



University
of Glasgow

Walker, John R. (2009) Investigation of isoform-specific fruitless mutants generated by gene targeting in *Drosophila melanogaster*. PhD thesis

<http://theses.gla.ac.uk/1283/>

Copyright and moral rights for this thesis are retained by the author

A copy can be downloaded for personal non-commercial research or study, without prior permission or charge

This thesis cannot be reproduced or quoted extensively from without first obtaining permission in writing from the Author

The content must not be changed in any way or sold commercially in any format or medium without the formal permission of the Author

When referring to this work, full bibliographic details including the author, title, awarding institution and date of the thesis must be given.

**Investigation of Isoform-specific *fruitless*
Mutants Generated by Gene Targeting in
*Drosophila melanogaster***

Submitted in fulfilment of the
requirements for the Degree of
Doctor of Philosophy

By
John R Walker

Division of Molecular Genetics
Anderson College
University of Glasgow
Glasgow G11 6NU, UK

April 2009

Abstract

fruitless (fru) is a pleiotropic gene which produces an array of variant transcription factor isoforms to fulfil a range of developmental and behavioural roles, from the regulation of axonal pathfinding during embryogenesis, all the way to the precise orchestration of individual steps of the *Drosophila melanogaster* male courtship ritual.

Much of the transcriptional differentiation is achieved through the use of multiple promoters, sex-specific splicing and variant C-termini. Alternative splicing at the 3' end enables generation of transcripts containing one of at least three zinc finger (Zn-F) domains (A, B or C). Due to the close proximity of these Zn-F-encoding exons at the *fru* locus, almost all extant *fru* mutants reduce or eliminate expression of all isoforms from a given promoter(s). This has prevented genetic dissection of their individual roles, and limited functional assignment to the zinc finger triumvirate as a whole.

Using gene targeting by homologous recombination, this project set out to generate precise null mutations for type-A and -B Fru isoforms in an attempt to determine which aspects of *fru* function are conferred by these isoforms. Isoform-specific antibodies were also generated to confirm the loss of individual isoforms within the generated mutants, and to investigate the expression of different isoforms throughout development.

Generation of such an antibody to Fru^B proteins enabled the developmental expression pattern of this isoform to be assessed for the first time, and expression in the male-specific serotonergic neurons of the abdominal ganglion suggested a possible role for male-specific Fru^B isoforms in male fertility. Investigation of the developmental expression patterns of Fru^C revealed a novel immunostaining pattern for this isoform in a group of coalescing cells which appear towards the end of embryonic development.

Isolation of specific-isoform mutants was achieved, giving rise to multiple mutant phenotypes, varying in severity between mutant lines. Analysis of mutants lacking type-A and -B Fru isoforms demonstrated the importance male-specific type-A and/or type-B isoforms in establishing male fertility, and suggested essential roles for sex-non-specific type-A and/or type-B isoforms in the viability and morphology of both sexes.

Table of Contents

Abstract	2
Table of Contents.....	3
List of Figures	6
List of Tables	7
Acknowledgements	8
Author's Declaration	9
Glossary	10
1 Introduction	12
1.1 <i>Drosophila melanogaster</i> as a Genetic Model to Study Behaviour	13
1.2 Courtship Behaviour in <i>Drosophila</i>	14
1.3 Male Courtship Behaviour is Mediated by <i>fruitless</i>	15
1.3.1 Discovery of <i>fruitless</i>	15
1.3.2 <i>fru</i> is a Member of the Sex Determination Hierarchy	16
1.3.3 <i>fru</i> Can Specify Most Male Courtship Behaviours.....	18
1.4 Phenotypes in <i>fru</i> P1 mutants	20
1.5 The roles of <i>fru</i> Promoters P2, P3 and P4	21
1.6 Expression Pattern of P1 Promoter	22
1.7 Expression Pattern of P2, P3 and P4 Promoters	27
1.8 Roles of different <i>fru</i> Isoforms	29
1.9 Conservation of <i>fru</i>	31
1.10 Gene Targeting by Homologous Recombination	34
1.11 Aims of this project	39
2 Materials and Methods.....	40
2.1 <i>Drosophila</i>	41
2.1.1 <i>Drosophila</i> Stocks.....	41
2.1.2 Rearing Conditions	42
2.1.3 <i>Drosophila</i> Microinjection	43
2.1.4 Dissection Techniques	45
2.2 Visualisation Techniques.....	46
2.2.1 Immunofluorescence.....	46
2.2.2 Confocal Microscopy	48
2.2.3 Image Processing	48
2.3 Bacterial Protocols	49
2.3.1 Strains and Plasmids	49
2.3.2 Culture Media	49
2.3.3 Antibiotics	50
2.3.4 Transformations	50
2.3.5 Isolation of Bacterial Artificial Chromosome (BAC) and Plasmid DNA from <i>E. coli</i>	51
2.4 Generation of Antibodies	51
2.4.1 GST Purification	51
2.4.2 pMAL Purification.....	52
2.4.3 Antibody Production	52
2.5 General Molecular Biology Protocols	53
2.5.1 Restriction Digestion of DNA.....	53
2.5.2 DNA Gel Electrophoresis.....	53
2.5.3 Visualization and Photography of Gels.....	53

2.5.4	Gel Extraction of DNA Fragments.....	53
2.5.5	Purification of Genomic DNA	54
2.5.6	Quantification of Nucleic Acids	54
2.5.7	Polymerase Chain Reaction (PCR)	54
2.5.8	DNA Sequencing	55
2.5.9	Southern Blotting of Fly Genomic DNA.....	57
3	Generation of Isoform-specific Antibodies	58
3.1	Introduction.....	59
3.2	Extant Fruitless Antibodies.....	59
3.3	Antigen design.....	60
3.4	Antigen production	62
3.4.1	Expression of fusion proteins	62
3.4.2	Purification of antigen.....	62
3.5	Antibody production.....	67
3.6	Testing Fruitless antibodies	68
3.6.1	Fru ^C proteins are expressed during embryonic development	68
3.6.2	Fru ^B and Fru ^C proteins are present in larval CNS	70
3.6.3	Fru ^B and Fru ^C co-localise with Fru ^M in male pupal CNS.....	72
3.6.4	Fru ^B is expressed in all the serotonergic neurons of the adult male abdominal ganglion	72
3.7	Discussion	77
3.8	Conclusions	80
4	Gene Targeting of <i>fruitless</i> Locus	81
4.1	Introduction.....	82
4.1.1	Mutagenesis at the <i>fru</i> Locus.....	82
4.1.2	Gene Targeting by Homologous Recombination	84
4.2	Design of Gene Targeting Construct	85
4.2.1	Targeting Vector.....	85
4.2.2	Choosing Targeting Homology Region	86
4.2.3	Introduction of Mutations into Donor DNA	90
4.2.4	Amplification of Donor DNA fragments	91
4.2.5	Cloning Strategy	92
4.3	Targeting the <i>fru</i> locus	92
4.3.1	Obtaining Targeting Construct Transformants.....	92
4.3.2	First Step Crosses: Integration at Target Locus	93
4.3.3	Analysis of Integration Events.....	95
4.3.4	Second Step Crosses: Resolution of Duplication.....	102
4.4	Discussion	103
4.4.1	Targeting Construct Design	104
4.4.2	Efficiency of Gene Targeting at Fruitless Locus.....	105
4.4.3	The I- <i>Crel</i> Endonuclease Recognition Site.....	106
4.5	Conclusions	107
5	Genetic Dissection of Gene Targeting Mutants	109
5.1	Introduction.....	110
5.2	Dissecting the Functions of <i>fruitless</i> Isoforms	110
5.3	Preparation of Gene Targeting Mutants for Phenotypic Analysis	112
5.4	Expression of <i>fruitless</i> Isoforms in Generated Recombinant Lines	112
5.5	Viability of Novel <i>fru</i> Mutants	116
5.5.1	Homozygote Viability	116
5.5.2	Complementation of Novel <i>fru</i> Mutants	118
5.5.3	Novel Mutants in Combination with Extant <i>fru</i> Null Mutants.....	119

5.6	Anatomical Defects in Novel <i>fru</i> Mutants	120
5.6.1	Disruption of Humeral Setae Formation	123
5.6.2	Defects in Genitalia Development	124
5.6.3	Abnormal Leg Development	125
5.7	Fertility of Novel <i>fru</i> Mutants.....	126
5.8	Discussion	129
5.9	Conclusions	132
6	Final Discussion	133
6.1	Further Characterisation of Novel <i>fru</i> Mutants	135
6.1.1	Do Both Fru ^{MA} and Fru ^{MB} Play a Significant Role in Establishing Male Fertility?	135
6.1.2	Are all three Fru ^{Com} Zn-F Isoforms Required to Confer Full Viability and Appropriate Morphology?	136
6.1.3	Are Fru ^{MA} or Fru ^{MB} Involved in Male Serotonergic Neuron Differentiation or MOL Development?.....	137
6.1.4	To What Extent is Male Courtship Affected in the Novel <i>fru</i> Mutants?.....	138
6.1.5	What Aberrant Splicing Events Occur at the <i>fru</i> Locus within the Novel Mutant Lines?.....	139
6.2	Novel Pattern of Fru ^C Embryonic Expression	141
6.3	Searching for Targets of Fru	142
	References	145

List of Figures

Figure 1.1 - Male Courtship in <i>Drosophila melanogaster</i>	15
Figure 1.2 - Molecular Map of <i>fru</i> Locus.	17
Figure 1.3 - The Sex Determination Hierarchy in <i>Drosophila</i>	19
Figure 1.4 - Regions of Male Brain Associated with Particular Aspects of Courtship.	25
Figure 1.5 - Fru ^M Expression in Pupal Male CNS.	26
Figure 1.6 - Conservation of <i>fru</i> Locus Organisation in <i>Anopheles gambiae</i>	32
Figure 1.7 - Conservation of <i>fru</i> Protein Domains in <i>Anopheles gambiae</i>	33
Figure 1.8 - Schematic Representation of Ends-out Targeting by Homologous Recombination.	37
Figure 1.9 - Schematic Representation of Ends-in Targeting by Homologous Recombination.	38
Figure 3.1 - Fruitless Isoform Antigens.	61
Figure 3.2 - Expression and Isolation of Fruitless-GST Fusion Proteins.	63
Figure 3.3 - Purification of Fruitless-GST Fusion Proteins B and C.	65
Figure 3.4 - Expression of MBP-Fru ^A Fusion Protein.	67
Figure 3.5 - Fru Isoform Immunostaining During Embryogenesis.	69
Figure 3.6 - Fru Isoform Expression in the Larval CNS.	71
Figure 3.7 - Fru Isoform Expression in the Pupal Male CNS.	73
Figure 3.8 - Fru Isoform Expression in the Adult Male CNS.	74
Figure 3.9 - Expression of Fru ^B in the Serotonergic Neuron Clusters of the Male Abdominal Ganglion.	76
Figure 4.1 - Genomic locations of Ten Extant <i>fru</i> Mutants and Deficiency Lines.	83
Figure 4.2 - Generation and Cloning of Donor Construct for Gene Targeting of <i>fru</i> Locus.	87
Figure 4.3 - Molecular Representation of Gene Targeting Process at the <i>fru</i> Locus.	89
Figure 4.4 - Genetic Crossing Scheme to Achieve Targeted Integration of Donor Construct at <i>fru</i> Locus.	94
Figure 4.5 - Verification of Re-integration Events by PCR.	97
Figure 4.6 - Verification of Targeted Events and Mutation Screens by PCR and Restriction Digestion.	98
Figure 4.7 - Southern Blot Analysis of Targeting Events.	101
Figure 4.8 - Genetic Crossing Scheme to Resolve Targeted Duplication at <i>fru</i> Locus.	103
Figure 5.1 - Expression of <i>fru</i> Isoforms in Adult Male CNS of Novel <i>fru</i> Mutants.	114
Figure 5.2 - Anatomical Defects Observed in Novel <i>fru</i> Mutants.	122

List of Tables

Table 2.1 - <i>Drosophila</i> Stocks used in this study.....	42
Table 2.2 - Primary antibodies used in this study.	47
Table 2.3 - Secondary antibodies used in this study.	48
Table 2.4 - Bacterial Strains	49
Table 2.5 - Table of plasmids.	49
Table 2.6 - Table of Primers.	56
Table 5.1 - Novel <i>fru</i> Mutant Lines and the Mutant Exons Incorporated During Gene Targeting.	113
Table 5.2 - Viability of Novel <i>fru</i> Mutants as Homozygotes and in Combination with Other <i>fru</i> Variants.	117
Table 5.3 - Frequency of Anatomical Abnormalities in Novel <i>fru</i> Mutants.	121
Table 5.4 - Fertility of Novel <i>fru</i> Mutants in Combination with other <i>fru</i> Variants.	127

Acknowledgements

Firstly I would like to thank my supervisor, Stephen Goodwin, for all his support and advice during this PhD. I would also like to thank all other members of the Goodwin lab - Tony, Suzanne, Jean-Christophe, Megan, Michael, Liz, Lizzy and Hania - for their friendship and help throughout the last few years. May the lab continue to prosper in Oxford.

I also thank the BBSRC for providing studentship funding, and my PhD assessors, Darren Monckton and Sean Colloms, for their advice.

Many thanks to my friends in Edinburgh and Glasgow, for all the laughs and good times.

Lastly, I would like to thank my parents for all their love and support.

Author's Declaration

I hereby declare that all the work reported in this thesis is my own unless stated otherwise in the text. None of the work has previously been submitted for any other degree at any other institution. All sources of information used in the preparation of this thesis are indicated by reference.

John R Walker

Glossary

5HT	5-Hydroxytryptamine
Abg	abdominal ganglion
bp	base pair(s)
BSA	bovine serum albumin
BTB	Broad-complex/Tramtrack/Bric-à-brac
°C	degrees Celsius
ChI	chaining index
CI	courtship index
CNS	central nervous system
<i>CS</i>	<i>Canton-S</i>
<i>CyO</i>	<i>Curly of Oster</i>
DFM	direct flight muscle
DNA	deoxyribonucleic acid
<i>dAbg</i>	dorsal serotonergic abdominal giant neurons
DSB	double strand break
<i>dsx</i>	<i>doublesex</i>
<i>e</i>	<i>ebony</i>
EDTA	Ethylene diamine tetraacetic acid
EGTA	Ethylene glycol tetraacetic acid
<i>elav</i>	<i>embryonic lethal, abnormal vision</i>
EtBr	ethidium bromide
FLP	Flippase site-specific recombinase
FRT	FLP recognition target
<i>fru</i>	<i>fruitless</i> gene
Fru	Fruitless protein
g	grams
g	centrifugal force equal to gravitational acceleration
GST	Glutathione S-Transferase
h	hour
<i>hid</i>	<i>head involution defective</i>
IPI	interpulse interval
IPTG	Isopropyl β -D-1-thiogalactopyranoside
kb	kilobase pairs
M	molar
MBP	maltose binding protein
MCS	multiple cloning site
mg	milligram
min	minute
mM	millimolar
MSg	meso-thoracic ganglion
mnDFM	motorneuron innervating direct flight muscle
ml	millilitre
MOL	Muscle of Lawrence
mRNA	messenger RNA
μ m	micrometre
<i>mw</i>	<i>miniwhite</i>
Myr	million years

NaOH	sodium hydroxide
ng	nanogram
PBS	phosphate buffered saline
PCR	polymerase chain reaction
<i>P</i> -element	<i>P</i> transposable element
<i>repo</i>	<i>reversed polarity</i>
s	second
<i>Sb</i>	<i>Stubble</i>
SP	sex-peptide
<i>srp</i>	<i>serpent</i>
<i>Sxl</i>	<i>sex -lethal</i>
T _M	melting temperature
Tra	<i>transformer</i>
Tra-2	<i>transformer-2</i>
UAS	upstream activator sequence
μg	microgram
μl	microlitre
<i>vAbg</i>	ventral serotonergic abdominal giant neurons
VNC	ventral nerve cord
<i>w</i>	<i>white</i>
WEI	wing extension index
Zn-F	zinc finger

1 Introduction

1.1 *Drosophila melanogaster* as a Genetic Model to Study Behaviour

Drosophila melanogaster has long been favoured for modelling the genetic systems that determine specific developmental outcomes. Its small size and short generation time make it an ideal organism for following the inheritance of different alleles, and studying the effects they produce in various genetic backgrounds. Genetic tools such as visible genetic markers, balancer chromosomes and *P*-element technology facilitate manipulation of the *Drosophila* genome and enable the genetic processes that underpin aspects of morphology and behaviour to be investigated. Complete sequencing of the *Drosophila melanogaster* genome (Adams *et al.* 2000), in conjunction with an array of mutagenesis techniques, has allowed genome-wide forward genetic screens to be performed, and the genetic basis of developmental functions to be identified. Besides the simple identification of the genes involved in particular traits, *Drosophila* is also a hugely powerful resource for the study of behavioural systems.

Several complex innate behaviours in *Drosophila* have been studied in great detail, including circadian rhythm (reviewed by Williams and Seghal, 2001) and courtship behaviour. How the brain develops to perform these innate behaviours is largely unknown, but genetic screens have revealed the genes involved in these behaviours, and explained how certain aspects of these behaviours are controlled.

Courtship behaviour in *Drosophila* is an excellent paradigm for the study of complex behaviour. Sexual dimorphism provides two naturally occurring behavioural variants, which facilitate investigation of how the developing nervous system can be differentially programmed to generate the potential for distinct innate behaviour between the sexes. The innate nature of the courtship repertoire has enabled its intricacies to be characterised in great detail, leading to accurate quantification of the series of sequential courtship steps, required to achieve mating success.

1.2 Courtship Behaviour in *Drosophila*

The courtship ritual of *Drosophila* is a complex series of behaviours performed by the male, which must be completed before the female will allow mating to take place (see Figure 1.1; reviewed by Hall 1994). The male will first follow a female and orient himself towards her. He then approaches the female from behind and begins tapping her abdomen with his forelegs. This act is believed to be involved in the detection of female cuticular pheromones using gustatory sensillae on the male's front legs (Robertson 1983). The male will then extend one wing, vibrating it, to produce a species-specific courtship song. The courtship song consists of two components, sine song and pulse song (Reviewed by Yamamoto *et al.* 1997). The time between song pulses, the interpulse interval (IPI), allows the female to recognise courtship song produced by males of her own species and increases her receptivity towards them. The male then approaches the female's abdomen and licks her genital plate with his proboscis. Finally, the male will bend his abdomen towards the female and attempt copulation. When successful, the male will mount the female, grasp her with his forelegs and make genital contact. If copulation is unsuccessful, the male will return to the initial stages of courtship before re-attempting copulation.

In *Drosophila melanogaster*, copulation lasts approximately 20 minutes. During this time the male transfers a complex mixture of sperm and seminal fluid to the female (reviewed by Wolfner 1997). In addition to providing reproductive potential to the female, this transfer also modifies her behavioural receptivity to subsequent male courtship. Accessory gland proteins carried in the seminal fluid reduce female receptivity and lead to an increase in active rejection responses to male courtship. Following successful copulation, females also show an increase in their egg laying rate (Kubli 2003). These postmating responses usually last for around one week. However, males that do not transfer sperm, but do transfer seminal fluid during mating, induce a short-term response of around one day. This indicates that the long term response is dependent upon the action of sperm. The short-term mating response is elicited by sex-peptide (SP), which is transferred in the seminal fluid (Liu and Kubli 2003).

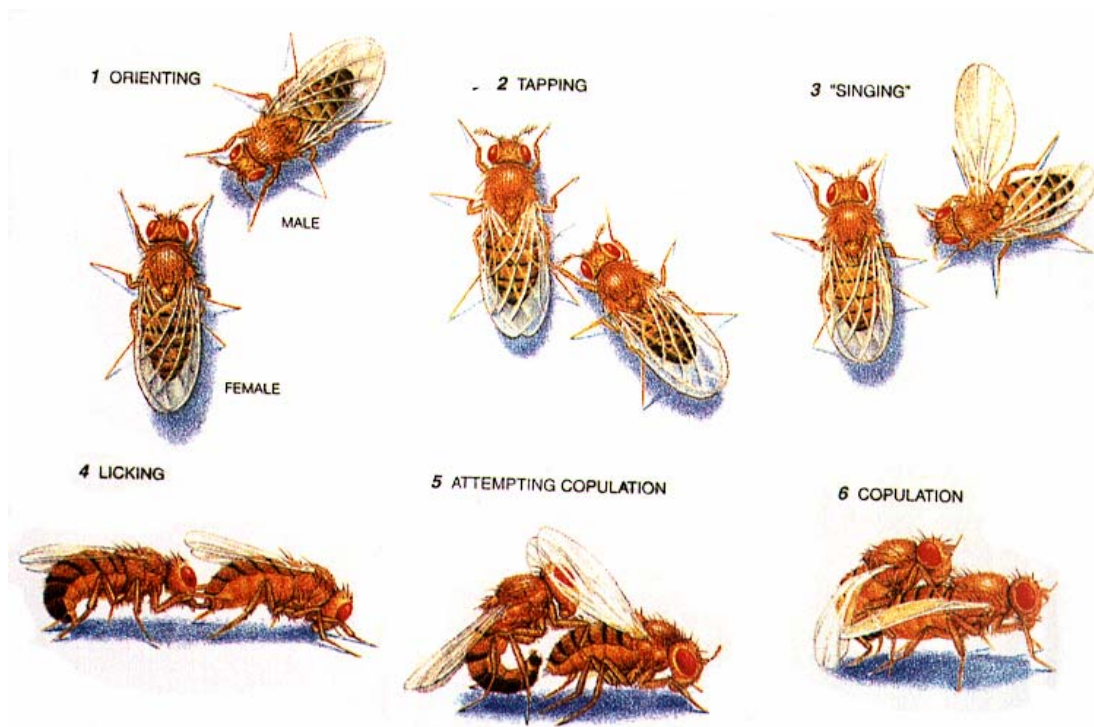


Figure 1.1 - Male Courtship in *Drosophila melanogaster*.

A male and a female fly are shown at six steps of the courtship ritual in *Drosophila melanogaster*. (From Greenspan 1995).

1.3 Male Courtship Behaviour is Mediated by *fruitless*

1.3.1 Discovery of *fruitless*

The importance of *fruitless* (*fru*) in male courtship was first identified in the isolation of an X-ray induced sterile mutant, *fru*¹ (Gill 1963). The genitalia of *fru*¹ males are normal, containing both sperm and seminal fluid, and the observed male sterility is due to a failure to copulate (Hall 1978a, Lee *et al.* 2001, Vellella *et al.* 2006). *fru*¹ mutant males perform indiscriminate courtship towards both males and females, but are behaviourally sterile as they fail to copulate. Additionally, *fru*¹ males passively elicit aberrant courtship from wild-type males.

The inter-male courtship observed in *fru*¹ males is characterised by the formation of courtship chains, in which each participant is courting the male in front and being simultaneously courted by the male directly behind it. The *fru*¹ mutation is caused by a small inversion which maps to the cytogenetic regions 90C and 91B and the abnormal phenotypes directed by and towards *fru*¹ males are caused by two separate genetic effects (Gailey and Hall 1989). It was

demonstrated by behavioural analysis of various deficiencies spanning the 90C-91B interval, that *fru* sterility and chaining behaviour maps to region 91B, whereas the elicitation of courtship maps to the interval 89F-90F.

The *fru* gene was cloned independently by two groups (Ito *et al.* 1996, Ryner *et al.* 1996), and spans approximately 140kb from cytogenetic location 91A7-91B3 (See Figure 1.2A). *fru* is pleiotropic, performing roles in establishing male sexual behaviour, in addition to influencing sex-non-specific requirements such as viability and external morphology (Ryner *et al.* 1996, Anand *et al.* 2001). The ability of *fru* to perform such a wide range of behavioural and developmental roles is enabled by differential promoter usage, and alternative splicing at both 5' and 3' ends, to combine complex *cis*-acting sequences (Ryner *et al.* 1996, Goodwin *et al.* 2000). *fru* transcripts are produced from four different promoters (P1, P2, P3 and P4), which encode closely related BTB (Broad-complex/Tramtrack/Bric-à-brac)-Zn-F putative transcription factors with C₂H₂ type zinc fingers (See Figure 1.2; Ito *et al.* 1996, Ryner *et al.* 1996). Accordingly, all *fru* transcripts contain one of four alternative 3' zinc finger ends, A, B, C or D (Ryner *et al.* 1996, Usui-Aoki *et al.* 2000). No functional role for type-D isoforms have been established thus far and it is known that sex-specific *fru* transcripts, which originate from P1, contain only A, B or C 3' termini (Billeter *et al.* 2006b).

1.3.2 *fru* is a Member of the Sex Determination Hierarchy

The male-specific outcomes of *fru* function are dependent upon P1 transcripts that are sex-specifically spliced at the 5' end (Ryner *et al.* 1996). In males, a male-specific 5' splice site is used that is located 1590 nucleotides upstream from the female-specific 5' splice site. Both 5' splice sites are then fused to a common 3' splice site more than 70kb downstream (Heinrichs *et al.* 1998). Translation of P1 transcripts in males produces a group of male-specific proteins, Fru^M, that have an amino-terminal extension of 101 amino acids preceding the BTB domain, compared to those produced from promoters P2-P4. Female-specific 5' splicing is induced by the binding of gene products from *transformer* (*tra*) and *transformer-2* (*tra 2*) to three 13bp *tra/tra-2* repeat elements, present upstream of the female-specific splice site (Figure 1.2B, Figure 1.3; Ryner *et al.* 1996, Heinrichs *et al.* 1998). *tra* is a key regulator in the sex determination

pathway and discovery that Tra mediates sex-specific splicing of *fru* transcripts, implicated *fru* as part of the sex determination hierarchy.

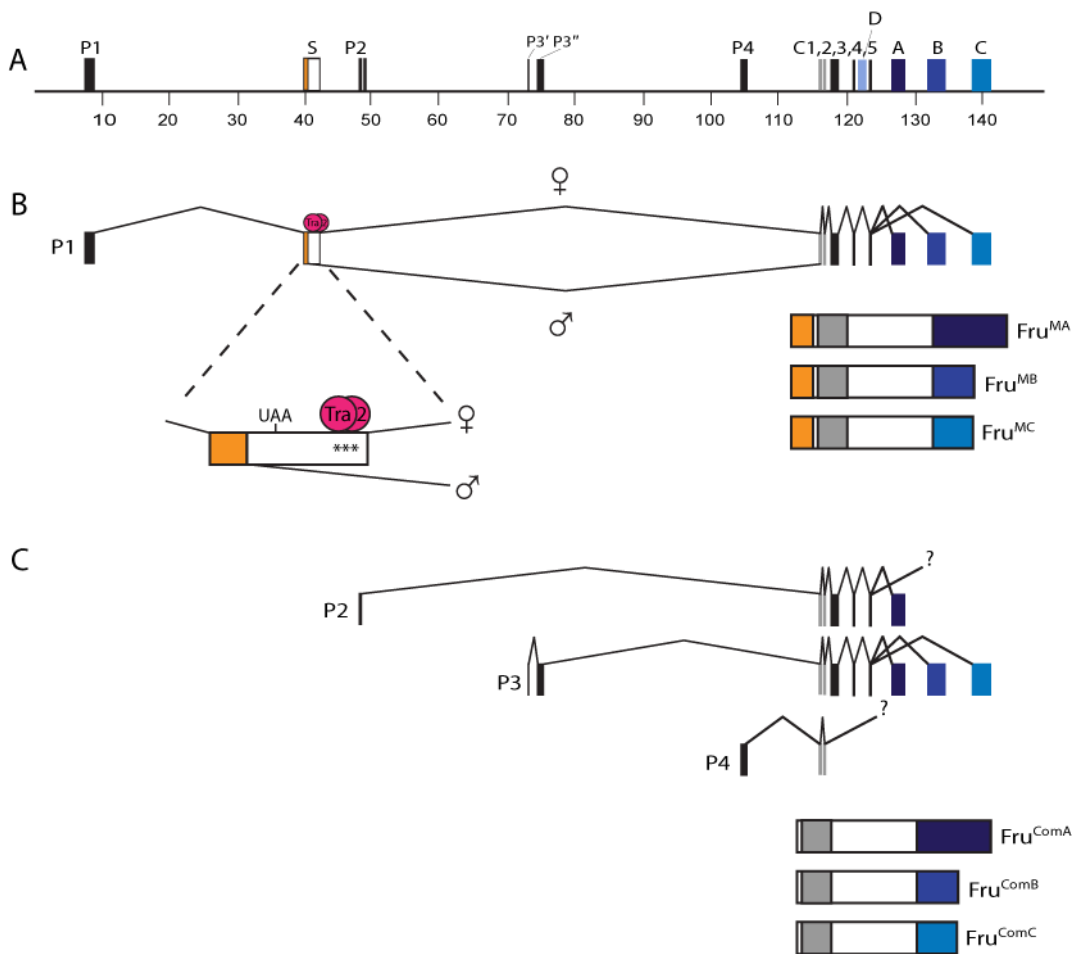


Figure 1.2 - Molecular Map of *fru* Locus.

(A) Genomic organisation of *fru* locus. Relative positions of the four promoters (P1-4), along with the five common exons (C1-5) and four potential Zn-F domain-encoding exons (A, B, C and D) are indicated. Also shown is the sex-specifically spliced exon (S) which is included in transcripts generated from P1. Distance is indicated in kb. (B) The transcripts produced by the P1 promoter. The P1 transcripts are sex-specifically spliced in females by Tra and Tra-2 binding to three transformer binding sites in exon S. This introduces a premature stop codon into female P1 transcripts. Due to an absence of Tra, male P1 transcripts follow a default splicing pathway. Asterisks indicate the 13-nt Tra binding sites. UAA shows the position of the transcriptional stop site in the female *fru* transcript. Also shown are the male-specific proteins (Fru^M) derived from the P1 transcripts (Fru^M). These contain a male-specific N-terminal domain (orange), a common BTB domain (grey), a common connector region (white) and zinc finger domain-containing C-terminus (blue). (C) Transcripts produced from the other promoters, and the Sex-non-specific proteins that they encode for (Fru^{Com}). These proteins lack the male-specific N-terminal domain, and it is not known whether all three Zn-F variant transcripts are produced from promoters P2 and P4. (Adapted from Anand *et al.* 2001).

Sex determination in *Drosophila* takes place on a cell by cell basis, where the sex of each cell is determined by the ratio of X chromosomes to autosomes present (See Figure 1.3; reviewed by Christiansen *et al.* 2002). This ratio controls the activity of an RNA splicing factor *Sex-lethal (Sxl)*. In females (XX) the ratio is 1, causing *Sxl* to be expressed. In males (XY), a ratio of 0.5 means that *Sxl* is not expressed. In females, *Sxl* regulates splicing of pre-mRNA from *tra* so that active Tra protein is expressed. Tra, in conjunction with Tra-2, acts in females to splice mRNA produced from *fru* and *doublesex (dsx)*, which are positioned downstream in the sex determination pathway. This sex-specific splicing produces a female-specific isoform of *dsx*, Dsx^F , and incorporates a premature stop codon into P1 *fru* transcripts in females. No proteins derived from P1 transcripts are detected in females and it is believed that female transcripts may be degraded by nonsense mediated RNA decay (reviewed by Amrani *et al.* 2006). In the absence of Tra, default splicing of *fru* and *dsx* occurs, producing male-specific Dsx^M and Fru^M isoforms respectively. While *fru* is involved in generating courtship potential in males, *dsx* primarily controls aspects of somatic differentiation and external morphology in both sexes (Cline and Meyer 1996).

1.3.3 *fru* Can Specify Most Male Courtship Behaviours

To investigate whether male courtship behaviour was conferred entirely by Fru^M it was necessary to recapitulate its expression in females. Development of homologous recombination technology in *Drosophila* enabled P1 transcripts in females to be constitutively spliced in a male-specific manner (Demir and Dickson 2005). Male-specific splicing in females was achieved by generating alleles in which the Tra/Tra-2 binding sites were deleted (*fru^M* and *fru^{Atra}*). Although Tra is still produced in these females, splicing follows the default male pathway, leading to the expression of Fru^M proteins.

Courtship analysis of these females found that they do indeed court wild-type females. *fru^M* and *fru^{Atra}* females orient, follow, tap, extend their wings and lick. These findings confirmed that *fru* is sufficient to perform most steps of male courtship behaviour. However, these females court at lower levels than wild-type males, and do not attempt copulation, demonstrating that the action of other genes is necessary to provide full courtship behaviour.

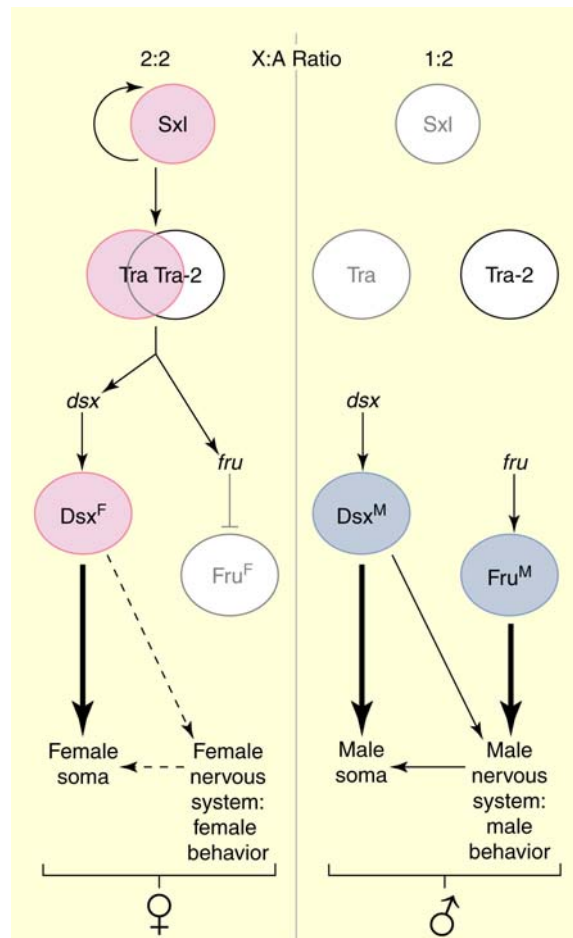


Figure 1.3 - The Sex Determination Hierarchy in *Drosophila*.

In females the ratio of X chromosomes to autosomes (X:A) is 2:2, resulting in active Sxl protein, which splices *tra* mRNA to produce functional Tra protein. The presence of Tra, in conjunction with the sex-non-specific Tra-2, causes a sex-specific splice in both *dsx* mRNA and *fru* mRNA produced from promoter P1. This female-specific splicing leads to production of Dsx^F and introducing a premature stop codon into female *fru* transcripts. No sex-specific Fru^F protein is made in females. In males the X:A ratio is 1:2 and Sxl is not produced, resulting in an absence of Tra. Splicing of *dsx* mRNA and *fru* P1 transcripts follow the default pathway in males leading to production of Dsx^M and Fru^M. (From Billeter *et al.* 2006a).

Courtship song analysis of *fru^M* and *fru^{Atra}* females shows that, although they are capable of wild-type wing extension, they spend significantly less time singing during courtship and produce no sine song (Rideout *et al.* 2007). Electrophysiology studies indicate that the activity of seven of the direct flight muscles (DFMs) are directly linked to the production of courtship song (Ewing 1979). The somata of the motorneurons innervating six of these muscles (mnDFMs) are located in the ventral thoracic ganglion, and five of these cell bodies are located in the meso-thoracic ganglion (Msg; Trimarchi and Schneiderman 1994).

Interestingly, a sexually dimorphic number of neurons are known to express P1 transcripts in the *Msg*, and studies with male-female mosaics have demonstrated that this region must be male for courtship song production (Lee *et al.* 2000, von Schilcher and Hall 1979). Analysis of the *Msg* in *fru^M* and *fru^{Atra}* females showed that expression of *Fru^M* was not present in as many neurons as in wild-type males, demonstrating that *Fru^M* alone is not sufficient to generate the sexually dimorphic neuronal population found in this region (Rideout *et al.* 2007).

Another gene known to be involved in song production is *dsx* (Lee *et al.* 2002). The discovery that *Dsx* colocalises with *Fru^M* in the *Msg*, coupled with the knowledge that *Dsx* exists in sex-specific isoforms, suggested that both proteins may co-operate to establish the sexually dimorphic neuronal populations found there (Rideout *et al.* 2007). Observation of a decrease in the number of *Fru^M* expressing neurons in the *Msg* of *dsx* null males, compared to wild-type males, showed that *Dsx* is also necessary to generate the sexual dimorphism required to produce courtship song (Rideout *et al.* 2007).

1.4 Phenotypes in *fru* P1 mutants

While promoters P2-P4 produce functional transcripts in both sexes, functional P1 transcripts are generated only in males. The importance of these male-specific P1 transcripts has been largely determined using various P1 mutants. Since the isolation of the first P1 mutant (*fru¹*), several other hypomorphic alleles have been generated by *P*-element insertion at the *fru* locus (*fru²*, *fru³*, *fru⁴* and *fru^{Sat}*; See Figure 1.2; Castrillon 1983, Moses 1989, Ito *et al.* 1996, Goodwin *et al.* 2000). The *fru²* mutant was isolated from the insertion of a tagged transposon at map location 91B. *fru²* males demonstrate a milder expression of the *fru* syndrome than in *fru¹* and are often able to fertilise females. Three further *fru* mutants (*fru³*, *fru⁴* and *fru^{Sat}*) due to *P*-element insertions were isolated on the basis of male sterility, and found also to map to 91B. Northern blot analysis of mRNA from the four *P*-element mutants demonstrated that the sex-specifically spliced transcripts from promoter P1, present in wild-type, were absent (Goodwin *et al.* 2000). This suggested that the mutant phenotypes observed in these alleles are due to disruption of P1 transcripts, and has subsequently been confirmed using deficiency lines which remove regions including the P1 promoter (Anand *et al.* 2001).

With the exception of *fru*², all homozygous *fru* P1 mutant males are sterile. The genitalia of these males are normal, containing both sperm and seminal fluid, and the observed sterility is due to a failure to copulate (Hall 1978a, Lee *et al.* 2001, Villella *et al.* 2006). In addition to an overall reduction or loss of fertility, these hypomorphic alleles are found to disrupt each step of the male courtship ritual. Different alleles induced various effects upon tapping behaviour, production of courtship song and licking of the female's genital plate and only *fru*² males ever attempted copulation (Gailey and Hall 1989, Villella *et al.* 1997, Goodwin *et al.* 2000).

In addition to its role in controlling male courtship behaviour, Fru^M also acts to mediate certain aspects of male morphology. Formation of the male-specific muscle of Lawrence (MOL) is dependent upon innervation by genetically male motor neurons during metamorphosis (Lawrence and Johnston, 1986; Currie and Bate, 1995; Usui-Aoki *et al.*, 2000). Fru^M expression in this motorneuron, present in both males and females, induces the recruitment of myoblasts from a sex-non-specific pool to form a larger male-specific muscle (Taylor and Knittel 1995). Although the precise function of this muscle is yet to be confirmed, it is proposed to be involved in the unbending of the male abdomen at the termination of copulation (Lee *et al.* 2001).

In females, lack of Fru^M means no MOL is formed, and the corresponding motorneuron innervates four smaller muscles. Similarly, mutant males lacking Fru^M (*fru*^M alleles) show abnormal or missing MOLs, and instead develop four smaller muscles, each innervated by the motor neuron that would normally innervate the MOL (Billeter and Goodwin 2004).

1.5 The roles of *fru* Promoters P2, P3 and P4

While *fru* transcripts from promoter P1 are required for successful courtship behaviour and certain aspects of morphology specific to the male, *fru* function is also essential for the viability of both sexes (Anand *et al.* 2001). Isolation of mutants lacking *fru* transcripts from different promoters has revealed those required for survival of both males and females. Although behaviourally sterile, males lacking P1 transcripts are still fully viable. Conversely, *fru* genotypes of both sexes lacking function from promoters P3 and P4 cannot eclose and die in

their pupal cases. If these mutants are released by hand from their pupal cases they display anatomical defects including defective leg joints and failure to evert imaginal discs (Anand *et al.* 2001). A similar pattern is observed in genotypes lacking P3 function only, although these individuals tend to reach a later stage of metamorphosis than those lacking P3 and P4 function.

The *fru* mutants that fail to emerge from their pupal cases have fewer motorneuron terminals on the lateral muscles of the abdomen. Additionally, innervation of the lateral abdominal muscles is concentrated in the lateral and middle zones, near the dorsal side of the body, and does not penetrate the medial zones as is the case in wild-type (Anand *et al.* 2001).

1.6 Expression Pattern of P1 Promoter

The expression patterns of P1 *fru* transcripts and the Fru^M proteins that they encode have been studied in detail throughout development and in mature adults (Lee *et al.* 2000). *in situ* hybridisation shows that P1 *fru* transcripts first appear in the CNS of 3rd instar larvae. Anti-Fru^M immunoreactivity is first detected in a few clusters of cells of the brain and the ventral ganglia at the same time, suggesting that expression of *fru* is controlled mainly at the transcriptional level. The signals produced by *in situ* hybridisation and Fru^M immunostaining peak, both in intensity and distribution, during the first two days of pupal development. The abundance of P1 transcripts then declines dramatically towards the end of the pupal stage and into adulthood. However, the pattern of expression in the mature CNS remains similar to that observed during metamorphosis. In contrast, levels of Fru^M immunoreactivity in the adult CNS are similar to those observed in 2-day pupae and remain constant throughout adulthood (Lee *et al.* 2000). While Fru^M proteins are only present in males, P1 transcripts are detected in both sexes during these stages. Female P1 transcripts are 1.5kb larger in size than male P1 transcripts due to sex-specific splicing mediated by Tra and Tra-2 (Ryner *et al.* 1996, Heinrichs *et al.* 1998, Goodwin *et al.* 2000). The incorporation of a premature stop codon into female transcripts prevents their translation into functional protein.

The appearance of Fru^M coincides with the remodelling of the CNS that occurs during metamorphosis. Ubiquitous expression of Tra can lead to loss of male

behaviour but only if it is expressed by early pupal stages, and not after (Arthur *et al.* 1998). Processing of information related to adult behaviours is controlled by dedicated interneurons formed during metamorphosis (Tissot and Stocker 2000, Consoulas *et al.* 2000). Formation of some of these neurons occurs only in males, mediated by Fru^M expression (Kimura *et al.* 2005).

Fru^M immunoreactivity produces signals which are located within the nuclei of cells within the male CNS. This supports protein sequence analysis, which infers that *fru* proteins are transcription factors. Fru^M also co-localises with the *elav* gene product, which is expressed solely in the nuclei of neurons (Yao *et al.* 1993), confirming that Fru^M expressing cells are neurons and not glia (Lee *et al.* 2000). Fru^M is expressed in approximately 1,700 neurons in the male pupal and adult CNS, which equates to around 2% of the neurons present in the nervous system at these stages. These Fru^M neurons, present in localised groups in brain, and also throughout the VNC, have been categorised into 20 defined clusters (Lee *et al.* 2000).

Fru^M expression can be found in all regions of the nervous system that are known to be important to male courtship behaviour (Fig 1.4; reviewed by Greenspan and Ferveur 2000, Billeter *et al.* 2006a). The key courtship dependent regions were identified by generating sex mosaics. The cell autonomous nature of sex determination in the fly has made it possible to generate gynandromorphs, which are female flies, containing clones of male tissue due to the loss of an X-chromosome in some tissues. Such sex mosaics are generated by random, somatic loss of an X chromosome from a diplo-X (female) to produce haplo-X (male) clones in an otherwise female background (reviewed by Greenspan and Ferveur 2000). Following behaviour studies, the sex of each region of a gynandromorph brain can be determined using an X-linked biochemical marker (reviewed by Hall 1978b). However, the random nature of X chromosome loss in gynandromorph studies means that focussed study of a particular region of the brain is difficult to achieve. An alternative route is to selectively feminise discrete regions of the male brain using the UAS/GAL4 system (Brand and Perrimon 1993). This can be accomplished by targeted expression of UAS-*tra*^F, under the control of GAL4-enhancer trap lines that express in specific regions of the CNS (Ferveur *et al.* 1995). Several *fru-gal4* constructs have been generated to manipulate expression in *fru* neurons. The *fru(16)-gal4* driver line, created

by fusion of a 16kb fragment of the P1 promoter to the yeast transcriptional activator Gal4, expresses in 16% of Fru^M neurons in the adult CNS (Billeter and Goodwin 2004).

Mosaic analyses revealed that the dorsal regions of the brain are required for the initial stages of courtship behaviour such as following, tapping and wing extension (Figure 1.4; Hall 1979). Five clusters of Fru^M expression are located in the dorsal brain (Lee *et al.* 2000). Three of these are found in the anterior superior protocerebrum: *fru-aSP1*, *fru-aSP2* and *fru-aSP3* (See Figure 1.5). The other two are located in the posterior superior protocerebrum: *fru-pSP1* and *fru-pSP2*. *fru-pSP2* is located in very close proximity to the calyx of the mushroom bodies. The mushroom bodies receive sensory information from a number of inputs and are crucial in courtship conditioning (McBride *et al.* 1999). The feminisation of these structures has been shown to result in inter-male courtship (O'Dell *et al.* 1995). A further cluster, *fru-P*, is also found broadly distributed ventral to the mushroom body calyx. Three clusters of expression are found in the lateral region of the brain: *fru-Lv*, *fru-Ld* and *fru-pL*. However, this region of the brain has yet to be implicated in any aspect of courtship behaviour.

Clusters *fru-M* and *fru-Lo* are expressed in the optic lobes. Vision is not necessary for courtship but visual cues form an important part in recognition of potential sexual partners (Joiner and Griffith 1997). A cluster of neurons is also found in the suboesophageal ganglion, *fru-SG* (Lee *et al.* 2000). This region of the brain contains projections from the maxillary palps and the mouthparts, which possess olfactory and gustatory receptors respectively (reviewed by Stocker 1994). Olfaction is involved in the perception of inhibitory female compounds during tapping of the female abdomen during courtship (Stocker and Gendre 1989). Gustatory receptors may play a similar sensory role when the male contacts the female genitalia with his mouthparts prior to copulation.

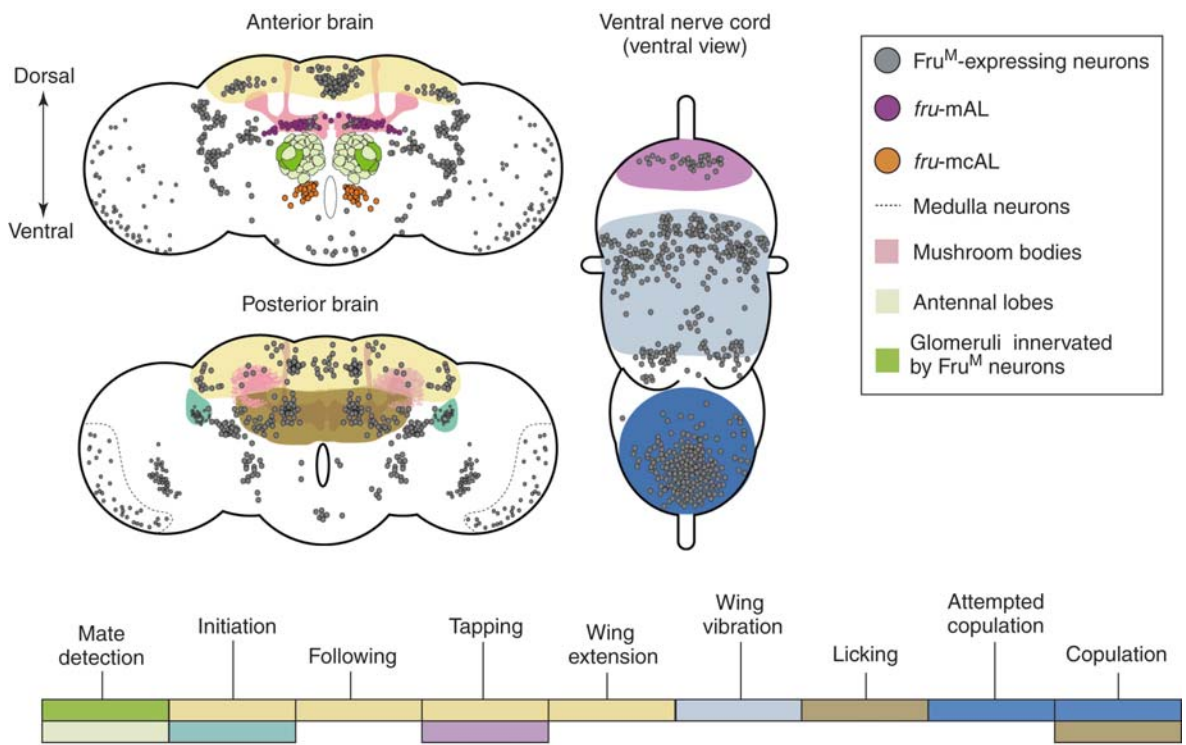
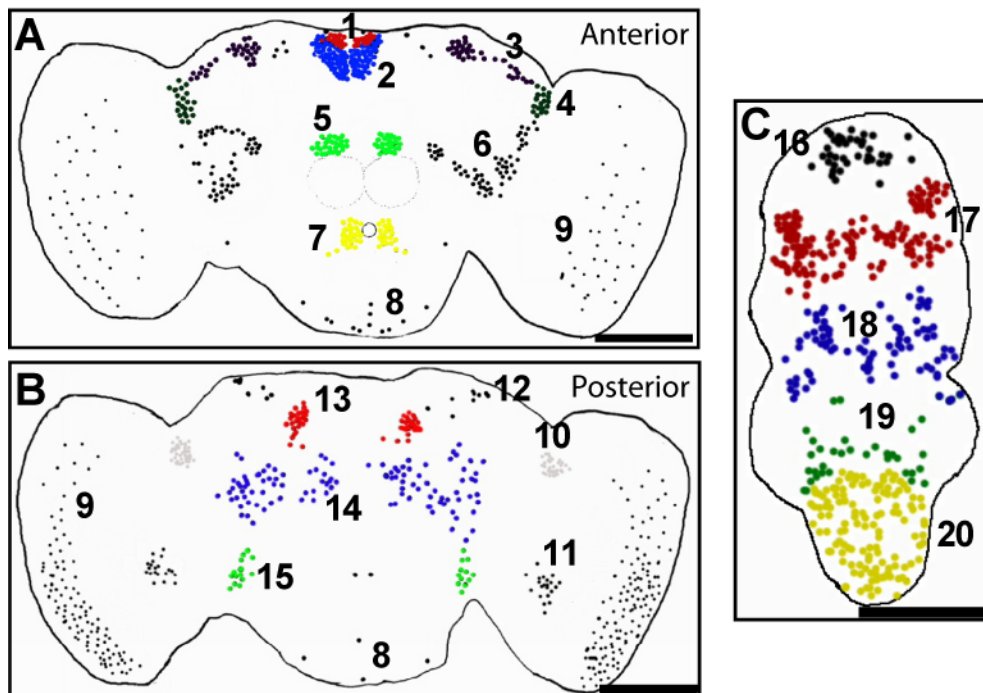


Figure 1.4 - Regions of Male Brain Associated with Particular Aspects of Courtship.

Expression pattern of Fru^M in the adult male CNS in relation to specific areas reported to be involved in particular aspects of male courtship. The coloured areas represent areas implicated in the performance of a particular courtship step, as indicated in the key below. (Billeter *et al.* 2006a).

Three clusters are located around the antennal lobes: *fru*-mAL, *fru*-AL and *fru*-mcAL. The antennal lobes are known to be involved in partner discrimination and the prevention of inter-male courtship (Ferveur *et al.* 1995). The antennal lobes process olfactory information received from the antennae and could be involved in pheromone recognition (reviewed by Stocker *et al.* 1994). The *fru*-mAL cluster contains Fru^M interneurons that are generated by Fru^M inhibition of cell death (Kimura *et al.* 2005). These interneurons send projections to the suboesophageal ganglion, and it is possible that these projections act as input sites for pheromonal information conveyed by gustatory neurons. *fru*¹ mutants lack Fru^M expression in this region of the brain and perform robust inter-male courtship (Gailey and Hall 1989, Lee and Hall 2001). High levels of inter-male courtship are also observed when these neurons are feminised or have their synaptic transmission blocked (Kitamoto 2002, Vilella *et al.* 2005). The *fru*-mcAL cluster is thought to control the sequential execution of courtship steps

(Manoli and Baker 2004). The cluster forms part of the median bundle, which receives information from various sensory systems throughout courtship.



1 : <i>fru</i> -aSP1	5 : <i>fru</i> -mAL	9 : <i>fru</i> -M	13 : <i>fru</i> -pSP2	17 : <i>fru</i> -PrMs
2 : <i>fru</i> -aSP2	6 : <i>fru</i> -AL	10 : <i>fru</i> -Ld	14 : <i>fru</i> -P	18 : <i>fru</i> -MsMt
3 : <i>fru</i> -aSP3	7 : <i>fru</i> -mcAL	11 : <i>fru</i> -Lo	15 : <i>fru</i> -pL	19 : <i>fru</i> -MtAb
4 : <i>fru</i> -Lv	8 : <i>fru</i> -SG	12 : <i>fru</i> -pSP1	16 : <i>fru</i> -Pr	20 : <i>fru</i> -Ab

Figure 1.5 - Fru^M Expression in Pupal Male CNS.

Spatial distribution of Fru^M-immunoreactive neurons in the male pupal CNS. (A) Anterior view of brain. (B) Posterior view of brain. (C) Ventral nerve cord (VNC), including both ventral and dorsal regions. Anterior is at the top. Scale bars=100µm. Table below shows the name of the numbered neuron clusters. (Modified from Lee *et al.* 2000).

Fru^M neurons are distributed more evenly throughout the ventral nerve cord (VNC). For this reason, neurons in this region are assigned to five groups based upon their position in a particular location of VNC. The anterior group is known as *fru*-Pr due to its position in the pro-thoracic ganglion. Three relatively posterior groups are found between the pro- and meso-thoracic (*fru*-PrMs), the meso- and meta-thoracic (*fru*-MsMt) and the meta-thoracic and abdominal ganglia (*fru*-MtAb). Feminisation studies using *tra*^F have shown the pro-thoracic ganglion to be involved in the early steps of courtships which may relate to chemosensory organs in the legs (Ferveur and Greenspan 1998).

Fru^M expression is known to co-localise with that of the male-specific *dsx* isoform (Dsx^M) in the *Msg*, acting to produce sexually dimorphic interneuron populations that are required for the production of courtship song (Rideout et al. 2007). Males lacking *fru*^M function are known to sing abnormally (Ryner et al. 1996, Vellella et al. 1997, Goodwin et al. 2000).

The fifth and final group is located within the abdominal ganglion, *fru*-Ab. Fru^M controls the production of two clusters of male-specific serotonergic neurons in the abdominal ganglion (Billeter et al. 2006b). Both of these clusters innervate the male reproductive organs and these serotonergic projections are thought to co-ordinate the release of sperm and seminal fluid (Acebes et al. 2004). Synchronised emission of sperm and seminal fluid is required to fertilise the female and prevent her remating, and lack of serotonin in these neurons is associated with infertility (Lee and Hall 2001, Billeter et al. 2004). The abdominal ganglion has also been implicated in the process of attempted copulation using sex mosaic studies (Hall 1977). The male-specific muscle of Lawrence (MOL) has been proposed as the muscle which may control unbending of the male abdomen to end copulation (Lee et al. 2001) and Fru^M has been shown to be necessary for the formation of this muscle (Billeter et al. 2006b).

1.7 Expression Pattern of P2, P3 and P4 Promoters

Although sex-specific *fru* transcripts are not produced until late in larval development (Lee et al. 2000), non-sex-specific (*fru*^{Com}) transcripts are widely expressed from early in embryonic CNS development. The role of *fru* in embryo development has been revealed using mutants possessing deletions or P-element insertions in the *fru* locus. Observations that embryos lacking most or all of *fru* function have defects in axonal projections led to the discovery that *fru* transcripts are required to regulate axonal pathfinding in the embryonic CNS (Song et al. 2002).

The transcripts present during embryogenesis are generated from *fru* promoters P3 and P4, which are believed to provide transcripts important for the viability of both sexes (Ryner et al. 1996; Anand et al. 2001). It has been shown, using antibodies specific to the Zn-F containing domains of *fru* proteins, that proteins possessing A-type or C-type 3' ends are present in the developing embryo. The

lack of an antibody to detect proteins with B-type 3' ends has prevented the presence of these proteins to be determined, but *in situ* hybridisation using 3' end riboprobes suggests that transcripts containing a B-type 3' end are present in the embryonic CNS (Song *et al.* 2002).

in situ hybridisation with anti-sense riboprobes, designed to detect all *fru* transcripts, has demonstrated that *fru* transcripts are expressed in a dynamic temporal and spatial pattern from the beginning of embryogenesis until stage 16. However, some *fru* transcripts are believed to be produced maternally and then sequestered in the oocyte (Song *et al.* 2002). These transcripts are uniformly distributed in the very early embryo and then are distributed into segregating pole cells. At the start of gastrulation heavily labelled cells are found in ventral and cephalic furrows. At the mid-point of embryogenesis (stages 7-9) the most prominent distribution of *fru* transcripts is found within the developing CNS, within mesectodermal and ventral neuroectodermal cells. Transcripts then become localised to delaminating neuroblasts and after stage 10, *fru* transcripts are detected in medial but not lateral neuroblasts. After stage 10, transcripts are detected in medial but not lateral neuroblasts, and expression then declines until stage 16 (Song *et al.* 2002). Immunocytochemistry, using antibodies to the 3' termini of Fru proteins demonstrated that Fru^{ComA} expression follows the overall expression pattern observed by *in situ* hybridisation. Fru^{ComC} is also consistent with this pattern until stage 12 when its CNS expression begins to decline (Song *et al.* 2002).

The sterility observed in *fru*⁴ mutant males is due to the insertion of a *P*-element 2kb upstream of the *fru* P3 promoter (Goodwin *et al.* 2000). Replacement of this *P*-element insertion with a GAL4 element produced reporter lines with an expression pattern like that of P3 and P4 (Dornan *et al.* 2005). Co-expression of the reporter lines and anti-Fru^{Com} (raised against the BTB domain common to all *fru* isoforms) is detected in the larval CNS, glia and support cells ensheathing neurite bundles. The expression in glial support cells and support cells is also shown to persist in the axonal bundles of pupae and adults of both sexes. Additionally, co-expression is observed in muscles cell of the thorax and the abdomen in adults of both sexes, and the accessory glands of testes in adult males (Dornan *et al.* 2005).

1.8 Roles of different *fru* Isoforms

It has been shown that *fru* is a pivotal regulator of both sex-specific and sex-non-specific developmental functions. *fru* is able to influence so many behavioural and morphological outcomes, in part, due to the vast array of transcripts it produces (Ryner *et al.* 1996, Anand *et al.* 2001). The functions of these transcripts have been studied using mutants that abolish certain subsets. Alleles lacking functional P1 transcripts have uncovered the behavioural and developmental functions of the male-specific transcripts (Goodwin *et al.* 2000, Usui-Aoki *et al.* 2000). Similarly, deficiencies removing large sections of the *fru* locus have revealed some of the essential, non-sex-specific functions conferred by transcripts from the other *fru* promoters (Anand *et al.* 2001). These findings highlight the importance of transcript variation generated by differential promoter usage and 5' sex-specific splicing, but what about 3' alternative splicing?

All wild-type *fru* transcripts contain one of four possible zinc finger 3' termini (A, B, C or D). These different zinc finger domains provide each type of isoform with potentially unique DNA binding specificities. Study of these individual isoforms thus far has been limited, as almost all extant *fru* mutants affect all transcripts produced by a particular promoter, or set of promoters. The exception to this rule was the isolation of the *fru^{AC}* allele. The *fru^{AC}* abolishes *fru^C* transcripts from all promoters allowing the contribution of both sex-specific and sex-non-specific isoforms to *Drosophila* development to be assessed (Billeter *et al.* 2006b). The loss of sex-non-specific Fru^{ComC} is associated with a reduction in the viability of both sexes, whereas loss of sex-specific Fru^{MC} disrupts several male developmental outcomes.

Phenotypic analysis of this mutant revealed that Fru^{MC} isoforms, exclusively, act in the formation of the male-specific muscle of Lawrence (MOL). Loss of Fru^{MC} also affects development of two male-specific clusters of serotonergic neurons in the abdominal ganglion and leads to diminished male courtship and behaviour (Billeter *et al.* 2006b). Further evidence of the role played by Fru^{MC} in these male-specific functions has been obtained using the UAS/GAL4 system of transcriptional activation (Brand and Perrimon 1993) to express different GAL4-responsive Fru^M isoforms, in an attempt to rescue function in mutants deficient

for particular Fru^M isoforms (Billeter *et al.* 2006b). The P1-specific *fru(16)-gal4* driver used to attempt rescue expresses in 16% of Fru^M neurons, including 25% of those located in the abdominal ganglion (Billeter and Goodwin 2004).

Expression of the UAS-*fru*^{MC} transgene in *fru*^{AC}/*fru*³ males (referred to as Fru^{MC}-nulls as they produce Fru^{MA} and Fru^{MB} isoforms but not Fru^{MC}) rescues fertility in a significant number of males but does not restore male courtship behaviour. Expression of Fru^{MC} in a *fru*³/*fru*³ background (referred to as Fru^M-nulls since they make no Fru^M isoforms) has no significant effect upon either male fertility or courtship behaviour, nor does expression of Fru^{MA} or Fru^{MB} in either Fru^{MC}-null or Fru^M-null mutant backgrounds (Billeter *et al.* 2006b).

The overwhelming majority of Fru^{MC}-null and Fru^M-null mutants lack any discernable MOL, and those that do possess only a vestigial MOL. Fru^{MC} expression rescues formation of the muscle in both of these mutant backgrounds, indicating that the Fru^{MC} isoform is both necessary and sufficient for MOL formation. This is also demonstrated by the finding that Fru^{MC} expression induces formation of a MOL-like muscle in wild-type females. No MOL induction is achieved by expression of Fru^{MA} or Fru^{MB} in either Fru^{MC}-null or Fru^M-null mutant males (Billeter *et al.* 2006b).

Both clusters of serotonergic neurons in the abdominal ganglion are absent in Fru^M-null mutants, and Fru^{MC}-nulls exhibit a reduction in the number of male serotonergic neurons in each cluster, with one cluster often completely absent. Fru^{MC} expression is able to rescue differentiation of both dorsal and ventral clusters in Fru^M-nulls. In Fru^{MC}-nulls rescue of the dorsal cluster is induced, with a smaller effect upon the ventral cluster. Differentiation of the dorsal cluster only in Fru^M-nulls can be rescued by Fru^{MB} expression, but expression has no significant impact upon the mutant phenotype in Fru^{MC}-nulls. Fru^{MA} expression does not significantly rescue serotonergic neuron differentiation in either mutant background, which is perhaps unsurprising given that Fru^{MA} is absent from the serotonergic neuron clusters of wild-type adult males (Billeter *et al.* 2006b).

The differential patterns of expression of each *fru* zinc finger isoform, and their varying ability to rescue certain developmental outcomes, suggests an important role of each variant isoform. The functional significance of these zinc finger

isoforms is also reinforced by the finding that the zinc finger domains are highly conserved within *Drosophilidae*, and other species such as the distantly related mosquito, *Anopheles gambiae* (Gailey *et al.* 2006).

1.9 Conservation of *fru*

The *fru* gene shows remarkable conservation amongst many species of *Diptera* and also within other insect orders (Bertossa *et al.* 2009). Indeed, organisation of the *fru* locus in *Anopheles gambiae* is almost to that found in *Drosophila melanogaster*, despite 250 Myr of evolutionary divergence (Gailey *et al.* 2006). As in *Drosophila*, *fru* utilises multiple promoters and alternative splicing in *A. gambiae* to generate an array of BTB-ZnF transcription factors. Sex-specific splicing also occurs in a manner strikingly similar to that employed by *Drosophila* (Gailey *et al.* 2006, Figure 1.6).

Tra/Tra-2 mediated sex-specific splicing in female mosquitoes leads to the incorporation of two female-specific sequences, one by exon inclusion, and the other by alternative 5' splice site usage. Absence of Tra protein in males induces default splicing and exclusion of these female sex-specific sequences by exon skipping and alternative 5' splice site usage. As with sex-specific *fru* mRNAs in *Drosophila*, only those produced in males are translated into full length BTB-ZnF proteins as female-specific mRNAs incorporate a premature stop codon (Gailey *et al.* 2006).

Tra/Tra-2 mediated sex-specific splicing in female mosquitoes leads to the incorporation of two female-specific sequences, one by exon inclusion, and the other by alternative 5' splice site usage. Absence of Tra protein in males induces default splicing and exclusion of these female sex-specific sequences by exon skipping and alternative 5' splice site usage. As with sex-specific *fru* mRNAs in *Drosophila*, only those produced in males are translated into full length BTB-ZnF proteins as female-specific mRNAs incorporate a premature stop codon (Gailey *et al.* 2006).

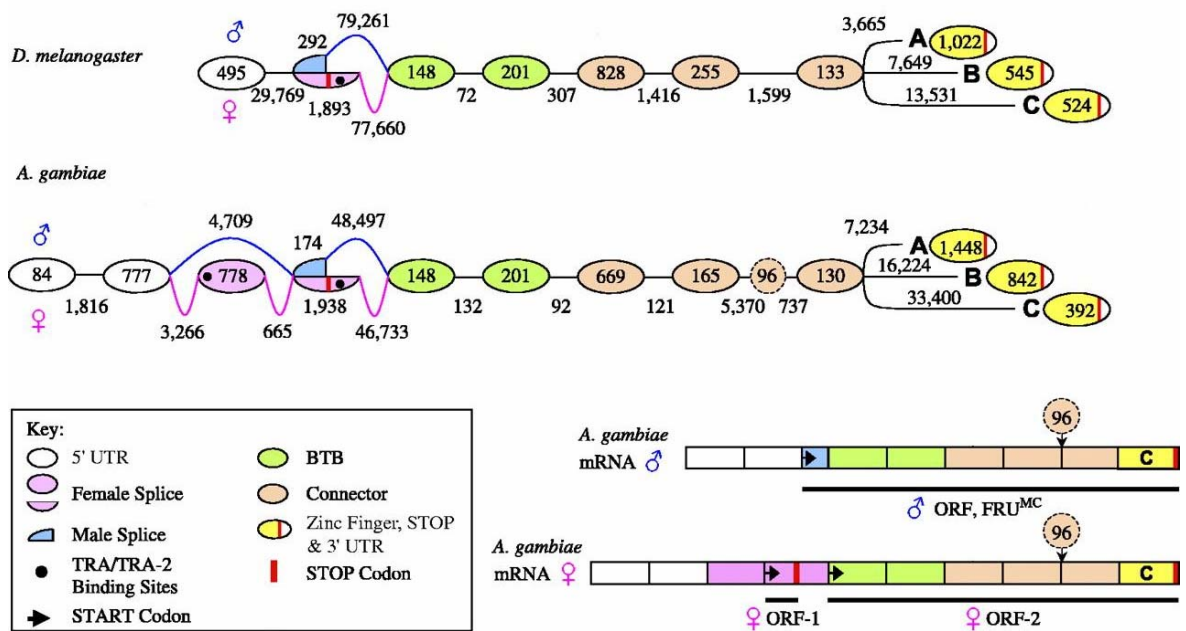


Figure 1.6 - Conservation of *fru* Locus Organisation in *Anopheles gambiae*.

Genomic organisation of *fru* locus is conserved in *D.melanogaster* and *A.gambiae*, but with 5' end variation. Ovals indicate exons and horizontal lines show introns processed out in both sexes. Curved blue and pink lines represent male- and female-specific splicing patterns respectively. Sizes of exons, and the distances between them, indicated in bp. Mosquito *fru* possesses two sex-non-specific 5' UTR exons and a third specific to females, whereas *Drosophila fru* contains only one. Alternative splicing of the Zn-F-encoding exons (A, B and C) is conserved in both species. Also shown are the mRNA ORFs generated from the distal promoter in *A.gambiae*. The sex-specific splicing pattern is homologous to that observed in *Drosophila*. The "96" represents an exon specific to *A. gambiae* that, when spliced, increases the connector region by 32 amino acids. (Modified from Gailey *et al.* 2006).

This conservation in *fru* is also reflected at a protein level. Conceptual translation of male-specific isoforms from both species revealed striking conservation of the BTB and the three C₂H₂ zinc finger domains (Figure 1.7). However, no such conservation is observed between the N-terminal extension and connector domains (Gailey *et al.* 2006).

The spatial and temporal expression of these Fru^M isoforms in *A. gambiae* mirrors that of *Drosophila* and has been shown to perform similar male-specific functions (Billeter *et al.* 2006b, Gailey *et al.* 2006). Remarkably, the partial rescue of *fru*^{MC} mutant male phenotypes using *fru(16)-gal4* and the *Drosophila* UAS-*fru*^{MC} transgene can also be achieved using a transgene expressing the corresponding *A. gambiae* isoform. Indeed the expression of the GAL4-responsive *A. gambiae* Fru^{MC} transgene (UAS-*Agfru*^{MC}) in the CNS of *Drosophila*

fru^{MC} males is sufficient to restore fertility and MOL formation is the vast majority of individuals. In fact, expression of UAS-*Agfru*^{MC} in males lacking all three Fru^M isoforms, or in females who do not otherwise develop this muscle, is also sufficient to induce MOL formation in the majority of cases (Billeter *et al.* 2006b, Gailey *et al.* 2006). Similarly, UAS-*Agfru*^{MC} is able to successfully rescue both clusters of serotonergic neurons in the abdominal ganglion of both *fru*^M and *fru*^{MC} mutant males. Additionally, expression UAS-*Agfru*^{MC} in wild-type females is sufficient to induce formation of a small number of ectopic serotonergic neurons at sites corresponding to those found in males (Billeter *et al.* 2006b).

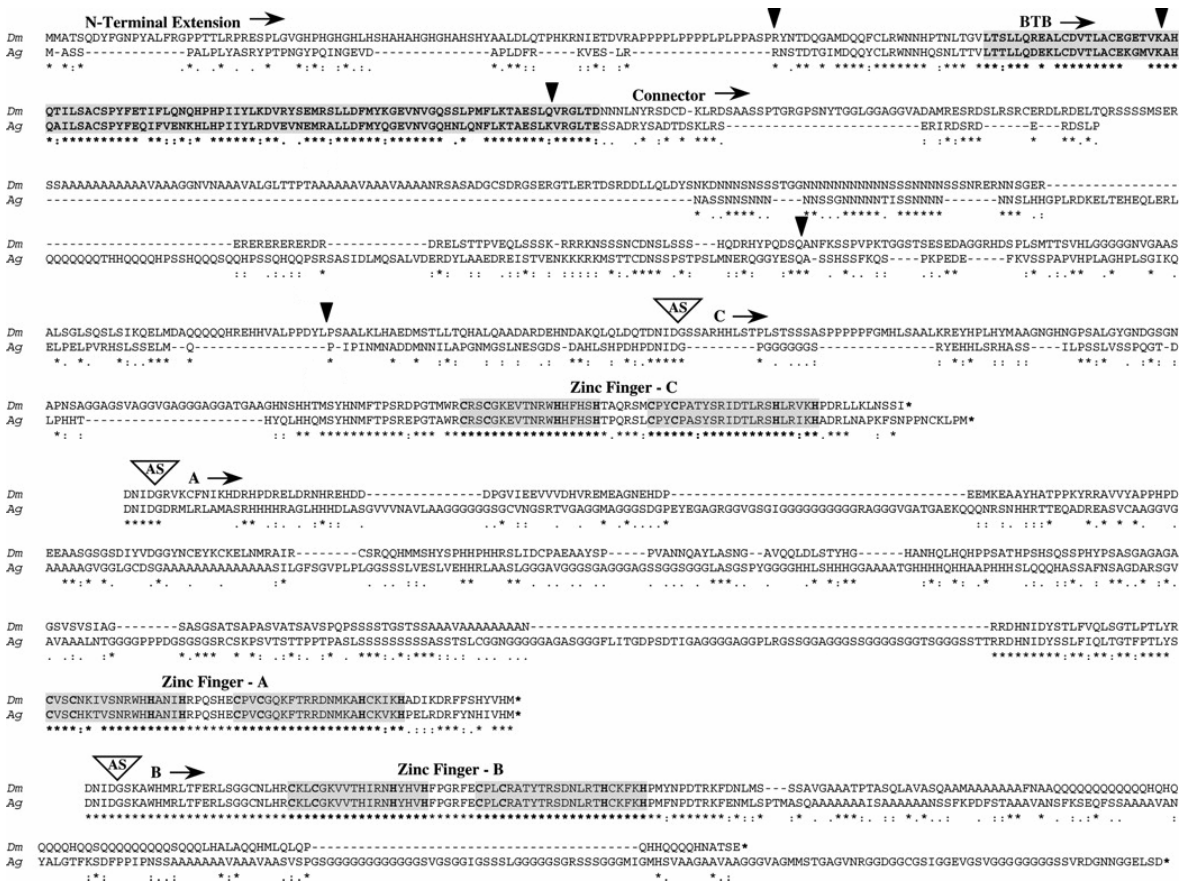


Figure 1.7 - Conservation of *fru* Protein Domains in *Anopheles gambiae*

ClustalW alignment of translated Fru^M cDNA sequences from *Anopheles gambiae* (Ag) and *Drosophila melanogaster* (Dm). The conserved BTB and alternative Zn-F domains are shaded. Both the N-terminal extension and connector domains were found to be divergent within the Fru^M proteins. Fru^M isoforms A-C are formed by alternative splicing of one of the Zn-F encoding exons at alternative splicing sites marked “AS”. Inverted black triangles indicate conserved splice sites in both species.

That ectopic expression of the *A. gambiae* Fru^{MC} isoform, as opposed to *fru(16)-gal4* driven expression of *Drosophila* Fru^{MA} or Fru^{MB} isoforms, is able to rescue

aspects of male-specific *fru* function in *Drosophila fru^{MC}* mutants highlights the highly-specific role played by the Fru^{MC} isoform in *Drosophila*. Generation of the *fru^{AC}* mutant was crucial in elucidating the role of this isoform. Isolation of type-A and -B isoform-specific mutants analogous to *fru^{AC}* would greatly enhance understanding of the contribution of each *fru* isoform to *Drosophila* development and behaviour. Within the past decade the technique of gene targeting by homologous recombination has become increasingly popular (Reviewed by Bi and Rong 2003). This is one way, in which to reliably introduce precise point mutations into, theoretically, any gene of interest within the *Drosophila* genome (Reviewed by Bi and Rong 2003).

1.10 Gene Targeting by Homologous Recombination

Gene targeting is a technique in which a cell's endogenous recombination machinery is used to integrate a piece of foreign DNA into its own genome at a locus homologous to the introduced exogenous DNA. Gene targeting was first pioneered in yeast (Hinnen *et al.* 1978) and, following the development of embryonic-derived stem cell technology (Evans and Kaufman 1981, Martin 1981), the technique was modified for use in mice (Mansour *et al.* 1988). In theory, gene targeting allows any endogenous gene of known sequence to be modified. Accordingly this technique is a powerful tool for modifying genes in organisms, like *Drosophila*, whose genomes have been fully sequenced.

The technique was adapted for use in *Drosophila* by generating linear donor DNA *in vivo*, removing the need for a compatible cell line (Rong and Golic 2000). There are two paths by which gene targeting by homologous recombination can be performed, designated as ends-out, or ends-in, targeting. Although the final outcome of each route is slightly different, the individual components used to achieve targeting in both techniques is largely the same. Both methods require a stretch of donor DNA containing homology to the target locus and also a modified region that is to be introduced at the target site. Additionally, a double-strand break (DSB) point within the donor construct is required to induce recombination, and a marker gene is necessary so that the integration events can be identified.

The relative positions of these components within the donor construct determine the path down which gene targeting will proceed. In ends-out targeting, the marker gene is placed between two regions of homology and double strand breakage of the donor construct DNA promotes the replacement of the target locus with modified homologous donor DNA (Figure 1.8). For ends-in the DSB point, but not the marker gene, is positioned within the stretch of homology and the entire donor construct integrates, resulting in a tandem duplication of the target locus (See Figure 1.9). In both cases a modified version of the target locus is integrated in addition to a marker gene to track the integration event.

P-element transformation is used to introduce the donor construct into the target germline (Rubin and Spradling 1983) and once a transformant line carrying the donor *P*-element is established, gene targeting can begin. Flies carrying the donor construct are mated with a strain carrying two transgenes under the control of heat-shock promoters which are induced to express two yeast derived enzymes. One of these, *FLP* recombinase, recognises 34bp *FLP* recognition target (FRT) sequences which are engineered into the donor construct (Golic and Lindquist 1989). When two FRTs are present in the same orientation, the intervening DNA can be excised as an extrachromosomal circle through the action of *FLP* recombinase. The other transgene, *I-SceI* endonuclease, also recognises a unique 18bp site in circularised donor construct, which it linearises by generating a DSB (Rong and Golic 2000). In both ends-in and ends-out strategies it is this DSB that promotes recombination at the target locus. The different applications and features of each approach are outlined below.

Ends-out

The ends-out technique is most commonly used if a null mutation, disrupting all gene products is desired. Frequently used in mice and yeast, initial attempts to perform ends-out targeting in *Drosophila* were unsuccessful (Bellaiche *et al.* 1999) and initial gene targeting in *Drosophila* was restricted to ends-in (Rong and Golic 2000, Rong and Golic 2001, Seum *et al.* 2002). However, by modifying the crossing scheme so that targeting occurred in females instead of males, it was shown that ends-out could be used to either repair or create mutations at the target locus (Gong and Golic 2003). This success achieved in females, and observations of higher targeting frequency in females (Rong and Golic 2000,

Rong *et al.* 2002), is believed to be due to the activity of the heat-shock promoters of the *I-SceI* and *FLP* transgenes being limited to only certain periods of spermatogenesis in males (Gong and Golic 2003). Additionally, *Drosophila* males do not undergo meiotic recombination.

Once the exogenous construct has been released from its insertion site and linearised, there are two basic methods by which ends-out modification of a target locus be executed. In using the target gene as the targeting homology in the donor construct, the endogenous target can be replaced by a modified version of the gene. Alternatively, if only flanking genomic regions are used as targeting homology, then a complete deletion of the gene can be achieved, replacing it with only the marker gene (reviewed by Bi and Rong 2003). However, the presence of this marker gene can interfere with analysis of the generated mutant phenotype. For example, ectopic expression of the *white* gene has been shown to induce high levels of male-male courtship (Zhang and Odenwald 1995). To insure against this type of interference, the marker gene may be flanked by direct *loxP* sites, to allow its removal by *I-CreI* site-specific recombinase post-targeting.

Ends-in

First implemented in *Drosophila* to rescue a mutation in the *yellow* gene (Rong and Golic 2000), ends-in targeting by homologous recombination was subsequently used to introduce mutations at several other loci (Rong and Golic 2001, Seum *et al.* 2002 , Rong *et al.* 2002). While ends-out targeting involves straightforward replacement of the target DNA, ends-in requires a second step to remove the resulting tandem duplication. Using *I-CreI* endonuclease, isolated from *Chlamydomonas reinhardtii* (Thompson *et al.* 1992), to recognise a unique cut site engineered into the donor construct, another DSB is induced between the two copies of the target DNA. In repairing the DSB, the cellular DNA repair machinery often reduces the duplication to a single copy and also removes the intervening marker gene. In a percentage of these reduction events, the introduced mutation(s) will be retained. Ends-in targeting has the advantage of allowing small point mutations to be introduced into endogenous genes. This facilitates the disruption of specific isoforms produced by a given gene, or the

introduction of amino acid substitutions into certain gene products, rather than a complete disruption of gene function.

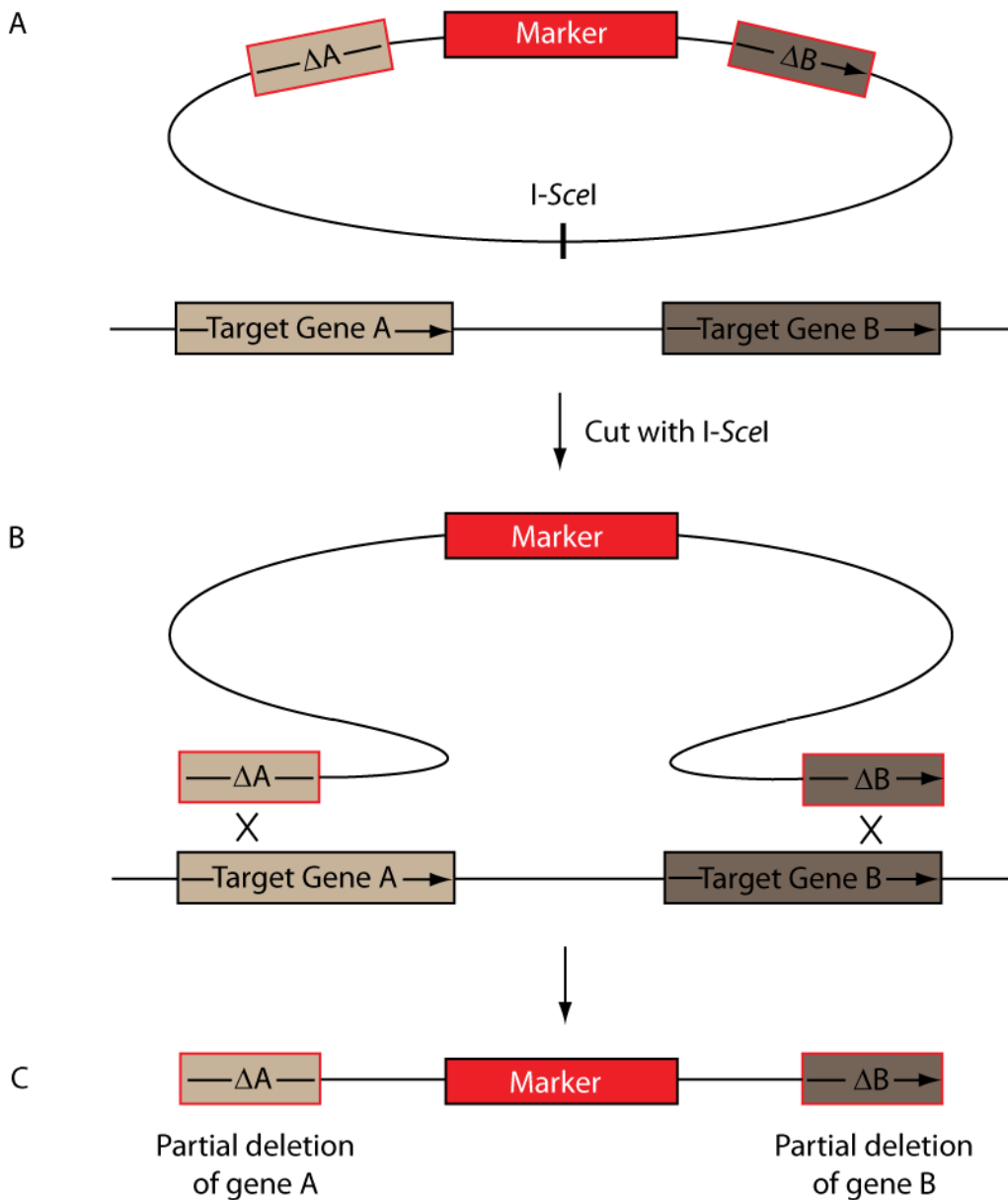


Figure 1.8 - Schematic Representation of Ends-out Targeting by Homologous Recombination. (A) Ends-out targeting of a locus containing two small genes. Circular targeting vector and target locus, corresponding to donor DNA stretch carried by targeting vector. The ends-out targeting vector contains a marker gene (red box) placed in between two regions of homology to target locus (ΔA and ΔB , boxes outlined in red). The vector also contains a I-SceI recognition site. (B) The targeting vector is cut using the site-specific I-SceI endonuclease. This produces a DSB and the targeting construct replaces the target locus by homologous recombination. (C) As the regions of homology are positioned at the extreme ends of the two genes, the genes are replaced by truncated versions and the intervening sequence is deleted.

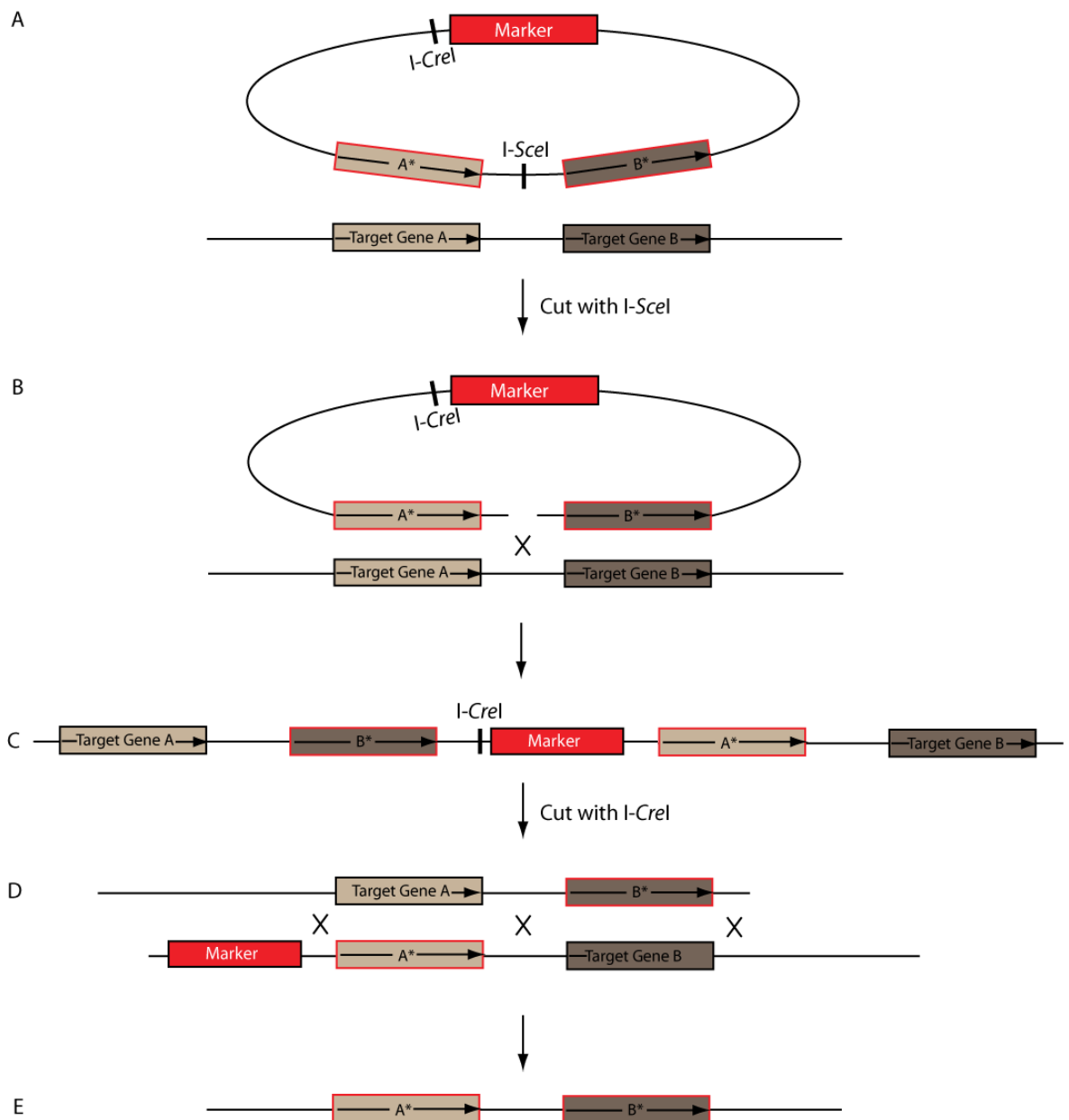


Figure 1.9 - Schematic Representation of Ends-in Targeting by Homologous Recombination. (A) Ends-in targeting of a locus containing two small genes. Circular targeting vector and target locus, corresponding to donor DNA stretch carried by targeting vector. The ends-in targeting vector contains an *I-SceI* recognition site placed in between two regions of modified homology to target locus, carrying small desired mutations (*A** and *B**, boxes outlined in red). The vector also contains a marker gene (red box) and an *I-CreI* recognition site. (B) The targeting vector is cut using the site-specific *I-SceI* endonuclease. This produces a DSB and the targeting construct is integrated at the target locus by homologous recombination. (C) A tandem duplication of the target region is produced, containing both wild-type and mutant copies of the genes of interest. (D) A DSB is produced using *I-CreI* endonuclease and the break is repaired by homologous recombination. This repair process removes the marker gene and reduces the targeted duplication to a single copy. In a percentage of resolution events the engineered mutations will be retained. Depending upon the positions of crossover points during repair, different mutant combinations can be obtained. (E) The resolved locus containing only a single copy of the target genes, each containing the engineered mutation.

1.11 Aims of this project

In light of the wealth of information gained from the study of the *fru*^{A^C} mutation, it was proposed that the main part of this project should focus upon the isolation of specific *fru* null-mutants for type-A and/or type-B isoforms. It was decided to use gene targeting by ends-in homologous recombination to introduce point mutations into the coding regions of the zinc-finger domain-encoding exons A and B.

To assess these mutants, isoform-specific antibodies were also to be generated. No antibody for Fru^B was currently available and, as such, the generation of this antibody took primary importance. Not only would this antibody enable identification of mutants lacking Fru^B expression, but it would also allow the spatial and temporal expression patterns of Fru^B to be characterised for the first time. Anti-Fru^A and anti-Fru^C were also to be generated, to replenish the existing, finite laboratory stock.

The final part of this study was to involve the characterisation of the mutants generated by gene targeting. Investigation was first to be performed using the generated antibodies, and then by screening the mutants for phenotypes associated with extant *fru* alleles such as loss of viability, anatomical defects and reduction in mating success.

2 Materials and Methods

2.1 Drosophila

2.1.1 Drosophila Stocks

A description of all the *Drosophila* stocks used in this work can be found in Table 2.1. A full description of all mutations and balancer chromosomes used can be found in FlyBase (<http://www.flybase.co.uk>).

Strain/Genotype	Description	Reference
<i>Canton-S (CS)</i>	Isogenic wild-type strain	Flybase
<i>y*,w*/Y,hs-hid;Sco,hs-I-Scel,hs-FLP/CyO</i>	P-element insertions on the Y and second chromosomes; used during first stage of gene targeting by homologous recombination to excise the donor P-element from genome and create a double-strand break in the extrachromosomal DNA prior to integration at the desired locus.	“M690” B.Dickson (unpub.*)
<i>y*,w*;ey-FLP</i>	P-element insertion on 2 nd chromosome, used during the first stage of gene targeting by homologous recombination.	“M699” B.Dickson (unpub.*)
<i>y*,w*,ey-FLP;Pin/CyO</i>	P-element insertion on X chromosome in a second chromosome balancer background, with <i>Pin</i> as a dominant marker for the other second chromosome; used during the first stage of gene targeting by homologous recombination.	“M700” B.Dickson (unpub.*)
<i>y*,w*,ey-FLP;+;Ly/TM3,Sb</i>	P-element insertion on X chromosome, in a third chromosome balancer background, with <i>Ly</i> a dominant marker for the other third chromosome; used during the first stage of gene targeting by homologous recombination.	“M701” B.Dickson (unpub.*)
<i>w*;+;hs-I-CreI,Sb</i>	P-element insertion on the third chromosome; used to create a double stranded break in the targeted locus to resolve the duplication created in the first stage of homologous recombination.	Rong <i>et al.</i> 2002

* - <http://www.imp.ac.at/research/barry-dickson/>

Strain/Genotype	Description	Reference
Df(3R) <i>fru</i> ^{Sat15} /TM3,Sb,e	Third Chromosome deficiency. Extends centromere-proximal from within <i>fru</i> ^{Sat} P-element insert. Removes entire <i>fru</i> common coding region, as well as several other genes.	Ito <i>et al.</i> 1996
Df(3R) <i>fru</i> ^{w24} /TM3,Sb,e	Third Chromosome deficiency breaking at <i>fru</i> locus. Breakpoints at 91A and 91D2-3	Ryner <i>et al.</i> 1996
Df(3R) <i>P141</i> /TM3,Sb,e	Third Chromosome deficiency breaking at the <i>fru</i> locus. Breakpoints at 90C2-D1 and 91B1-2	Gailey and Hall 1989
Df(3R) <i>Cha</i> ^{M5} /TM3,Sb,e	Third Chromosome deficiency breaking at the <i>fru</i> locus. Breakpoints at 91B3 and 91D1	Gailey and Hall 1989
<i>fru</i> ^{ΔC} /TM3,Sb,e	Micro-deletion in <i>fru</i> exon C	Billeter <i>et al.</i> 2006b
<i>w</i> ¹ ; <i>ap</i> ^{Xa} /CyO,+	Strain isogenised to wild-type Canton-S strain. Second chromosome balancer (<i>CyO</i>) and dominant marker (<i>ap</i> ^{Xa}).	Flybase, 2007
TM3,Sb,e/TM6B,Tb,Hu,e	Strain isogenised to Canton-S. Third chromosome balancers.	Flybase, 2007
<i>w</i> ¹	<i>w</i> mutant isogenised to Canton-S.	Billeter, 2003
<i>w</i> ¹¹¹⁸	<i>w</i> mutant used for microinjections	Flybase, 2007

Table 2.1 - *Drosophila* Stocks used in this study. “*w*” or “*y*” indicates that the precise allele of *w* or *y* is unknown.

2.1.2 Rearing Conditions

Drosophila stocks were raised on ‘Glasgow’ medium. Stocks were maintained at room temperature in the laboratory or at 18°C. For genetic crosses and experiments, the flies were mated and their progeny raised either in an incubator or a designated fly room at 25°C with 12:12 hour light-dark cycles.

Glasgow Medium: 10 g agar, 15 g sucrose, 30 g glucose, 35 g dried yeast, 15 g maize meal, 10 g wheat germ, 30 g treacle, and 10 g soy flour per litre of distilled water.

Drosophila adult females were allowed to lay eggs on apple juice agar plates for approximately 16 h, after which the embryos were collected from the plates.

Apple Juice Agar: 20 g agar, 26 g sucrose, 52 g glucose, 7 g dried yeast, and 9% (v/v) apple juice (The Organic Juice Company) per litre of distilled water.

For these media, distilled water was heated to boiling to dissolve the agar. The remaining reagents were then added and allowed to dissolve. The media was allowed to cool to 60°C before being supplemented with Nipagin M (4-hydroxybenzoic acid methylester, 10% (w/v) in absolute ethanol) to inhibit fungal growth.

2.1.3 *Drosophila* Microinjection

2.1.3.1 DNA Solution

Plasmids for microinjection were purified from *E. coli* DH5 α , using the Plasmid Maxi Kit (QIAGEN), following the standard protocol. The helper plasmid pUCHS π Δ 2-3 (Laski *et al.* 1986) was co-injected with the non-autonomous *P*-element transformation vector containing the transgene to provide a source of transposase (ratio of helper:non-autonomous *P*-element = 1:5). The mixture was then injected at an approximate concentration of 100 μ M/ml.

2.1.3.2 Microinjection

Drosophila embryos of genotype w^{1118} were microinjected with the DNA solution described above using standard microinjection procedures by Genetic Services Inc. (Cambridge, MA).

2.1.3.3 Selecting *P*-element Transformants

Larvae were returned by post approximately 48 hr after injection. They were allowed to develop into adults in a food vial at 25°C. Single adults were collected after eclosion and mated with w^{1118} flies of the opposite sex. The progeny of these crosses were screened for the presence of red eyes, indicating *P*-element integration. The *P*-element used in this study contained the *mini-white* (*mw*) gene, which confers red eye colour to flies when in a w^{1118} genetic background.

2.1.3.4 Determination of Chromosomal Insertion

P-element lines were crossed to different balancer chromosomes with dominant genetic markers to determine the chromosome of insertion. Since all the *P*-elements used in this work contain the *mW* gene as a marker, all genetic crosses were carried out using flies with balancer chromosomes in a *w* background. The *P*-elements were followed using the eye colour conferred by the presence of the *mW* transgene.

To determine whether an insertion occurred on the second chromosome, flies heterozygous for the presence of the *P*-element were crossed to $w^h;ap^{Xa}/CyO$. The $w^h;+/CyO$ progeny with orange eyes were then backcrossed to $w^h;ap^{Xa}/CyO$. Insertion on the second chromosome was determined by the absence of $w^h;ap^{Xa}/CyO$ progeny with orange eyes.

Insertions on the third chromosome were determined similarly, but this time by crossing the *P*-element line to $w^{118};+;TM3,Sb,e/TM6B,Tb,Hu,e$. For insertion on the first chromosome (X), males carrying the *P*-element insertion were crossed to w^h females. Integration on the first chromosome was determined by the absence of male progeny with orange eyes (inherited the *mW* marker). After excluding insertions on the first, second and third chromosome, the insertion was determined to have occurred on the fourth chromosome. No insertions were found on the Y chromosome.

Once the chromosome bearing the *P*-element was determined, the insert was balanced with the appropriate chromosomal balancer. Homozygous viable lines were kept both as homozygous stocks and as heterozygotes with an appropriate balancer chromosome. Lethal insertion lines were kept as heterozygotes with the appropriate balancer chromosome.

2.1.3.5 Outcrossing of Gene Targeting Mutants into a *Canton-S* Background

All generated gene targeting mutants were outcrossed to isogenise their genetic background with that of a *Canton-S* wild type strain. White-eyed virgin females of the *Canton-S* (w^h) strain were collected and crossed to red-eyed males of the line of interest. The *mini-white* marker was used to follow the transgene

throughout the outcrossing procedure. At the F1 stage, one orange-eyed virgin female was crossed to three *Canton-S* (w^h) males. At the F2 stage, one orange-eyed virgin female was crossed again to *Canton-S* (w^h) males. This process was repeated for at least five generations. After outcrossing, a single virgin female was collected and crossed to three sibling males, and the homozygous progeny from this cross were used to generate the final outcrossed stock.

2.1.4 Dissection Techniques

2.1.4.1 Whole Mount Dissection of the Adult CNS

Flies were aged for 5 days before dissecting, except in the case of pharate adults. After light CO₂-anaesthesia, flies were immersed in ethanol for 5 s. They were then transferred into phosphate-buffered saline (PBS; 137 mM NaCl, 2.7 mM KCl, 10 mM Na₂HPO₄, 2 mM KH₂PO₄) in a dissecting dish lined with silicon gel (Sylgard, Dow-Corning). Their wings and legs were removed using dissection forceps. The brain was isolated by first removing the proboscis, and then by tearing the head capsule in half by pulling at the lower corner of each eye. The brain was left attached to the rest of the body. The abdomen was then severed and the legs were cut removed using dissection scissors. The forceps were used to cut the thoracic cuticle transversely from anterior to posterior above the base of the legs. The oesophagus was removed to reveal the dorsal part of the ventral nerve cord (VNC), and the VNC gently lifted from the thorax.

2.1.4.2 Whole Mount Pupal CNS

Wandering 3rd instar larvae make their way to the side of the vial, where they eventually evert their spiracles and stop moving (Bainbridge and Bownes, 1981). These pre-pupae were collected and sexed by the size of their gonads (Ashburner, 1989).

Individuals were then transferred to a 50 mm Petri dish humidified with a wet tissue, and the pupae were aged at 25°C for 48 hours. Pupa at the desired stage were transferred to PBS for dissection. The operculum was first removed using forceps. The rest of the pupal case was then gently peeled off to reveal the pupa. A slit was made with the forceps along the dorsal part of the thorax, extending to just below the head. A Gilson P20 micropipette fitted with a yellow

tip was used to jet 20 µl of PBS in and out of this opening, which cleared the inside of the thorax and allowed the visualization of the pupal CNS. The abdomen was then severed using forceps. Eventually, the PBS current dislodged the CNS from the head capsule, and the whole CNS was isolated.

2.1.4.3 Whole Mount Larval CNS

Wandering 3rd instar larvae were gently selected with metal tongs and transferred to PBS. Larvae were sexed according to the size of their gonads (Ashburner, 1989). Forceps were then used to grab the mid-part of the body. The forceps were pulled apart, and the brain lifted out of the remains.

2.1.4.4 Embryo Collection

Approximately 50 females and 25 males were pooled in an inverted plastic beaker and allowed to lay eggs on a plastic Petri dish containing apple juice agar medium with a dab of yeast paste (dried yeast in distilled water, heat inactivated) covering the open bottom of the beaker. Flies were allowed to lay overnight at 25°C on the plate, and the plate was removed the following morning for collection. Embryos were detached from the egg laying plate using a paintbrush and a stream of distilled water, and collected in a fine-mesh sieve.

2.2 Visualisation Techniques

2.2.1 Immunofluorescence

Samples were dissected in PBS and fixed in 2% paraformaldehyde (in PBS) for 30 min on ice. They were washed three times in PBS for 15 min each, three times in PBT (1xPBS, 0.4 % Triton X-100), and incubated for 1 hour in PTN (PBT, 5% normal goat serum (Scottish Diagnostics and Molecular Probes)). The specimens were incubated at 4°C overnight in PTN containing the primary antibody at the appropriate concentration (see table 2.2). They were washed four times in PBT for 1 hour each and incubated in PTN containing the appropriate species-specific fluor-conjugated secondary antibody (see table 2.3) either for 4 hours at room temperature or overnight at 4°C. They were washed four times in PBT for 1 hour and three times in PBS for 30 min. Stained specimens were mounted in VectaShield (Vector Lab) on Polylysine treated microscope slides (BDH).

Embryos were collected as described previously in this section, and dechorionated by placing the sieve into a 50% solution of bleach in distilled water for exactly 3 min, after which the embryos were washed thoroughly with distilled water to remove all traces of bleach. The embryos were then transferred to 5 ml heptane in a glass container using a paintbrush, and 5 ml of 4% paraformaldehyde (in PBS) was added, and the solution was shaken vigorously. The embryos were fixed for 10 min at room temperature. After fixation, the aqueous bottom layer was completely removed, and a 5 ml solution of 95% methanol/5% EGTA (ethylene glycol tetra-acetic acid, pH 8.0) was added to the glass container, and swirled gently. De-vitellinized embryos sank to the bottom of the container. Embryos were then transferred to a clean 1.5 ml Eppendorf tube containing 1.0 ml of PBS. After the embryos had fallen to the bottom of the tube, most of the PBS was removed and several drops of PAT (PBS, 1% Triton-X, 0.1% bovine serum albumin (BSA)) were added. The embryos were then washed an additional three times with PAT, followed by two washes in PBS. To mount, the PBS was removed and VectaShield (Vector Lab) was added, and the embryos were transferred to a polylysine slide for viewing.

Antibody	Description	Dilution	Source/Reference
Anti-Fru^M	Rabbit, polyclonal against male-specific 101 aa domain of Fru ^M	1:300* or 1:400*	Billeter <i>et al.</i> , 2006b
Anti-Fru^A	Rat, polyclonal against zinc finger domain of Fru ^A	1:100	Song et al. 2002
Anti-Fru^B	Rat, polyclonal against zinc finger domain of Fru ^B	1:200	This study
Anti-Fru^C	Rat, polyclonal against zinc finger domain of Fru ^C	1:200	This study
Anti-Repo	Mouse, monoclonal against glial cell marker Repo	1:50	Developmental Studies Hybridoma Bank, University of Iowa
Anti-5HT	Rabbit, polyclonal against 5-Hydroxytryptamine (serotonin)	1:2000	Sigma

Table 2.2 - Primary antibodies used in this study. “*” - 1:300 dilution used for pupal CNS, 1:400 dilution used for adult CNS.

Antibody	Description	Dilution	Source/Reference
Anti-rat IgG-Alexa Fluor 488	Goat, polyclonal against rat IgG, conjugated to Alexa Fluor 488.	1:300	Molecular Probes, Inc.
Anti-rabbit IgG-Alexa Fluor 546	Goat, polyclonal against rabbit IgG, conjugated to Alexa Fluor 546.	1:300	Molecular Probes, Inc.
Anti-mouse IgG-Alexa Fluor 546	Goat, polyclonal against mouse IgG, conjugated to Alexa Fluor 546.	1:300	Molecular Probes, Inc.

Table 2.3 - Secondary antibodies used in this study.

IgG stands for Immunoglobulin Gamma.

2.2.2 Confocal Microscopy

Stained whole mounts were examined with a Zeiss LSM 510 Meta confocal microscope equipped with x10, x20, x40 (oil immersion), and x63 (oil immersion) objectives. The Ar/HeNe lasers of the Zeiss can excite fluorochromes with the following wavelengths in the visible spectrum: 458 nm, 476 nm, 488 nm, 514 nm, 543 nm and 633 nm. Alexa fluor-488-conjugated secondary antibodies were excited with the 488 nm line, and emit in the green spectrum. TRITC-conjugated phalloidin and the Alexa Fluor 546-conjugated secondary antibodies were excited with 543 nm line, and emit in the red spectrum.

For double-labelling, the 488 nm and 543 nm lines were used sequentially for each optical section through the sample to excite both fluors individually and avoid bleed-through. Stacks of optical sections were generated at 1.7 μm spacing.

2.2.3 Image Processing

After acquisition of confocal images, the images files were opened with Ziess LSM software and transformed into "Maximum-Z-Projections" which superimpose serial optical sections into a single image. The brightness and contrast of images were altered in Photoshop (Adobe).

2.3 Bacterial Protocols

2.3.1 Strains and Plasmids

The following *E.coli* bacterial strains were used in this thesis.

Strain	Genotype
DH5 α (Hanahan 1983)	F ⁻ , ϕ 80d <i>lacZ</i> Δ M15 Δ (<i>lacZYA-argF</i>)U169 <i>deoR recA1 endA1 hsdR17</i> (r _k ⁻ , m _k ⁺) <i>phoA supE44</i> λ <i>thi-1 gyrA96 relA1</i>
BL21-CodonPlus (DE3) RP (Stratagene)	B B F <i>ompT hsdS</i> (r _B ⁻ m _B ⁻) <i>dcm</i> ⁺ Tet ^r <i>gal</i> λ (DE3) <i>endA Hte</i> [<i>argU proL Cam</i> ^r]
TB1 (New England Biolabs)	F ⁻ <i>ara</i> Δ (<i>lac-proAB</i>) [ϕ 80d <i>lac</i> Δ (<i>lacZ</i>)M15] <i>rpsL</i> (Str ^R) <i>thi hsdR</i> = JM83 <i>hsdR</i>

Table 2.4 - Bacterial Strains.

The plasmids used in this study are listed below.

Plasmid	Size (bp)	Description	Antibiotic Resistance	Source or Reference
pGEX 6P-1	4,984	Expression vector to express GST fusions in bacteria.	Ampicillin	Invitrogen
PCR [®] 2.1-TOPO [®]	3,900	Sub-cloning vector for cloning PCR products using topoisomerase.	Ampicillin	Invitrogen
pTV2	8,163	Vector for gene targeting by homologous recombination. Contains multiple cloning sites, <i>P</i> -element transposition sequences, a mini-white marker gene and I- <i>CreI</i> recognition site.	Ampicillin	Rong <i>et al.</i> 2002
pED7	8,090	Vector for gene targeting by homologous recombination. Contains multiple cloning sites, <i>P</i> -element transposition sequences, a mini-white marker gene and I- <i>CreI</i> recognition site.	Ampicillin	Gift from B.Dickson, unpub.
pGEM-T Easy	3,016	Cloning Vector with 5' T overhangs	Ampicillin	Promega

Table 2.5 - Table of plasmids.

2.3.2 Culture Media

SOC: 2% tryptone, 0.5% yeast extract, 10 mM NaCl, 2.5 mM KCl, 10 mM MgCl₂, 10 mM MgSO₄, 20 mM glucose, pH 7.0

L-Broth (LB): 10 g Bacto-tryptone (Difco), 5 g yeast extract (Difco), and 10 g NaCl per litre of water; pH was adjusted to 7.0 with NaOH.

L-Agar: As above with the addition of Bacto-agar (Difco) to 1.5%.

All culture media were sterilised by autoclaving at 120°C for 15 min.

2.3.3 Antibiotics

When necessary, antibiotics were added to culture media for plasmid selection. Antibiotics were added to broth at room temperature and to molten agar at 50°C. Final concentrations of antibiotic used were as follows: 100 µg/ml for ampicillin and 20 µg/ml for chloramphenicol. All antibiotics were purchased from Sigma.

2.3.4 Transformations

2.3.4.1 Preparing Competent *E. coli* Using Chemical Treatment

The Hanahan method (Hanahan *et al.* 1995) was used for the generation and long-term storage of high efficiency competent DH5α bacteria. Bacteria transformed for protein expression were one of two strains. BL21-CodonPlus (DE3) RP for use with the GST-fusion proteins and TB1 for expression of MBP-fusion proteins (See section 2.4). These cells were prepared fresh for each transformation. A 25ml culture of BL21 cells was initiated from an overnight culture and grown to OD600 = 0.4. The cells were harvested by centrifugation at 3,000g at 4°C and resuspended in 25ml 0.1M CaCl₂. The cells were centrifuged again at 3,000g and resuspended in 5ml 0.1M CaCl₂. The fresh competent cells were then kept on ice until use.

The general protocol for bacterial transformation was as follows. 3µl of a ligation mix or 0.5µl of purified plasmid was mixed with 100µl of competent cells and left for 30 minutes. The cells were then heat-shocked at 42°C for 1 minute and cooled on ice for 2 minutes. 700µl of LB broth were added and the

cells were allowed to recover at 37°C for one hour. The cells were then harvested by centrifugation at 6,000g, resuspended in a small volume of LB and spread on LB plates containing an appropriate antibiotic.

2.3.5 Isolation of Bacterial Artificial Chromosome (BAC) and Plasmid DNA from E. coli

2.3.5.1 Small-Scale Isolation of BAC and Plasmid DNA by Alkaline Lysis

DNA was purified from 5-10 ml of overnight culture grown in L-Broth at 37°C with shaking in the presence of the appropriate concentration and type of antibiotic. BAC and plasmid DNA were both isolated using the alkaline lysis method (Sambrook and Russell, 2001). Plasmid DNA for sequencing and cloning was isolated using the QIAprep spin miniprep kit (QIAGEN) according to the manufacturer's instructions.

2.3.5.2 Large-Scale Isolation of Ultra-Pure BAC and Plasmid DNA

Large-scale preparations of BAC and plasmid DNA were performed using the Maxiprep kit (QIAGEN) according to the manufacturer's instructions.

2.4 Generation of Antibodies

2.4.1 GST Purification

PCR products representing the chosen antigenic fragments of each protein were cloned in frame into the pGEX-6P-1 vector (Amersham). The pGEX constructs were transformed into BL21 CodonPlus (DE3) RT. Bacteria were grown from overnight cultures in 1.2l of LB with ampicillin and chloramphenicol to OD₆₀₀=0.5. The temperature of the incubator was lowered to 30°C and the bacteria were induced with 0.5mM IPTG for 3h. The cells were harvested by centrifugation at 4,000g for 10min at 4°C. The cells were resuspended in 50ml PBS + 1mM PMSF + 0.3% mammalian protease inhibitor cocktail (Sigma). The concentrated cells were burst by sonicating (3x30s bursts, 27% amplitude, 4°C [VibraCell, Sonics and Materials, Newton, CT, USA]). The lysed cells were centrifuged at 12,000g for 10min at 4°C to separate the soluble and insoluble

phase. GST-fusion proteins were purified from the soluble phase using GSTrap FF 1ml Sepharose columns or 1ml of Glutathione Sepharose 4B (Amersham) following the manufacturer's protocol.

2.4.2 pMAL Purification

PCR products representing the chosen antigenic fragments of each protein were cloned in frame into the pMAL-c2 vector downstream from the MalE gene, which encodes maltose binding protein (MBP) (New England Biolabs). The pMAL constructs were transformed into TB1 cells. Bacteria were grown from overnight cultures in 1l of LB with glucose and ampicillin to OD₆₀₀=0.5. Glucose is necessary to repress *E.coli* maltose genes, one of which is amylase which can degrade the amylose affinity resin used later. IPTG was added to a final concentration of 0.3mM and cells were incubated for 3h. The cells were harvested centrifugation at 4,000g for 20min and cells were resuspended in 50ml column buffer (20mM Tris-HCl, 200mM NaCl, 1mM EDTA, 1mM PMSF + 0.3% mammalian protease inhibitor cocktail (Sigma)). The cells were then frozen overnight at 20°C. The concentrated cells were broken open by sonicating in 15s bursts. Between each burst the release of protein was assessed using a Bradford assay. 10µl of sonicate were added to 1.5ml Bradford reagent and mixed. This process was repeated until the released protein reached a maximum, indicated by the colour of the solution (usually a total sonication time of around 2 min). The lysed cells were centrifuged at 9,000g for 30min at 4°C to separate the soluble and insoluble phase. MBP-fusion proteins were purified from the soluble phase using an amylose resin column (New England Biolabs) following the manufacturer's protocol.

2.4.3 Antibody Production

Purified GST fusion proteins were sent to Diagnostics Scotland (Penicuik, Lothian) for injection into rat. Returned sera were aliquotted and stored at -20°C.

2.5 General Molecular Biology Protocols

2.5.1 Restriction Digestion of DNA

DNA was digested in the appropriate buffer for the enzyme(s) according to manufacturer recommendations (New England Biolabs). 2 units of enzyme were used per μg of DNA to ensure complete restriction of DNA. Digests were carried out at 37°C for 4 hours.

2.5.2 DNA Gel Electrophoresis

DNA fragments were resolved on agarose (Boehringer Mannheim) gels. The DNA solution was mixed with loading buffer and loaded into agarose gels containing 1 X TAE (40 mM Tris/AcOH (pH 8.2), 20 mM NaOAc, 1 mM EDTA). A range of agarose concentrations (0.5%-2.0%) were used depending on the size of the fragments to be resolved (Sambrook and Russell, 2001). The gels were run from 1 hour to overnight at voltages ranging from 25 mV to 120 mV. DNA size markers were the 100 bp or the 1 kb ladders (New England Biolabs).

2.5.3 Visualization and Photography of Gels

DNA was visualized by UV-induced fluorescence on either a short wave (254 nm) or long wave (365 nm) transilluminator after staining the agarose gels in an ethidium bromide (EtBr) solution (0.5 $\mu\text{g}/\text{ml}$) in a shaker tray for 40 min. Gels were photographed using a Polaroid camera loaded with Polaroid 667 film and fitted with a Kodak Wratten filter No. 23A.

2.5.4 Gel Extraction of DNA Fragments

Size-selected DNA fragments were excised from agarose gels using a clean razor blade, on the long wave (365 nm) UV transilluminator. Purification of the DNA fragment from agarose, salt and enzymes was carried out with the QIAquick gel extraction kit (QIAGEN), or the QIAEXII Gel Extraction Kit (for fragments >10 kb)(QIAGEN) following manufacturer's instructions.

2.5.5 Purification of Genomic DNA

Fly genomic DNA (gDNA) was prepared by a modification to the procedure described in Hamilton and Zinn (1994). 0.04 g of flies (approx. 30 flies) were frozen on dry ice and homogenized with a micro-pestle in 200 μ l of grinding buffer (5% sucrose, 80 mM NaCl, 100 mM Tris, pH 8.5, 0.5% SDS, 50 mM EDTA). The homogenate was then incubated at 70°C for 30 min, supplemented with 35 μ l of 8 M KOAc, transferred to ice for 30 min and centrifuged at 12000 g for 10 min at 4°C. The supernatant was then transferred into a clean tube. Excess protein was extracted from the solution using a phenol:chloroform:isoamyl alcohol extraction (25:24:1; Sigma) (as described in Sambrook and Russell, 2001). The DNA was then precipitated by adding 150 μ l of isopropanol to the supernatant and allowed to stand at room temperature for 5 min. The genomic DNA was pelleted by centrifugation at 12000 g for 15 min at 4°C. The pellet was rinsed with 500 μ l of 70% EtOH and allowed to dry at room temperature. The pellet of genomic DNA was resuspended in 200 μ l of TE (10 mM Tris-HCl, 1 mM EDTA, pH 8.0) with 0.1 mg/ml of RNase A (Sigma).

2.5.6 Quantification of Nucleic Acids

The amount of DNA in a sample was estimated by taking Optical Density (O.D.) measurement at a wavelength of 260 nm using a spectrophotometer. An O.D.₂₆₀=1 corresponded to ~50 μ g/ml of double stranded DNA.

Estimation of DNA concentration in an agarose gel was also done by comparing a given band with the 3 kb band of the 1 kb ladder (New England Biolabs), which contains approximately 125 ng of DNA when ladder is prepared according to manufacturer's instructions.

2.5.7 Polymerase Chain Reaction (PCR)

Taq polymerase (New England Biolabs) was used for diagnostic PCR, and Phusion high fidelity DNA polymerase (New England Biolabs) was used for applications requiring high fidelity amplification. The PCR mix was set according to manufacturer's instruction. For PCR using *Taq* polymerase (New England Biolabs) the conditions were the following: initial denaturation- 5 min at 95°C;

denaturation- 50 sec at 94°C, annealing- 40 sec 40-60°C, extension- 1 min at 72°C, where denaturation through extension was repeated for 30-35 cycles, followed by a final extension at 72°C for 5 min. For high fidelity PCR with Phusion DNA Polymerase (New England Biolabs) the conditions were the following: initial denaturation step- 30 sec at 98°C; denaturation- 15 sec at 98°C, annealing- 30 sec at 40-60°C, extension- 15 sec per kb at 72°C, where denaturation through extension was repeated for 30-35 cycles, followed by a final extension at 72°C for 10 min.

2.5.7.1 Primer Sequences

The primers and oligonucleotides used in this work are shown in Table 2.6 overleaf.

2.5.7.2 Primer Design

Primers used in this study were designed with the help of MacVector 7.2.2 (Oxford Molecular) software purchased from Invitrogen. The T_m of primers was calculated using MacVector software. The primers were ordered from Sigma-Aldrich (Dorset, UK). A description of the primers used for PCR and sequencing can be found in Table 2.6.

2.5.7.3 Cloning PCR Products

PCR products were cloned into vector pCR®2.1-TOPO® using the TOPO-TA cloning kit (Invitrogen) following manufacturer's instructions.

2.5.8 DNA Sequencing

Automated sequencing was carried out by the Geneservice Inc. (Cambridge, UK). Geneservice uses Applied Biosystems 3730 DNA Analyzer sequencers, which detect DNA molecules labelled with fluorescent dyes and automatically analyzes data using Sun ultra10 sparcstations for sequence analysis. Primers used for sequencing can be found in Table 2.6.

Plasmid	Sequence	Tm (°C)
AbZnA-f-EcoRI	CCGGAATTCCGCTGCAAGTGTTTTAACATTAAGC	70.0
AbZnA-r-XhoI	CCGCTCGAGGTTTGCTTGATTCTTGGTACTTAG	68.6
ZnF B-for\EcoRI	GGGGGAATTCTCCAAGGCCTGGCACATGCGG	66.6
ZnF B-rev\XhoI	CCGCTCGAGGACGCCAGGCGCCGTAGTTCC	79.2
AbZnC-f-EcoRI	CCGGAATTCAGCAGCGCCCCGCCACCACCTG	80.5
AbZnC-r-XhoI	GCCGCTCGAGCGGTGATGGGCTGCACTTGGGC	82.6
Not_3	GCGGCCGCTGGTGAAAAGTTAGCATTAGC	69.6
Sall_rev3.1	GTCGACGGTTCGTGCTTAATGTAAAAAC	64.4
Sall_for3	GTCGACCGGATCGGGAAGTGGATC	65.3
HindIII_3	AAGCTTCTCTGGCCAAACGGCTTG	63.5
MluI_3	ACGCGTTTGGACGCTCTGCTGATCTAT	65.6
HR_ZnFB_NheI_f2	GGGGGGCTAGCTTTCGAGCGCCTCT	78.6
NheI_rev3	GCTAGCGCATGTGCCAGGC	59.0
Avall_1	GGCACAAATGTCTGACAGG	48.2
HR4.3seq	TGCGAGGAGGAATCCAATG	53.2
KPN_three	GGTACCGCATTTCGTGGGCTTGCTTC	67.6
new_I-SceI_sense	AGCTTTAGGGATAACAGGGTAATA	59.8
new_I-SceI_antisense	AATCCCTATTGTCCATTATGCGC	69.1
A_probe_for	CATTCACACCCACCGTACAC	50.7
B_probe_for	TCAAATCGAATCGAAACG	46.6
B_probe_rev	CTTTTGTGTAGTTCCTAGTGC	45.8
dREPCRAfor	GCCAAGATTTGATCCCTATTCC	53.4
dREPCRArev	GGTGGGTGTTTTGCCAAAG	52.7
REPCRB2for	TTCCCATCCCGTTCAAAGTG	56.2
REPCRB2rev	GCCGACGAGGACATTAGG	50.2
HRFRT1R1	CAACTGAAGGCGGACATTG	51.3
HR_start	TATAATACATCCCATTTTCAT	41.2
HR1.2seq	GCGTTCAAGAAAAGCGAG	48.4
HR1.3seq	TTCCAAACCCCGAGACAAG	52.3
HR1.4seq	CGATACTCTCCACACCATC	49.0
HR1.5seq	CACACACTCAAATACACTCGC	48.0
HR1.6seq	TGAAAAATCCCGCACCCAG	55.6
HR1.7seq	TGATTTCCAGGCTTCGCAG	53.7
HR1.8seq	TAGACACCATTACACCCACCG	56.9
HR2.2seq	ATCAGCCACACATCCCAGTC	51.8
HR2.3seq	AATCCAGAGTGAGGAGCCAACAGC	56.9
HR3.2seq	CCAAAAACAATCGTCCCC	49.9
HR3.3seq	GGGGTGTGAATGAAATGTG	49.9
HR4.2seq	GCCCTTCAACTTCTATGCC	48.8
HR4.4seq	TTAGGAGCAAACACCGAAC	47.6
HR4.5seq	GCCGAGTTTGTATCCAGTC	48.8
HR4.55seq	AGCAGGAGAGTTGAGCGTTG	52.1
HR4.6seq	CAAAAACACACACAGCC	46.3

Table 2.6 - Table of Primers.

2.5.9 Southern Blotting of Fly Genomic DNA

30 μ g of gDNA was digested with an appropriate restriction enzyme for 8 hours. The DNA was then separated by electrophoresis on a 0.8% TAE gel overnight at 25V. The DNA was then visualised by staining with EtBr to check that the DNA had been electrophoresed correctly. The gel was then placed in denaturation solution for 30 minutes, and subsequently washed in neutralisation solution. The Southern blot was set up to transfer to a Hybond N+ nylon membrane (Amersham, Buckinghamshire). The DNA was then crosslinked to the membrane in a Stratelinker (Stratagene) using the auto-crosslink feature. The membrane was pre-hybridised overnight in hybridisation buffer (1% SDS, 6xSSC, 5x Denhardt's, 50mM Phosphate buffer (pH 6.8), 100 μ g/ml sheared salmon sperm DNA) at 65 °C.

The probe was generated using Prime-it II Kit (Stratagene) following the manufacturer's instructions. The probes were purified using Micro Bio-Spin P-30 columns, following the manufacturer's instructions. The activity of the probe was determined using a liquid scintillation counter. The probe was applied to the membrane with fresh hybridisation buffer (10⁶ cpm/ml of hybridisation solution). Hybridisation was carried out for a minimum of 16 hours. After hybridisation, the filters were washed in 2X SSC for 15 min, 1 X SSC, 0.1% SDS for 10 min and then a final wash of 0.1 X SSC, 0.1% SDS 5 min. Prior to autoradiography, filters were blotted dry and covered in Saran Wrap™. Autoradiography of probed filters was carried out at -70°C in a cassette with an intensifying screen and exposed to Konica Medical film, for as long as required. Films were developed using a Kodak X-Omat film processor.

3 Generation of Isoform-specific Antibodies

3.1 Introduction

As it was the intention to generate mutants for particular *fru* isoforms, a reliable method was required to confirm that the targeted isoforms had been specifically affected in these mutants. The engineered mutations could be detected molecularly, but it would also be necessary to ensure that the presence or absence of proteins specific to the variant isoforms could be confirmed. Immunohistochemistry using isoform-specific *fru* antibodies is one way in which not only the presence or absence of such isoforms may be determined but also the level of expression in previously described neuronal clusters (Lee *et al.* 2000, Song *et al.* 2002, Billeter *et al.* 2006b).

In this chapter the generation of antibodies to detect specific Zn-F containing domains of *fru* proteins is described. This entails how the antigens to raise these antibodies were designed and how the protein expression and purification systems were assessed. Testing of the produced antibodies is evaluated and the expression pattern of the *fru* B isoform is described for the first time.

3.2 Extant Fruitless Antibodies

Antibodies to the sex-specific domain of male Fru proteins (Fru^M) and to a common region (Fru^{Com}; Lee *et al.* 2000), found in both sex-specific and non-sex-specific Fru proteins, have been used to document the expression patterns of *fru* in both wild-type and mutant animals (Lee *et al.* 2000, Usui-Aoki *et al.* 2000). More recently, use of antibodies to the alternative C-terminal Zn-F domains A and C found in both sex-specific and non-sex-specific *fru* isoforms have revealed subtle differences in the expression patterns of the *fru* isoforms, suggesting distinct yet overlapping roles (Song *et al.* 2002, Billeter *et al.* 2006b). To date, the absence of an antibody to the Zn-F B domain has left part of the isoform story untold. The intention was to generate antibodies to each of the C-terminal Zn-F ends, particularly type B, to further investigate the expression pattern and functional role of each *fru* isoform.

3.3 Antigen design

All three variant Zn-Fs belong to the C₂H₂ class of zinc fingers and share the Zn-F domain consensus sequence C-X₂-C-X-K-X-V-X₅-H-X₃-H-X₆-C-P-X-C-X₅-R-X-D-X₄-H-X₃-K-H, where C and H are the cysteines and histidines that comprise the C₂H₂ domains, and X represents non-conserved amino acids. However, the alternative C-terminal exons vary in both length and in the positioning of the Zn-F domains within the exon. This variation within the rest of the exon has enabled isoform-specific antibodies to be raised against Zn-Fs A and C without cross-immunoreactivity within signals (Song *et al.* 2002).

Antigens for production of antibodies to Zn-F A and C containing *fru* isoforms were generated with primers identical to those employed to amplify the exonic regions used to raise the existing Fru^A and Fru^C antibodies (Song *et al.* 2002). Both antigens are designed to include the entire coding region of the corresponding exon, including the specific Zn-F domains (see Figure 3.1). It is believed that Zn-Fs A and C share a more recent common ancestor than with the more distantly related Zn-F B (Bertossa *et al.* 2009), potentially reducing the possibility of Fru^A and Fru^C proteins being detected with a Fru^B antibody. With this in mind, the recombinant protein used to raise the *fru* Zn-F B antibody was also generated by amplifying a 582bp fragment, which comprised the entire coding region of *fru* exon B.

The exonic regions were amplified as single fragments by polymerase chain reaction and sequenced to verify that no mutations had been introduced during amplification.

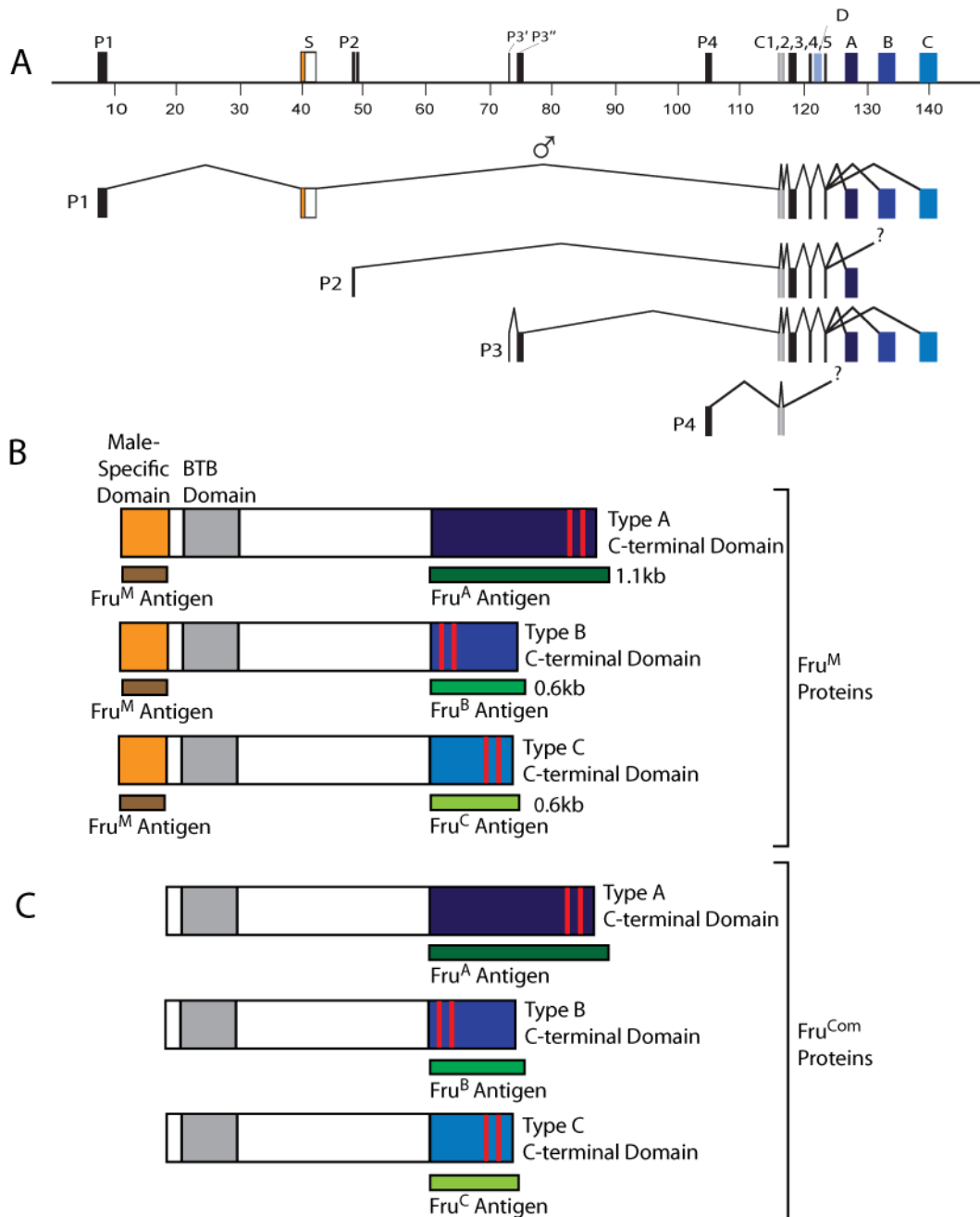


Figure 3.1 - Fruitless Isoform Antigens. (A) *fru* Locus and the transcripts generated by each promoter. P1 transcripts are only translated into functional protein in males. (B) Three isoforms of Fru^M protein, differing in identity of the Zn-F containing domain at the carboxy terminus. The grey coloured box represents the BTB protein-protein interaction domain and the blue boxes represent the different Zn-F domains present in each isoform. The relative positions of the two Zn-F motifs within each of the C-terminal ends are illustrated by two vertical red lines. The green boxes represent the regions chosen to make antigens for each of the Fruitless isoforms and their relative sizes. The orange box represents the male-specific domain, found only in Fru^M proteins, and the brown box shows the 281bp antigenic region used to generate the Fru^M antibody used in this study (Lee *et al.* 2000 and Billeter *et al.* 2006b). (C) Three isoforms of Fru^{Com} protein are found in both sexes (Anand *et al.* 2001).

3.4 Antigen production

All three exonic regions (A, B and C) were cloned in-frame into a bacterial expression vector using restriction sites engineered into the PCR primers that they were derived from. Fusion proteins were then expressed in bacteria and the bacterial cells were then broken open by sonication prior to fractionation and purification.

3.4.1 Expression of fusion proteins

The pGEX-6P1 expression vector was used for production of all three fusion proteins and each produced immunogen was fused to a glutathione *S*-transferase (GST) tag (Amersham Biosciences). Initial small scale expression of the GST fusion proteins in BL21 *E.coli* cells was performed and all three exhibited solubility (see Figure 3.2). Each culture was then scaled up for expression and isolation of Fru-GST fusion proteins.

3.4.2 Purification of antigen

Following fractionation by centrifugation, the bacterial lysates were separated into soluble and insoluble phases. The supernatant fractions containing the soluble fusion proteins were then purified to obtain the antigens for antibody production.

3.4.2.1 Batch purification

Initial purification was performed by batch method using Glutathione Sepharose beads. Here, GST fusion proteins are purified from bacterial lysates by affinity chromatography. When added to Glutathione Sepharose beads the GST tag portion of the proteins binds to the ligand. The bound fusion proteins are then washed several times and eluted under mild non-denaturing conditions. The protein of interest can be cleaved from its GST affinity tag prior to elution by cutting it with a site-specific enzyme, PreScission Protease (Amersham Biosciences).

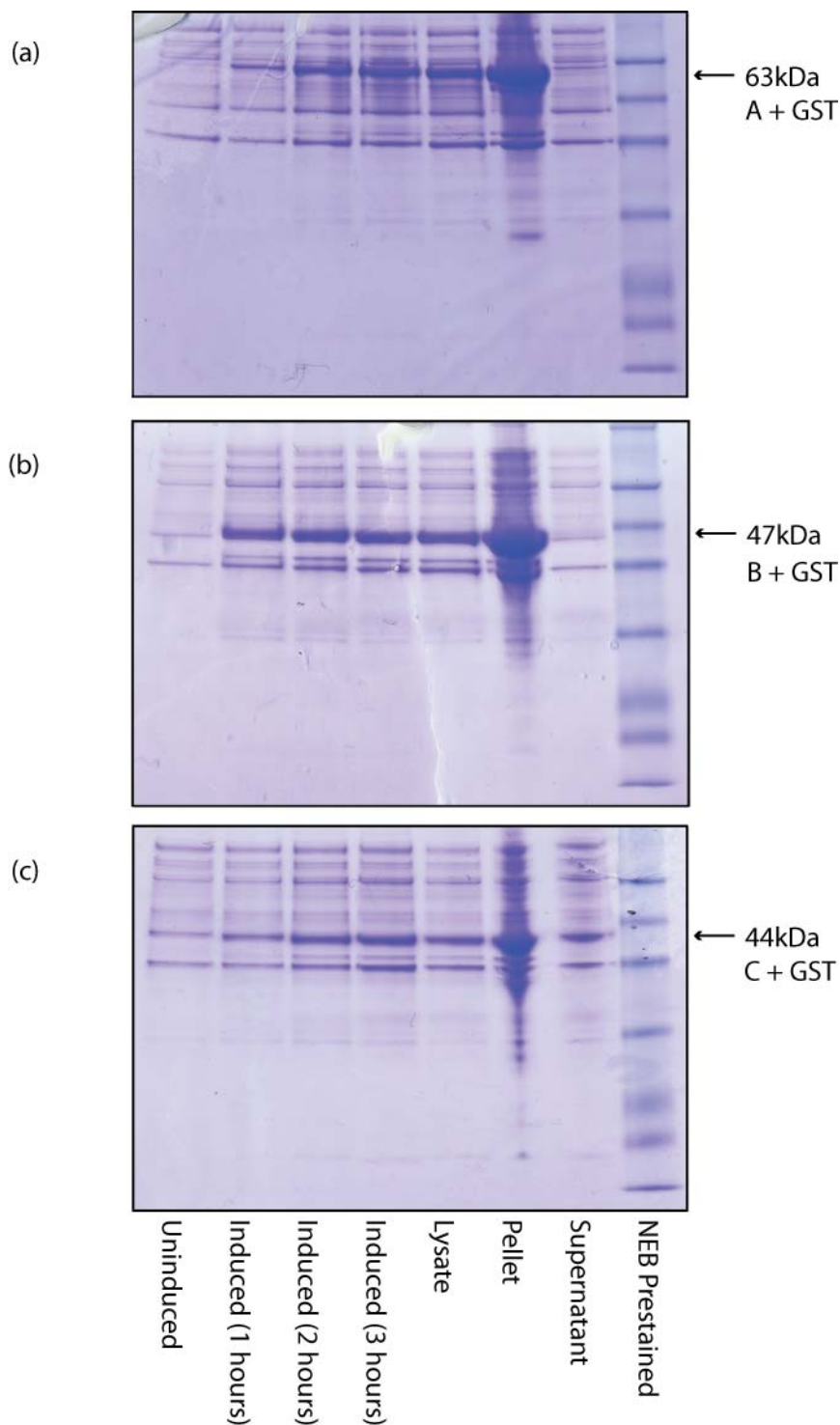


Figure 3.2 - Expression and Isolation of Fruitless-GST Fusion Proteins. (a-c) NuPAGE 12% Bis-Tris gels showing protein expression in *E.coli* cells transformed with one of three pGEX-Fru plasmids (A, B or C). Expression is shown prior to induction and at one hour intervals following addition of IPTG. Lysate was derived by bursting the bacterial cells with sonication and centrifugation was used to separate the lysate into soluble (Supernatant) and insoluble (Pellet) fractions. Lysate, Supernatant and Pellet fractions were diluted tenfold prior to loading. The GST-fusion proteins A, B and C run at 63kDa, 47kDa and 44kDa respectively.

In spite of the observed fusion protein solubility, early purification attempts recovered only minimal recombinant protein yields. Prior to purification each recombinant protein was observed at high levels in the supernatant, but was then found only at very low levels following cleavage from the GST tag. As a consequence, purification was performed in the absence of PreScission Protease to determine whether or not cleavage had had an adverse effect upon protein yield. This involved simply eluting the recombinant proteins from the glutathione sepharose with the GST tag still attached. By eluting without cleavage, the yield of Zn-F protein was increased. However, in each eluate there were significantly higher levels of GST alone (indicated by a 26kDa band) than recombinant protein attached to GST. This showed that most of the GST had become detached from the Zn-F protein, even in the absence of PreScission protease. Additionally, these liberated Zn-F proteins were not detected in the eluate, suggesting that the recombinant protein-GST fusions were unstable and the Zn-F proteins were readily degraded if separated from the GST tag.

It was therefore decided to raise antibodies against recombinant proteins with the GST tag still attached. As GST is not present in flies it was concluded that the attached GST tag should not lead to any additional immunoreactivity. Furthermore once the immunogenic sera are obtained, they can be affinity purified to remove any antibodies that react with GST.

3.4.2.2 Improving fusion protein stability

The duration of the protein expression step and that of the sonication and purification process were around six hours each, and for purely time management the bacterial cells were often frozen following the expression step. However, it was found that by performing protein sonication and purification directly after protein expression, degradation was significantly reduced. When resuspending bacterial cells phenylmethylsulphonyl fluoride (PMSF) and protease inhibitors were used to reduce protein degradation. It was also found that addition of a Complete EDTA-free protein inhibitor tablet (Roche Diagnostics) also reduced degradation.

Expression and purification the recombinant proteins within a 12 hour time window, in combination with the new protease inhibitor tablets, allowed higher

quantities of Zn-F protein to be obtained, though still not at quantities recommended to raise antibodies in rat with (five 50 μ l aliquots, each containing a minimum of 15-20 μ g; Diagnostics Scotland, Penicuik).

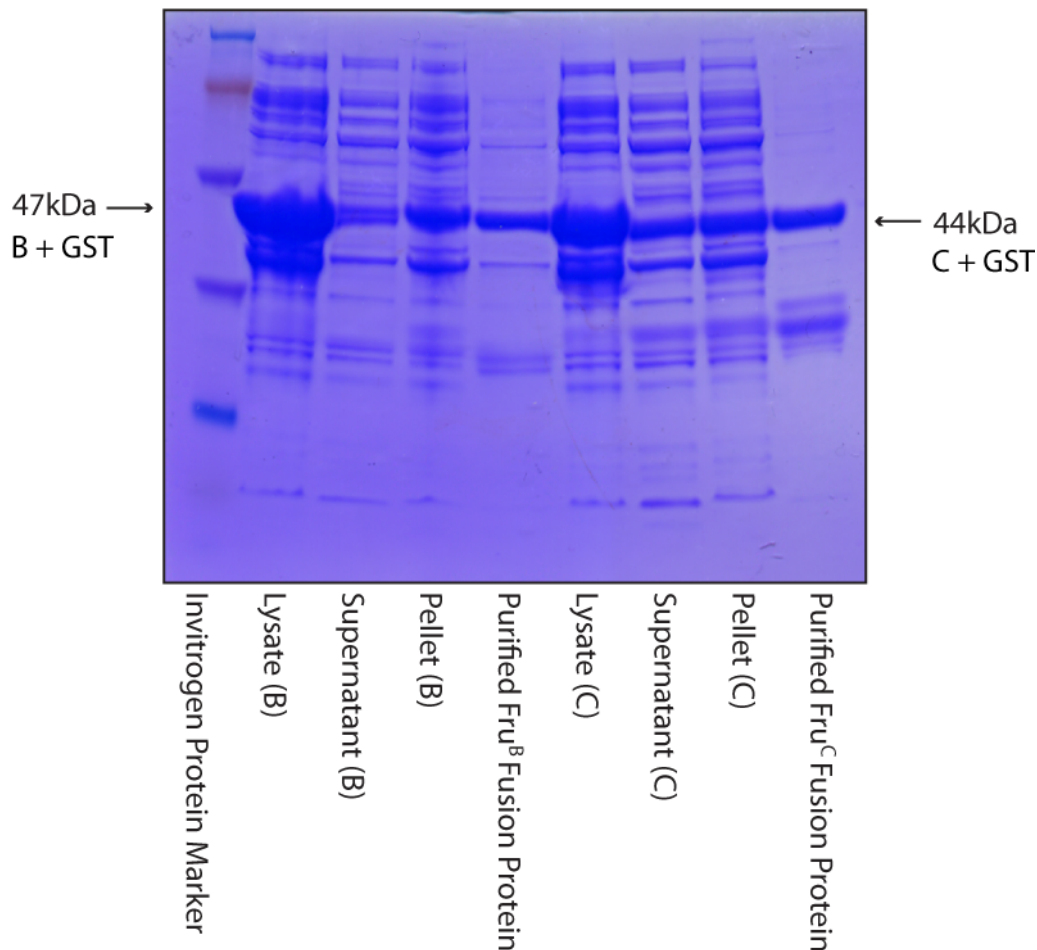


Figure 3.3 - Purification of Fruitless-GST Fusion Proteins B and C. NuPAGE 12% Bis-Tris gel showing purification of GST fusion proteins. For each fusion protein the lysate, soluble fraction (supernatant) and insoluble fraction (Pellet) are shown, in addition to the purified protein itself following washing and elution from GSTrap columns. The GST-fusion proteins B and C run at 47kDa and 44kDa respectively.

3.4.2.3 GSTrap FF column purification

To achieve the necessary levels of proteins it was decided to use GSTrap FF columns (Amersham Biosciences) instead of the Glutathione Sepharose beads during the purification process. The GSTrap columns work by the same principles as the Glutathione Sepharose beads, however the Glutathione Sepharose is fixed within a column, allowing the supernatant to be passed over the GST binding sites at a constant rate using a syringe. By implementing

column purification, a significant increase in the yield of both Fru^B and Fru^C recombinant proteins was achieved. Using a Coomassie (Bradford) Protein assay the concentration of these purified proteins was estimated to be 0.52µg/µl for the Fru^B antigen and 1.60µg/µl for the Fru^C antigen. 250µl of each antigen was then sent to Diagnostics Scotland for injection into rats. Rat was chosen to raise the antibodies as *fru* antibodies have been successfully raised in this organism in the past, and to facilitate double-staining with the Fru^M antibody that was raised in rabbit (Billeter *et al.* 2006b).

In contrast to the high levels of purified Fru^B and Fru^C fusion proteins, the yield of the purified Fru^A fusion protein was barely detectable. Following several attempts to improve the yield of purified protein, it was decided that this antigen should be expressed and purified using a different method.

3.4.2.4 The pMAL expression system

In the pMAL protein fusion and purification system a cloned gene is inserted into the pMAL vector downstream from the MalE gene, which encodes maltose binding protein (MBP; Guan *et al.* 1987). This enables expression of an MBP-fusion protein which can be purified using amylose resin. The expressed MBP has been engineered to achieve strong binding to amylose and the MBP-fusion protein is then washed before elution from the resin using a column buffer containing maltose. The pMAL system generally provides reliable expression with substantial yields of up to 100mg of fusion protein per litre of culture (New England Biolabs). Fusion to MBP has also been shown to enhance solubility of proteins expressed in *E.coli* (Kapust and Waugh, 1999).

Initial expression attempts were unsuccessful but, by reducing the growing temperature from 30°C to 23°C and doubling the expression time, fusion protein expression was achieved. Small-scale expression and purification of the Fru^A-MBP-fusion protein produced a strong product of expected size, observed in the resultant supernatant fraction. A weaker product was also observed in the eluate following purification (see Figure 3.4). Expression was repeated at an increased volume to obtain sufficient protein to use as an antigen. Despite several attempts to recapitulate previous levels of solubility, using various growing conditions, it was not possible to obtain sufficient soluble protein or

subsequent purified fusion protein to use as an antigen for production of a new Fru^A antibody. However, analysis of Fru^A expression in generated mutant lines would still be possible using the extant Fru^A antibody (Song *et al.* 2002).

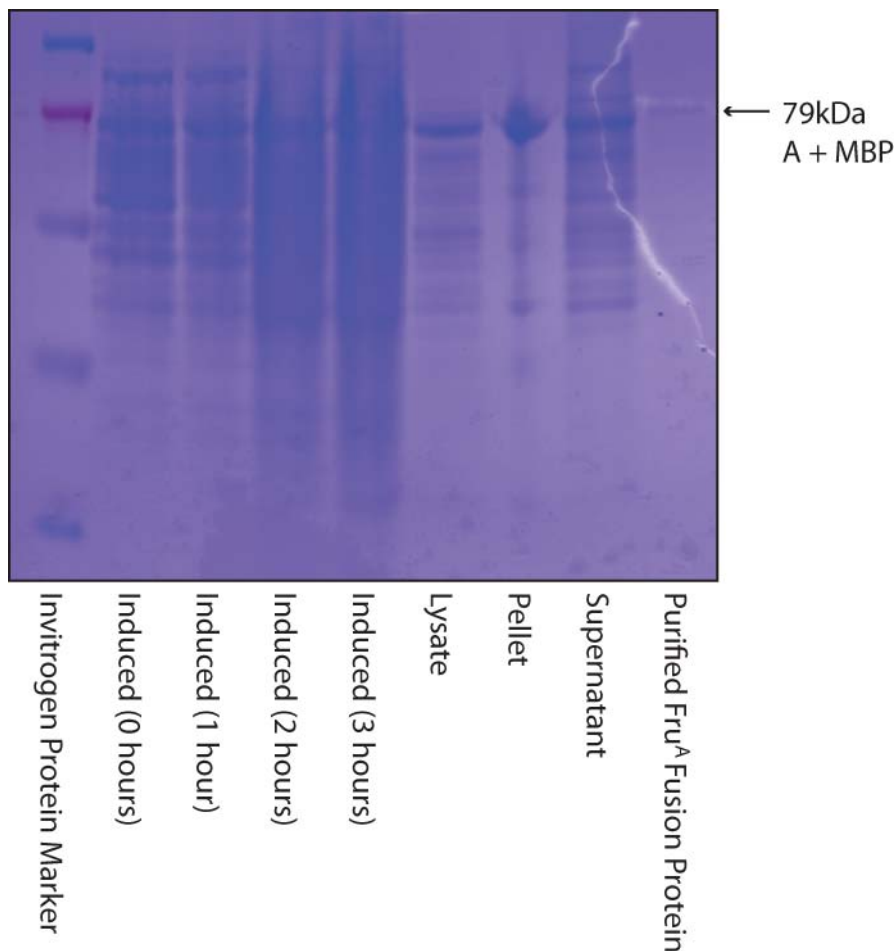


Figure 3.4 - Expression of MBP-Fru^A Fusion Protein. NuPAGE 12% Bis-Tris gel showing small scale expression and purification of MBP-Fru^A fusion protein using the pMAL protein fusion and purification system. Expression is shown prior to induction and at one hour intervals following addition of IPTG. Lysate was derived by breaking the bacterial cells with sonication and centrifugation was used to separate the lysate into soluble (Supernatant) and insoluble (Pellet) fractions. The purified MBP-Fru^A fusion runs at 79kDa.

3.5 Antibody production

Purified Fusion proteins were sent to Diagnostics Scotland (Penicuik, Lothian) for injection into rat. As previously stated, rat was chosen due to the previous success of raising Fru antibodies in this organism and also to allow co-localisation studies with the extant Fru^M antibody raised in rabbit (Billeter *et al.* 2006b). Returned Sera were tested, then aliquotted and stored at -20°C.

3.6 Testing Fruitless antibodies

To assess the novel generated *fru* isoform antibodies, the expression patterns generated by the novel antibodies were compared to previously characterised patterns of expression of extant Fru antibodies. The specificity of these expression patterns were confirmed through changes in expression in mutants deficient for the isoform assayed.

The histochemical signals produced by the Fru^C antibody were compared to those generated by the existing Fru^C antibody (Song *et al.* 2002), and these signals were also assessed in the *fru^{AC}* mutant (Billeter *et al.* 2006b). The Fru^B antibody was used in immunofluorescence assays in conjunction with the Fru^M antibody raised in rabbit to confirm that the cells labelled by anti-Fru^B express Fru protein. To demonstrate that the observed Fru^B signals are in fact detecting Fru^B proteins, immunofluorescence examination of mutants lacking Fru^B proteins was performed (see Chapter 5, Figure 5.1).

3.6.1 Fru^C proteins are expressed during embryonic development

In the latter stages (stages 12-13) of embryogenesis Fru^C immunostaining localises with nuclei in a group of cells which migrate towards the anterior end of the embryo (Figure 3.5B). Positionally, these cells strongly resemble precursors of the Garland cells which form here late in embryo development. At stage 15 in embryonic development a group of 15-20 Garland cells form around the oesophagus near the proventriculus (Riziki 1978). Garland cells function as nephrocytes in *Drosophila* by removing waste products from the haemolymph by endocytosis (Kosaka and Ikeda 1983). Another possibility is that these cells are haemocytes, which are known to migrate throughout the embryo during stages 12 and 13. The vast majority of embryonic haemocytes become macrophages and function as part of the immune system in *Drosophila* (Tepass *et al.* 1994).

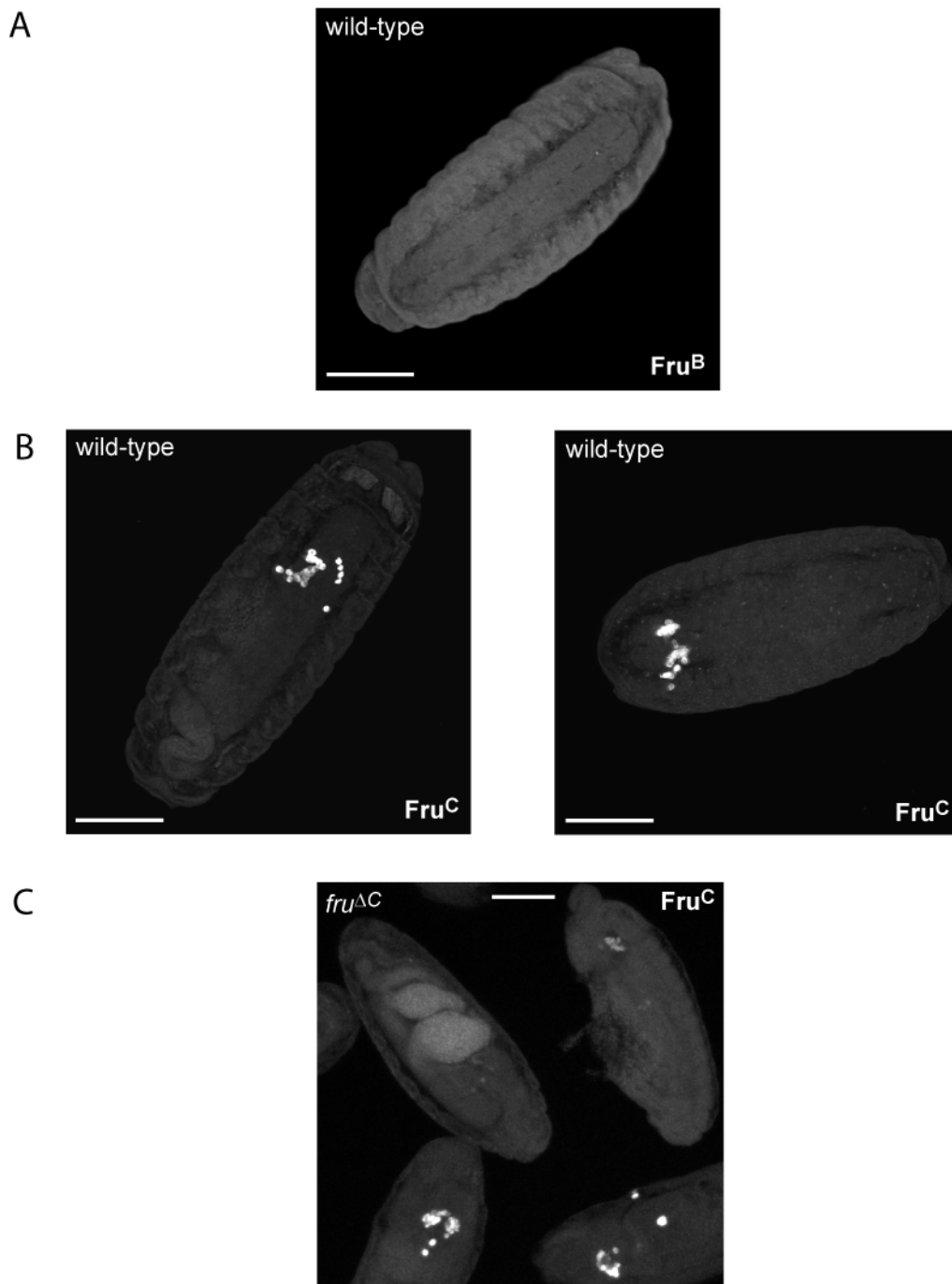


Figure 3.5 - Fru Isoform Immunostaining During Embryogenesis. (A) Anti-Fru^B immunostaining in wild-type (*Canton-S*) stage 13 embryo. No anti-Fru^B signals detected. (B) Anti-Fru^C immunostaining in *Canton-S* stage 13 embryo. (C) Anti-Fru^C immunostaining in *fru*^{ΔC} mutant stage 13 embryo. Of the four embryos shown, anti-Fru^C signals were detected in the two lower embryos, but absent from two upper embryos. Scale bars=100μm.

To verify that the identified cells were indeed expressing Fru^C proteins, the assay was repeated with anti-Fru^C in *fru^{ΔC}* embryos, which are unable to synthesise Fru^C proteins. As male *fru^{ΔC}* homozygotes show incompletely penetrant sterility (Billeter *et al.* 2006b) it was necessary to use heterozygotes in combination with a third chromosome balancer to obtain embryos. The balancer chromosome also carried GFP to allow *fru^{ΔC}* heterozygote embryos to be identified. However, it was subsequently discovered that the GFP marker gene had been lost from that line, preventing GFP detection in heterozygotes.

In spite of this, immunostaining revealed an absence of Fru^C signals in a significant number of the collected embryos (See Figure 3.5C). These embryos were presumably homozygous for *fru^{ΔC}* since all wild-type stage 13 embryos displayed Fru^C immunostaining. To clarify the matter, the original stock should be checked to confirm that the GFP marker gene has been lost, and re-ordered if necessary. As a negative control, Fru^C immunostaining of embryos collected from a stock of *fru^{ΔC}*, in heterozygous combination with the functional GFP balancer, should be performed and assessed for the presence of anti-Fru^C signals.

In immunocytochemistry of wild-type embryos with anti-Fru^B, no signal was apparent during embryogenesis (See Figure 3.5A). To verify the apparent absence of Fru^B proteins from wild-type stage 13 embryos, a positive control should be performed. This could be achieved by driving expression of Fru^B using the UAS/GAL4 system. Expression of GAL4-responsive Fru^B isoform transgene could be induced by a pan-neuronal driver line such as *Sca-Gal4*, which has an expression pattern similar to that of Fru proteins (Song *et al.* 2002).

3.6.2 Fru^B and Fru^C proteins are present in larval CNS

Immunostaining in 3rd-instar larvae (L3) with anti-Fru^B produced signals in a large number of cells in the VNC in both sexes. The larvae were sexed prior to immunostaining, but the expression patterns appeared to be the same in both males and females. This is consistent with previous studies (Lee *et al.* 2000). Signals were also detected in cells within neurite bundles which connect imaginal discs to the larval CNS (See Figure 3.6).

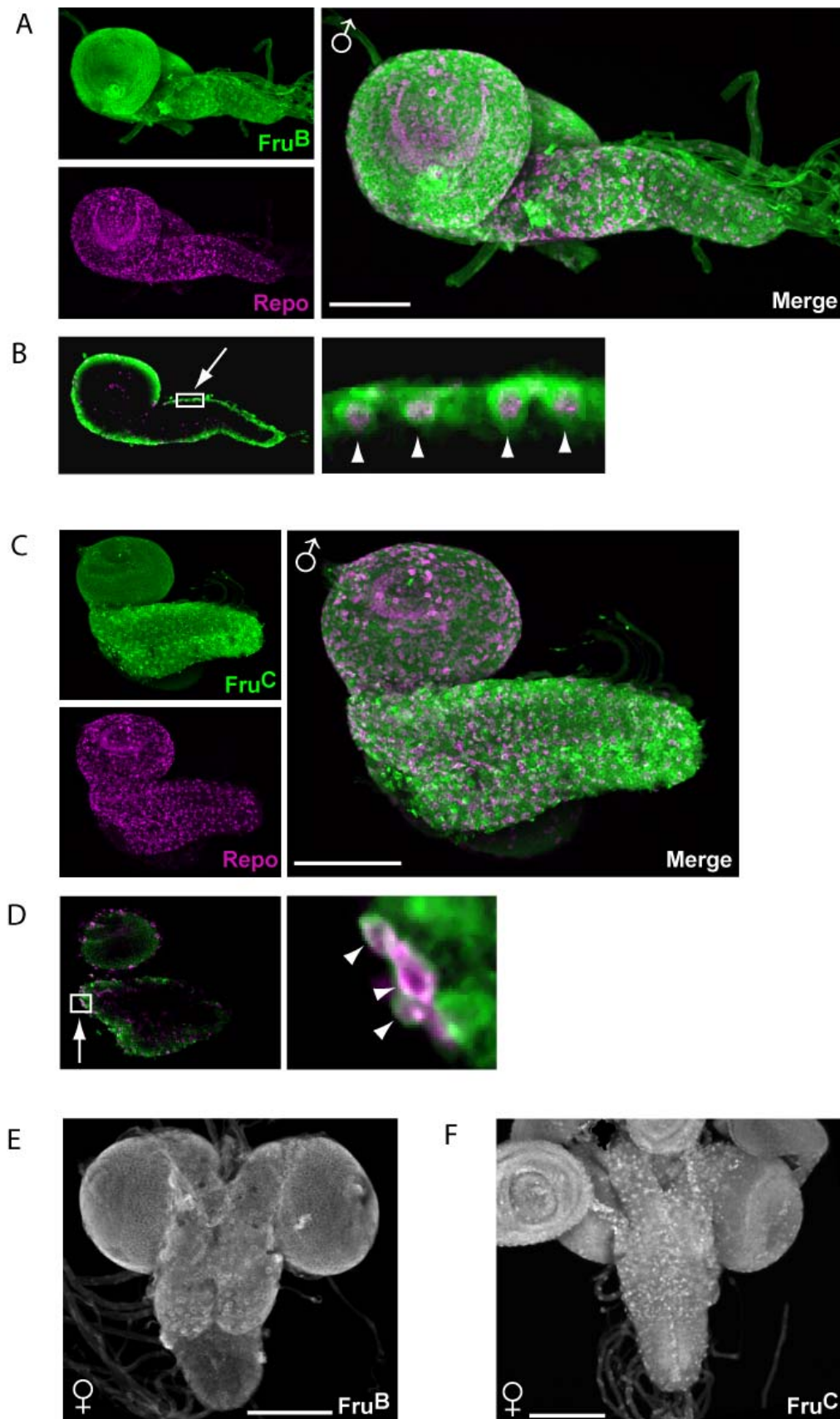


Figure 3.6 - Fru Isoform Expression in the Larval CNS. (A) Wild-type L3 larval male CNS co-labelled with anti-Fru^B and anti-Repo. (B) Single confocal Z-slice of image (A), showing nuclear co-localisation of Fru^B and Repo in a population of neurons. (C) Wild-type L3 larval male CNS co-labelled with anti-Fru^C and anti-Repo. (D) Single confocal Z-slice of image (C), showing nuclear co-localisation of Fru^C and Repo in a population of neurons. (E-F) Wild-type L3 larval female CNS labelled with anti-Fru^B (E) or anti-Fru^C (F). Scale bars=100µm.

Anti-Fru^C immunoreactivity detected Fru^C proteins in the L3 CNS of both sexes. A large number of cells in both the brain and VNC were stained, in addition to cells within neurite bundles attached to the CNS. Non-neuronal Fru expression has been previously reported in L3 larvae, and to investigate whether the observed Fru signals in the L3 larval CNS were derived from glia, double-labelling experiments were performed with anti-Repo, which stains glial cells. Colocalisation between anti-Repo and the Fru antibodies signals was observed only in a small number of cells for both Fru^B and Fru^C (See Figure 3.6B and D), suggesting that the majority of Fru^B and Fru^C expressing cells in L3 larvae are not glia.

3.6.3 Fru^B and Fru^C co-localise with Fru^M in male pupal CNS

Anti-Fru^B and anti-Fru^C both immunostained a large number of cells in the brain and VNC of male pupae. The signals produced from both antibodies overlapped very closely with anti-Fru^M signals (Lee *et al.* 2000) when double-labelling experiments were performed in 2-day old male pupa (See Figure 3.7). Fru^B is expressed in almost all of the cells in which Fru^M is expressed in the CNS. Fru^C is expressed in all Fru^M positive cells in the brain and the vast majority of the Fru^M expressing cells in the VNC. Females do not produce Fru^M proteins and accordingly, no anti-Fru^M signal was detected in the CNS of 2-day old female pupae (Ryner *et al.* 1996, Lee *et al.* 2000). Similarly, no signal was detected for anti-Fru^B and anti-Fru^C.

3.6.4 Fru^B is expressed in all the serotonergic neurons of the adult male abdominal ganglion

As in pupae, Anti-Fru^B and anti-Fru^C both immunostained a large number of cells throughout the adult male CNS. Again, in double-labelling experiments with anti-Fru^M, the signals produced by both anti-Fru^B and anti-Fru^C closely overlapped those generated by anti-Fru^M (See Figure 3.8).

However, although expression of all three Fru^M isoforms is present in the overwhelming majority of all Fru^M cells, there is one region in which isoform expression is known to be finely regulated. In the male abdominal ganglion, there are two clusters of male-specific serotonergic neurons, positioned dorsally and ventrally (α 5Abg and ν 5Abg, Billeter *et al.* 2006b).

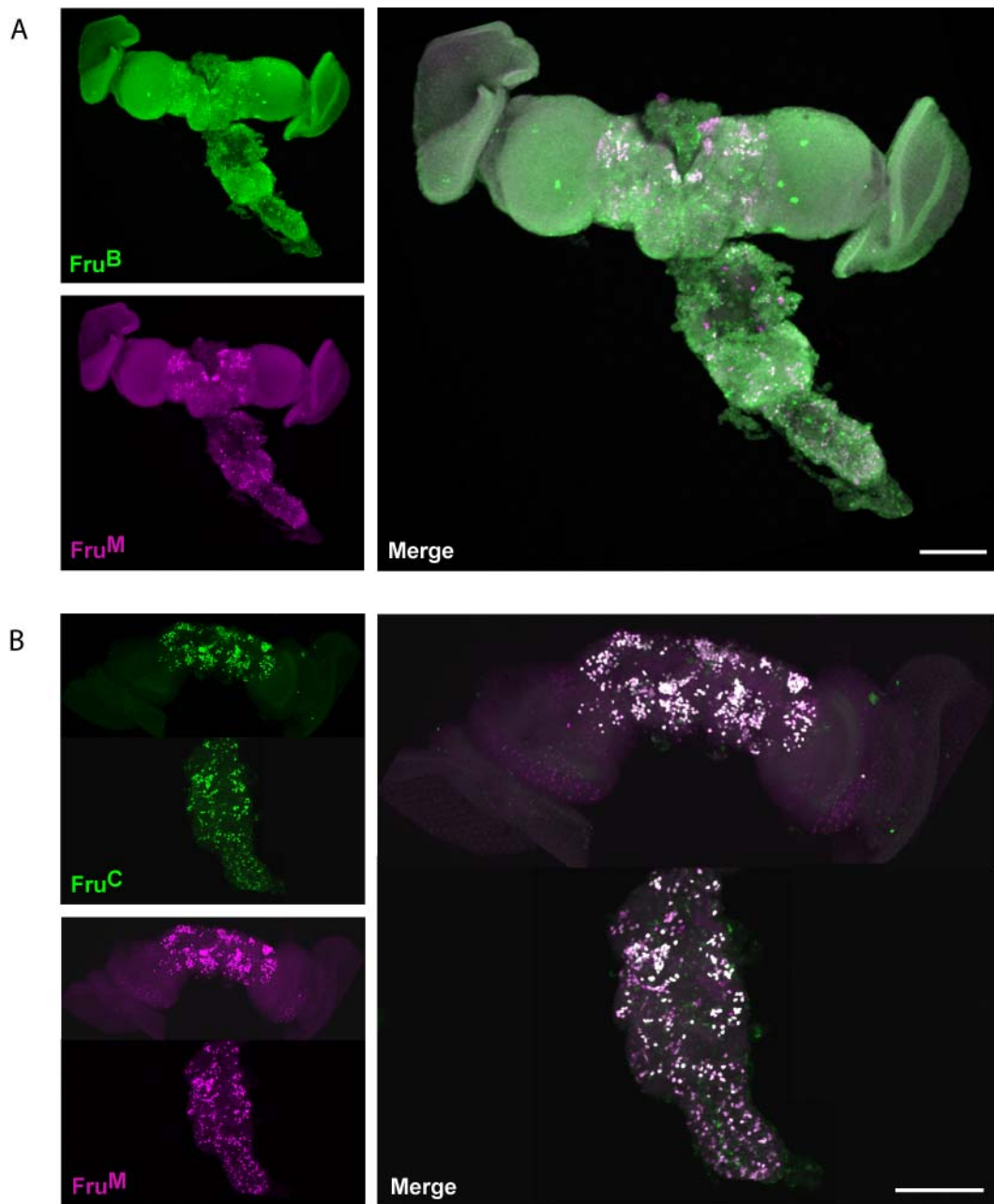


Figure 3.7 - Fru Isoform Expression in the Pupal Male CNS. (A) Wild-type 2-day old pupal male CNS co-labelled with anti-Fru^B and anti-Fru^M. (B) Wild-type 2-day old pupal male CNS co-labelled with anti-Fru^C and anti-Fru^M. Scale bars=100μm.

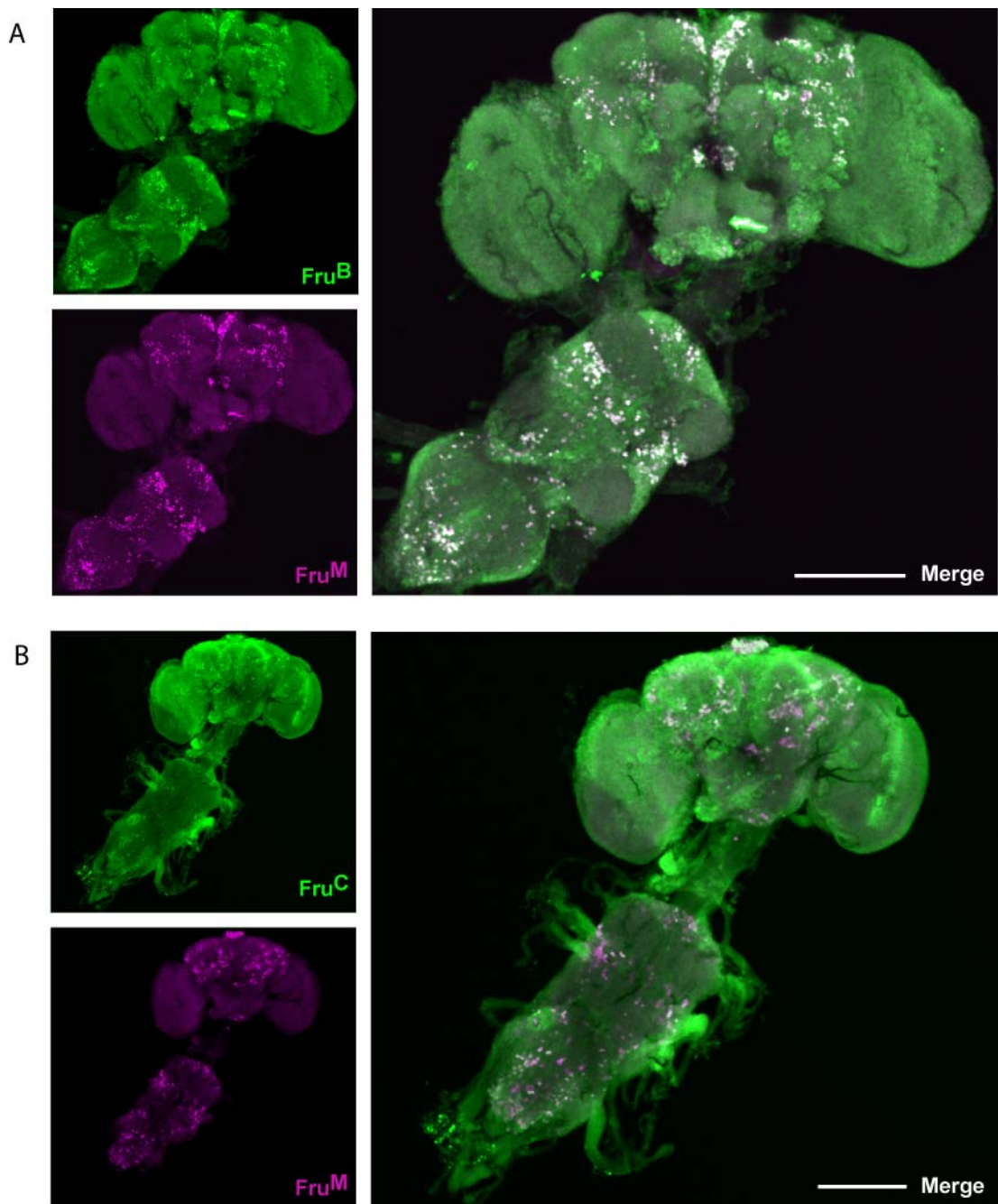


Figure 3.8 - Fru Isoform Expression in the Adult Male CNS. (A) Wild-type 5-day old adult male CNS co-labelled with anti-Fru^B and anti- Fru^M. (B) Wild-type 5-day old adult male CNS co-labelled with anti-Fru^C and anti- Fru^M. Scale bars=100 μ m.

These serotonergic neuron clusters are involved in the control of sperm and seminal fluid transfer, and their development is partly controlled by the presence of Fru^M proteins (Lee and Hall 2001, Lee *et al* 2001). It is also known that not all of the Fru^M isoforms are expressed in these neurons. Fru^{MC} proteins are expressed in all neurons of both clusters whereas Fru^{MA} proteins are completely absent from both clusters (Billeter *et al.* 2006b). The expression of Fru^{MB} proteins in the male-specific serotonergic neuron clusters is previously unassessed, as a Fru^B antibody has not been available until now.

In a separate experiment by Jean-Christophe Billeter, double-labelling of the male abdominal ganglion using anti-Fru^B, generated in this study, and a serotonin antibody, anti-5HT (5-Hydroxytryptamine), was performed. This enabled expression of Fru^{MB} in the serotonergic neuron clusters of the abdominal ganglion to be assessed for the first time. Fru^{MB} expression was observed in all of the serotonergic neurons in the adult male abdominal ganglion in both the α SAbg and ν SAbg clusters (See Figure 3.9). This finding shows the expression pattern of Fru^{MB} isoforms in the serotonergic clusters of the adult male abdominal ganglion is like that of Fru^{MC} and not like that of Fru^{MA}, which is entirely absent from both clusters.

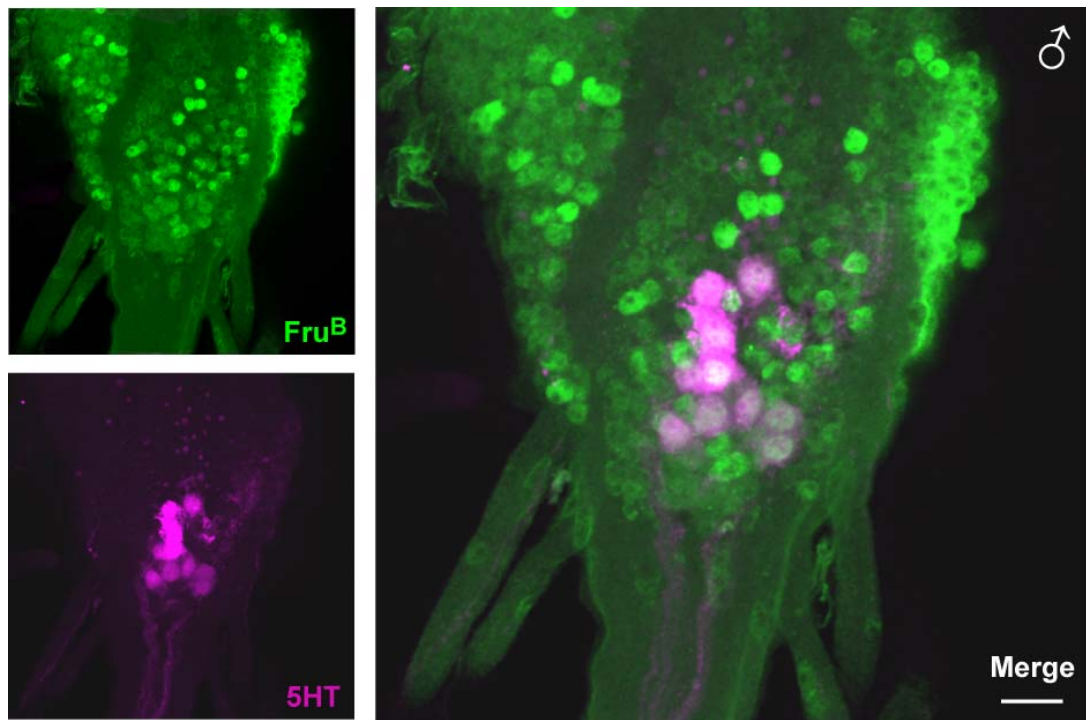


Figure 3.9 - Expression of Fru^B in the Serotonergic Neuron Clusters of the Male Abdominal Ganglion. Co-labelling of wild-type 5-day old adult male abdominal ganglion co-labelled with anti-Fru^B and anti-5HT. Experiment performed by J-C.Billeter. Scale bars=10 μ m.

3.7 Discussion

The co-localisation of signals produced from anti-Fru^B and anti-Fru^C with those generated by anti-Fru^M, coupled with the apparent absence of anti-Fru^C signals in *fru*^{A^C} animals, indicated that the Fru^B and Fru^C antibodies were immunolabelling the correct groups of cells. The failure to obtain sufficient purified Fru^A fusion protein in both expression systems used may have been caused by several factors. The secondary structure of the fusion protein may have been toxic to the *E.coli* cells that were expressing it, or alternatively, the protein may be unstable in vitro and rapidly degraded following expression.

Embryo immunohistochemistry was performed towards the end of embryogenesis as it has been shown that *fru* transcripts present in the initial stages of embryo development are maternally derived (Song *et al.* 2002). The different spatial and temporal expression of Fru^B and Fru^C shows that the choice of each Zn-F domain-containing isoform and its corresponding expression pattern is finely regulated. As sex-specific *fru* transcripts are not produced until late in larval development (Lee *et al.* 2001), it can be concluded that Fru^C proteins detected in the embryo are sex-non-specific proteins (Fru^{ComC}). Detection of Fru^{ComC} protein in the developing embryo is consistent with previous immunohistochemistry and *in situ* hybridisations, which detected type C non-sex-specific transcripts from P3 and P4 promoters and described them as the most abundant *fru* isoforms during embryogenesis (Song *et al.* 2002). The two promoters involved are believed to provide transcripts important for the viability of both sexes (Ryner *et al.* 1996; Anand *et al.* 2001). The role of *fru* in embryo development has been revealed using mutants possessing deletions or P-element insertions in the *fru* locus. Observations that embryos lacking most or all of *fru* function have defects in axonal projections led to the discovery that *fru* transcripts are required to regulate axonal pathfinding in the embryonic CNS (Song *et al.* 2002). The discovery of a novel pattern of Fru^C expression in stage 13 embryos is interesting. Much is known of *fru*'s role in generating the potential for male courtship behaviour and to a lesser extent its essential role in the viability of both sexes, but almost nothing is known of *fru*'s role in other more subtle biological outcomes. Verification of the identity of these cells may

uncover further functional roles and targets of sex-non-specific Fru proteins (also see section 6.2).

This is the first investigation to immunostain embryos with a Fru^B antibody and the absence of any detectable signal may indicate that Fru^B proteins are not expressed at all in the embryo. Alternatively it may be the case that the methods used in the course of this project are not sensitive enough to detect Fru^B proteins. To achieve immunostaining, embryos were ruptured. In previous studies, filleted embryos were used and *in situ* hybridisation using a B type specific riboprobe detected B 3' end transcripts during embryogenesis (Song *et al.* 2002). However, the expression patterns detected by the new *fru* antibodies are consistent with previous findings that transcripts with a C-type 3' end are most abundant in the developing embryonic CNS (Song *et al.* 2002).

Larval immunostaining was performed with mature 3rd-instar larvae (L3). Expression of sex-specific transcripts from the P1 promoter begins at this stage, just prior to the beginning of pupariation (Lee *et al.* 2000). However, as these transcripts are only found in a few small clusters in the male L3 larvae (Lee *et al.* 2000), almost all of the signals detected with anti-Fru^B and anti-Fru^C in males and all signals in females are likely to represent expression of non-sex-specific Fru^{com} proteins. This is consistent with the finding that expression of both Fru^B and Fru^C in L3 larvae is very similar in both sexes. Double-labelling of male L3 larvae with anti-repo, and anti-Fru^B or anti-Fru^C, showed that most of the detected Fru expression is not within glia.

As Repo (*reversed polarity*) expression is nuclear, the small number anti-Fru^B and -Fru^C signals that co-localised with anti-repo in glial cells must also be nuclear. This is consistent with fact that Fru proteins are transcription factors. To assess whether the remaining signals anti-Fru^B and -Fru^C signals are neuronal, larvae should be co-labelled with either anti-Fru^B or -Fru^C and the antibody to the *elav* gene product, which is only expressed in the nuclei of neurons from the early stages of development (Yao *et al.* 1993).

In contrast the low levels of Fru expression detected L3 larvae glial cells in this study, previous investigations using an antibody raised against the region common to all *fru* transcripts have suggested that non-neuronal Fru expression is

more prevalent at this developmental stage (Lee *et al.* 2000). A reason for this variation could be due to expression of Fru^A, which would be detected by anti-Fru^{Com} but not anti-Fru^B and anti-Fru^C. However, it is more likely that Fru^B and Fru^C proteins are present in non-neuronal tissues of L3 larvae, but are more readily detected by the Fru^{Com} antibody. An explanation for this could be that the Fru^{Com} antibody was raised against a region containing part of the BTB domain. This domain is known to be involved in protein-protein interaction (Albagli *et al.* 1995) and as such, may be presented in an exposed position on the surface of the Fru protein, facilitating immunoreactivity.

Immunohistochemistry was performed in 2-day pupae as levels of Fru expression in the CNS peak at this stage of development (Lee *et al.* 2000, Usui-Aoki *et al.* 2000). Double-labelling with anti-Fru^M revealed that expression of both Fru^B and Fru^C follows very closely the expression pattern of Fru^M in male pupae. The absence of any female pupal Fru immunostaining, in addition to the co-localisation of Fru^B and Fru^C with Fru^M, suggests that the vast majority Fru^B and Fru^C proteins detected in in 2-day pupae are sex-specific proteins derived from transcripts generated by the P1 promoter. The cells that express Fru in the male pupal CNS and then into adulthood have been well characterised and described in 20 separate clusters according to immunohistochemical signals detected with a Fru^M antibody (Lee *et al.* 2000, Billeter and Goodwin 2004). Fru^B and Fru^C expression was detected in 19 of the 20 clusters, the noticeable exception being the absence of immunostaining in the medulla optic lobes. Anti-Fru^M immunostaining in this region was quite weak compared to the other clusters and this apparent variation may be due to the sensitivity of the individual antibodies. Indeed in all anti-Fru^M double-labelling experiments the signal detected by anti-Fru^M was consistently stronger than that of either that of either anti-Fru^B or anti-Fru^C. Nevertheless, expression of both Fru^B and Fru^C in all but one of these cell clusters backs up the assertion that the observed signals represent Fru^M proteins. It also shows that at this stage the expression patterns of Fru^{MB} and Fru^{MC} appear to be identical, suggesting that they may be performing similar or closely related functions.

The pattern of Fru^B and Fru^C expression in the 5-day adult male CNS was reminiscent of that in 2-day male pupae. Fru^B and Fru^C expression was detected in all of the 20 clusters except for the medulla optic lobe, and these signals co-

localised with those of anti-Fru^M. This may indicate that although levels of *fru* mRNA transcripts observed in the adult CNS are significantly lower than those detected in 2-day pupae (Lee *et al.* 2000), high levels of both Fru^{MB} and Fru^{MC} proteins persist into adulthood. The finding that Fru^{MB} is expressed in all of the serotonergic neurons in the male abdominal ganglion is interesting as it completes the picture with respect to expression of male-specific isoforms in this region. It is known that Fru^{MC} is expressed in all of the serotonergic neurons in the male abdominal ganglion, whereas Fru^{MA} is expressed in only a subset of these cells (Billeter *et al.* 2006b). This illustrates that the choice of Zn-F domain in male-specific Fru proteins is as closely regulated as it is in Fru proteins common to both sexes.

3.8 Conclusions

In the course of this chapter, antibodies were generated to detect individual *fru* isoforms and the successful generation of a Fru^B antibody enabled the presence of this specific subset of Fru proteins to be detected for the first time. Using these novel antibodies, the expression patterns of these isoforms was assessed throughout the main stages of development, allowing comparison to the results of other studies and, in some cases, enabling the findings of other investigations to be extended.

The findings from the investigations using these novel antibodies gave a valuable insight into the expression pattern of the corresponding isoforms and hinted at potential functional roles, both of which will be invaluable in assessing the expression patterns and phenotypic outcomes of the mutants to be generated by gene targeting.

4 Gene Targeting of *fruitless* Locus

4.1 Introduction

In the previous chapter, the generation of isoform-specific Fru antibodies was described. These antibodies were used to document the expression patterns of the corresponding Fru isoforms at stages and anatomical locations previously unexplored for these particular protein subsets. However, the main aim of generating these reagents was to enable specific detection of the presence, or absence, of each of these zinc finger variant isoforms of Fru in different mutant lines. By assessing which isoforms are expressed in various *fru* mutants and by comparing the phenotypes associated with these alleles it should be possible to illuminate the roles played by *fru* both during development and in the regulation of male adult courtship behaviour.

4.1.1 Mutagenesis at the *fru* Locus

Mutant alleles of *fru* have been pivotal in unravelling the complexity of the gene and the roles it plays. However, most of these mutants have been shown to abolish or greatly reduce all transcripts produced from particular *fru* promoters or indeed the entire locus (Figure 4.1; Gailey and Hall 1989, Castrillon *et al.* 1993, Ryner *et al.* 1996, Ito *et al.* 1996, Goodwin *et al.* 2000, Anand *et al.* 2001).

These alleles can reveal the contribution of all transcripts produced by a particular promoter, or group of promoters, but tell nothing of the roles played by each of the variant zinc finger isoforms produced from each promoter. The only known mutation that affects a specific subset of the transcripts produced at a given *fru* promoter is the *fru^{AC}* mutation (Billeter *et al.* 2006b). This mutation is a small 7bp deletion in the exon encoding for the type-C zinc finger domain, causing a frameshift and inclusion of a premature stop codon, ensuring no functional type-C isoforms are produced. In *fru^{AC}* animals both Fru^{ComC} and Fru^{MC} are disrupted, yet other non-sex-specific and sex-specific isoforms are unaffected. The *fru^{AC}* mutation provided a unique opportunity to investigate the functional role of type-C isoforms, by determining which aspects of the *fru* syndrome are attributable to the disruption of only type-C isoforms (Billeter *et al.* 2006b).

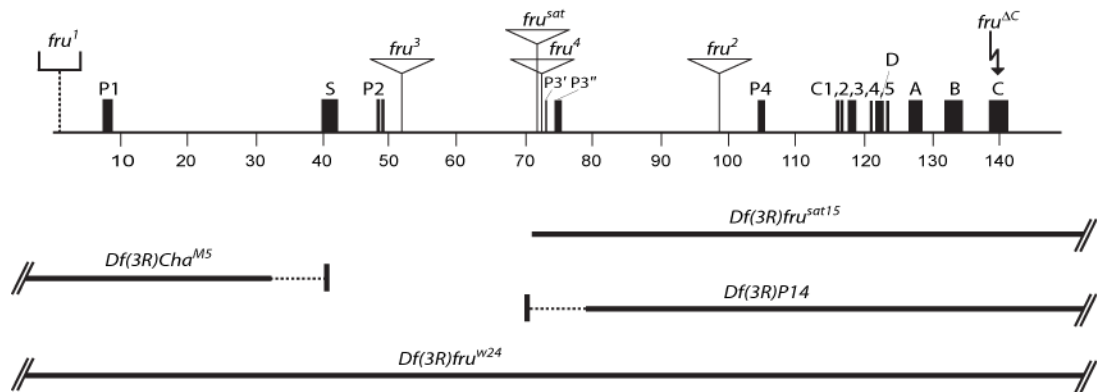


Figure 4.1 - Genomic locations of Ten Extant *fru* Mutants and Deficiency Lines.

Relative genomic locations of ten extant *fru* mutants within the *fru* locus. *fru* mutants caused by insertion of a *P*-element at the *fru* locus are represented by an inverted triangle (*fru*², *fru*³, *fru*⁴ and *fru*^{sat}). The horizontal lines below the *fru* locus depict the extent of the genomic deletions which characterise each of the *fru* deficiency lines used in this study (*fru*^{sat15}, *Cha*^{M5}, *P14* and *fru*^{w24}). Also depicted are the small deletion which causes the *fru*¹ mutation and the micro-deletion of *fru*^{AC} within exon C. Size of locus shown in kb.

The main reason that such a mutation has been isolated only once lies in the method of mutagenesis. Existing mutants have been generated by one of three methods; *P*-element remobilisation or mutagenesis using EMS or X-rays. EMS screens have the potential to generate small micro-deletions, as in the case of *fru*^{AC}, but such mutagenesis is largely unpredictable in terms of the size and location of the lesions produced. X-ray induced lesions tend to be larger and often involve complex inversions and translocations, such as the first *fru* allele (*fru*¹, Gill 1963). Instead of producing null mutations, such events, can lead to novel splicing patterns, which can complicate the assessment of a gene's functionality.

If *P*-element inserts are already present, in close proximity to the target locus, then the chance of recovering a mutation within the region of interest by *P*-element remobilisation will be increased. However, the size and type of mutations produced vary greatly and the effects on transcription at a given locus can be quite complex. Translocations and inversions can lead to reduced or differential patterns of expression, as opposed to the abolition of functional gene products. Additionally, *P*-elements themselves can act as splice sites if they are introduced into a particular locus, leading to novel transcripts and aberrant expression. Such novel transcripts have been observed as a result of *P*-elements at the *fru* locus (Goodwin *et al.* 2000). Here the novel transcripts of *P*-

element insertions at the same genomic location within the *fru* locus were shown to vary depending on the type of element present. In this case, the *P*-elements causing the *fru^{sat}* and *fru²* alleles are inserted at the same approximate genomic location, but produce vastly different novel *fru* transcripts. The *fru^{sat}* allele produces an array of transcripts identical to that of the *fru²* allele, despite the insertions being almost 30kb apart. The *fru³* and *fru⁴* alleles also produce identical transcript arrays and are approximately 20kb apart. A likely reason for this is that The *fru³* and *fru⁴* are due to *P*-element insertion of the same transposon, *P{PZ}*, while *fru^{sat}* and *fru²* are due to the insetion of different transposons (*{P(w⁺ry⁺)A}* and *P{IwB}* respectively), which share some sequence similarity (Goodwin *et al.* 2000). Insertion of an identical *P*-element in alternate orientations has also been shown to produce different arrays of novel transcripts at the *fru* locus (Dornan *et al.* 2005).

A method of introducing small and precise mutations into the exons encoding *fru* type-A and -B zinc finger domains was required so that the functional contribution of isoforms containing each of these domains could be assessed. The recently described technique of gene targeting by homologous recombination is one such method that lends itself well to these requirements.

4.1.2 Gene Targeting by Homologous Recombination

Gene targeting by homologous recombination is a powerful strategy which can be used to mutagenise genes and investigate their function. First performed in yeast (Hinnen *et al.* 1978), the technique was successfully adapted to enable modification of *Drosophila* genes *in vivo* (Rong and Golic 2000), and has since been implemented at more than 20 different loci. Targeting efficiency varies from locus to locus, perhaps dependent on chromatin structure (Reviewed by Gong and Rong 2003). However, efficient gene targeting has been accomplished at the *fru* locus before (Demir and Dickson 2005, Stockinger *et al.* 2005, Manoli *et al.* 2005), suggesting that it may be possible to efficiently disrupt individual isoforms of *fru*.

There are two routes available to achieve gene targeting by homologous recombination: ends-in and ends-out (see Figures 1.8 and 1.9). Ends-in targeting has been shown to be more efficient than ends-out targeting in yeast and mammalian cells (Hasty *et al.* 1991, Hastings *et al.* 1993), and initial attempts to

perform ends-out in *Drosophila* were unsuccessful (Bellaiche *et al.* 1999). More recently ends-out targeting has been achieved in *Drosophila* with targeting efficiency comparable to that attained with ends-in. However, there are features of ends-in targeting which make this route more suitable for the precise manipulation of endogenous genes.

Instead of replacing the target locus with a truncated copy or deleting it entirely, as is the case with ends-out targeting, ends-in can be used to introduce small, precise mutations which accurately modify the gene products of the locus, rather than simply abolishing all function (Rong *et al.* 2002). Ends-in targeting has also been successful in simultaneously disrupting two small genes within a small gene cluster (Dolezal *et al.* 2003), and it is reasonable to speculate that this strategy could be used to simultaneously target the adjacent A- and B-type zinc finger domain encoding exons of the *fru* locus.

Additionally, with ends-out targeting, the marker gene is retained once targeting is complete unless recombination sites such as *loxP* are also engineered into the donor construct. The second step of ends-in targeting automatically eliminates the marker gene, so that it cannot interfere with subsequent phenotypic analysis. Given that *fru* plays such a crucial role in male courtship behaviour, any gene targeting strategy to modify this gene by homologous recombination must eliminate this marker from the final targeted locus. In light of these concerns it was decided to follow an ends-in protocol to specifically target, by homologous recombination, the type-A and -B zinc finger encoding exons of the *fru* locus.

4.2 Design of Gene Targeting Construct

4.2.1 Targeting Vector

The *P*-element vector pTV2 was selected for use as the targeting vector as it had been used in previous, successful ends-in targeting studies (Rong *et al.* 2002, Dolezal *et al.* 2003). The vector has transposition sequences at the extreme 5' and 3' ends to facilitate integration into the target genome. Inside those *P*-element ends are directional FRT sequences, which allow *FLP* recombinase to excise the donor section of the targeting construct as an extrachromosomal circle. The region of donor DNA, which acts as homology in the targeting

process, is inserted into the vector using a multiple cloning site (MCS). A marker gene, *mw*, allowing the integrant to be phenotypically scored during the targeting process is included, as is an I-*Crel* site-specific endonuclease recognition site, which will be used to induce a double strand break (DSB) in the final step of targeting to resolve the gene duplication.

4.2.2 Choosing Targeting Homology Region

Two main factors must be considered when choosing a genomic stretch of DNA to act as donor DNA in ends-in gene targeting. Firstly, DNA with sufficient sequence homology to the target locus must be selected to enable efficient targeting *in vivo*. Extended donor-target homology has been shown to increase targeting efficiency (Deng and Capecchi 1992, Papadopoulou and Dumas 1997, Rong *et al.* 2002). While 40bp of donor-target homology is sufficient to allow gene targeting to occur in yeast, at least 2kb of homology is necessary to direct gene targeting in mouse ES cells (Deng and Capecchi 1992). Gene targeting has been performed in *Drosophila* using as little as 2kb of homology (Rong and Golic 2001), but for efficient targeting it has been recommended to include at least 4kb (Rong and Golic 2000, Reviewed by Bi and Rong 2003). The second important point to consider is the positioning of the I-*Scel* site, which will be used to induce the DSB. When homologous recombination occurs at this DSB, gene conversion can repair to wild-type any mutations close to the DSB, by using the homologous chromosome as a template. Given that the average length of conversion is approximately 1.3kb (Gloor *et al.* 1991), the distance between the I-*Scel* site and engineered mutations within the targeting construct must be chosen carefully.

As the type-A and -B zinc finger encoding exons are adjacent within the *fru* locus it was decided to target both of them using one targeting construct. In addition to reducing fly screening numbers by half, this may allow different combinations of Fru^A and Fru^B mutants to be generated, depending upon gene conversion and final resolution events. To help ensure that no functional protein was produced for each of the targeted zinc finger isoforms, mutations were introduced near to the beginning of each exon. Premature in-frame stop codons were introduced into each exon as shown in Figure 4.2B.

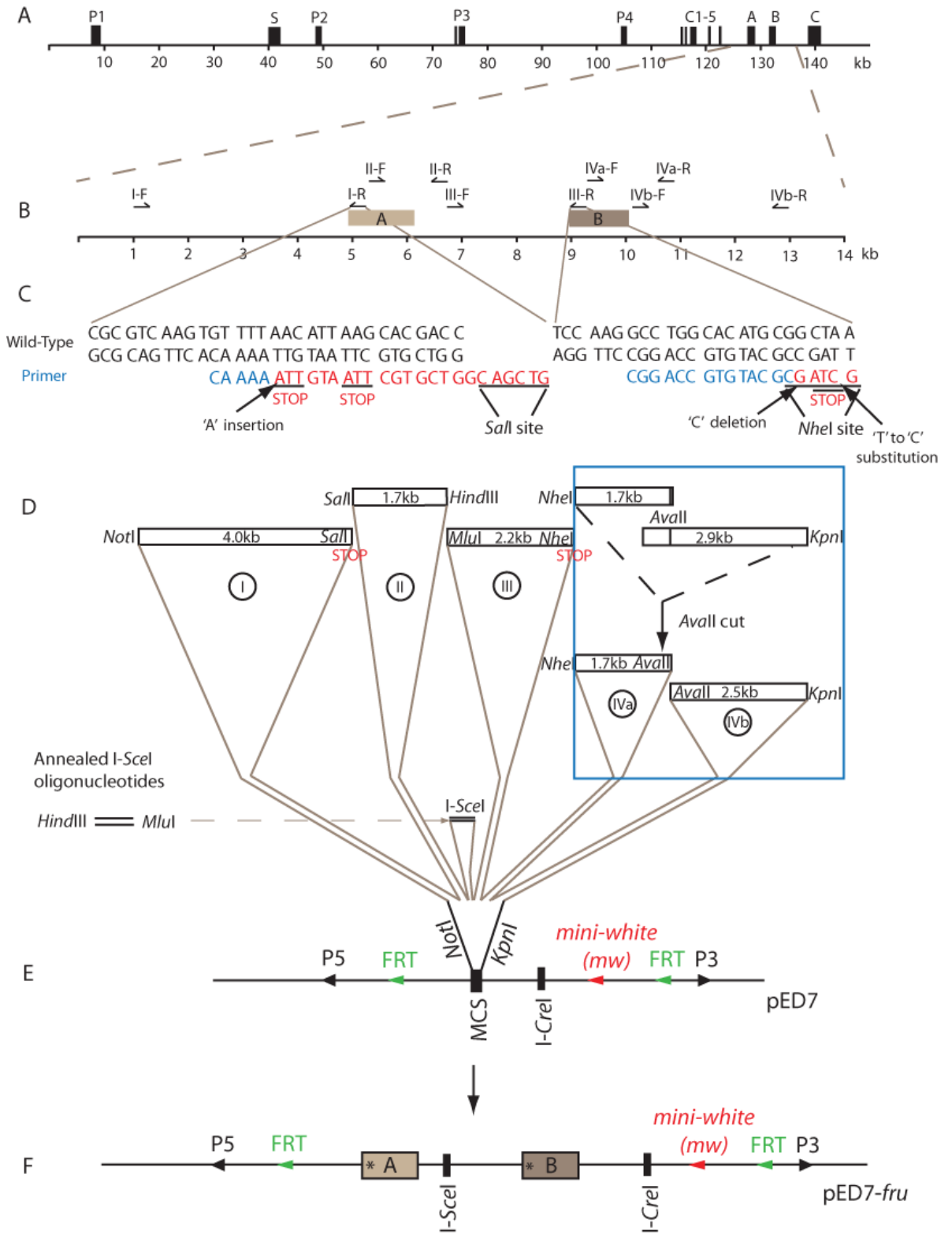


Figure 4.2 - Generation and Cloning of Donor Construct for Gene Targeting of *fru* Locus.

Figure 4.2 - Generation and Cloning of Donor Construct for Gene Targeting of *fru* Locus. (A) Entire *fru* locus. Promoters and exons represented by black boxes. Size of locus indicated in kb. (B) Enlarged view of target locus. PCR primer positions, forward (F) or reverse (R) are indicated by half arrows. Numbers on arrows indicate the fragment (I-IV) amplified by a particular primer set (fragment IV was amplified in two pieces, 'IVa' and 'IVb'). Exons A and B are represented by grey boxes. (C) Nucleotide sequence of primers used to introduce point mutations into coding sequences of exons A and B, compared to wild-type sequence. Induced point mutations and resultant stop codons are indicated as are the novel diagnostic restriction sites engineered into the primers. (D) Sizes of PCR fragments used to assemble the donor construct. Generation of sequence required for fragment 'IV' by restriction digestion of fragments 'IVa' and 'IVb', indicate by area inside blue box. Restriction sites used to clone PCR fragments and annealed oligonucleotides into pED7 vector. (E) Restriction sites of pED7 vector used to clone donor construct and relative positions of elements within the vector. (F) Final assembled gene targeting construct, pED7-*fru*. Introduced exon mutations represented by a star (*).

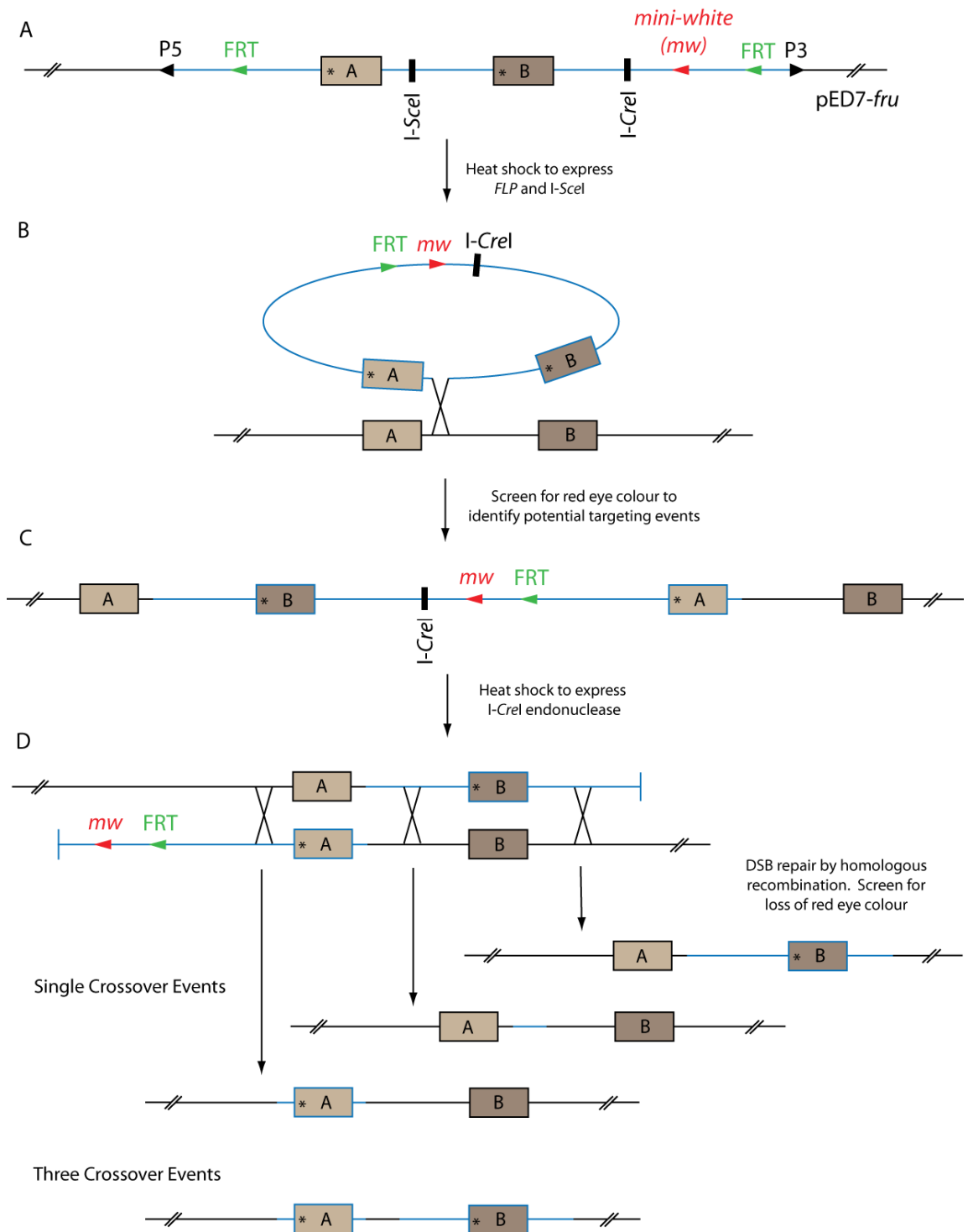


Figure 4.3 - Molecular Representation of Gene Targeting Process at the *fru* Locus. (A) Donor construct integrated at random location on second chromosome. Endogenous DNA represented by black line, DNA of targeting construct shown by blue line. Arrowheads indicate components of targeting construct; *P*-element ends (black), FRT sequences (green) and *mw* marker gene (red). I-SceI and I-CreI endonuclease sites are represented by thick black lines. (B) Excision and circularisation of donor construct through the action of FLP recombinase. Induction of DSB by I-SceI endonuclease and insertion of donor construct. (C) Red-eyed re-integrants are isolated and mapped to chromosome of insertion. (D) Formation of DSB by I-CreI endonuclease, inducing resolution of targeted duplication by homologous recombination, characterised by loss of eye colour. Potential resolution events and resulting mutant combinations of exons A and B.

The distance between the beginning of exon A and exon B is 4kb and accordingly it was decided to locate the *I-SceI* site roughly equidistant from the start of each exon. Taking the issue of gap expansion into account, this position was chosen to promote equal inclusion of each mutation at the target locus. It was also decided to include approximately 4kb of sequence homology upstream of exon A and 4kb downstream of exon B to produce a 12kb donor stretch of DNA. This should not only enable efficient targeting, but also promote equal frequencies of recombination events between the introduced mutations during the duplication resolution step of gene targeting (see figure 4.2D and Figure 4.3D). Depending on the sites of recombination during resolution, different combinations of mutations may be obtained, and the phenotypes of such single and double mutants would be very informative with regard to the specific, individual and combinatorial functions of each zinc finger containing domain.

4.2.3 Introduction of Mutations into Donor DNA

It was decided to amplify the 12kb stretch of donor DNA by PCR in four adjacent fragments. PCR primers were designed so that the three internal junctions between these fragments were located at the beginning of exon A, the beginning of exon B and a third in the middle of these two points (see Figure 4.2B). The positioning of these junctions enabled the desired mutations to be engineered into the PCR primers and subsequently incorporated into the exons encoding the A- and B-type zinc finger domains. A novel restriction enzyme cut site was also engineered into each PCR primer to enable the individual fragments to be ligated together for assembly of the final targeting construct. These restriction sites also served another equally important purpose. As both generated mutations were now associated with a novel restriction site, these sites could be used diagnostically, post-targeting, to determine the presence or absence of the mutations carried by the donor DNA. The third and central junction, between exons A and B, was utilised to introduce the *I-SceI* novel restriction site into this section of donor DNA. Complementary oligonucleotides containing the recognition sequence for *I-SceI* endonuclease were annealed to generate a double stranded *I-SceI* restriction site. Also included in these oligonucleotides were the restriction sites found at the ends of the two fragments of the central donor junction. A different restriction site was used at each side of the junction

to ensure that only one *I-SceI* site would be incorporated into the final construct in one orientation.

4.2.4 Amplification of Donor DNA fragments

To generate the quartet of fragments required to obtain 12kb of donor:target homology, four PCR primer pairs were designed. Numerous trials, using different DNA templates, DNA polymerases and various PCR amplification conditions were performed to generate the desired regions. Several subtle variations on each primer pair were designed and after optimisation of each reaction, three of the four desired fragments were isolated. It was not possible to amplify the final 4kb fragment, which included most of the B exon, in one piece. This was due to the low GC content of the region around exon B, forcing the melting temperatures of 5' primers to be very low and making PCR amplifications of the complete 4kb product very difficult. Thus, it was decided that the final fragment should be amplified in two separate parts (see Figure 4.2D).

In the previous chapter a 582bp fragment was amplified by PCR from the start of exon B to use to raise a polyclonal antibody. The 3' primer from that reaction was used with the 5' primers designed for use in amplifying fragment IV. That these newly paired primers were able to generate the expected product showed that the 5' primers designed to generate the final donor fragment were indeed able to amplify DNA fragments from the within the zinc finger B exon. The existing 3' primers designed to amplify the fragment were used in conjunction with 5' primers, previously designed for sequencing the fragment, to amplify progressively larger portions of desired region. 5' sequencing primers of increasing distance from the position of the 3' donor construct primers were employed until PCR could not generate fragments of the expected size. At this point a 3' primer was designed to use in conjunction with the existing 5' fragment IV primers. This new primer was designed to amplify a 1.7kb DNA fragment from the beginning of B exon end that would overlap the largest fragment (2.9kb) obtained in amplification from the distal end. The sequence of the overlap region was chosen so that it contained a restriction enzyme cut site, *Avall*, that was not present elsewhere in either fragment. This unique restriction site enabled both products to be cut with *Avall* and ligated together to form the final donor fragment of the targeting construct. All PCR products

were purified and cloned into the TOPO TA Cloning vector (Invitrogen). Plasmids that contained the desired insert were purified and sequenced twice to verify that no mutations, other than the ones specifically engineered into the construct, were incorporated during PCR amplification.

4.2.5 Cloning Strategy

The multiple cloning site (MCS) of the pTV2 targeting vector was cut with the two restriction enzymes whose sites had been engineered at opposite ends of the designed section of donor DNA. However, following size fractionation, the observed DNA bands were not as predicted. The source of this vector, *Drosophila* stock centre (Bloomington, University of Indiana), was consulted, and confirmation was received of errors in the sequence of the vector. As a result of this, the vector was withdrawn from their catalogue. Attempts to obtain a bona fide version of pTV2 from other sources were unsuccessful and, hence, another compatible gene targeting vector had to be found. An unpublished vector for ends-in gene targeting, pED7, was generously provided by B. Dickson (IMBA, Austria). This vector included all of the important features of the pTV2 vector, including the required restriction enzyme sites necessary for inclusion of the donor DNA insert. The donor region fragments and annealed oligonucleotides for I-SceI site were ligated into the pED7 vector as shown in Figure 4.2E. The sequence of the assembled pED7-*fru* construct was then verified by DNA sequencing.

4.3 Targeting the *fru* locus

4.3.1 Obtaining Targeting Construct Transformants

Before gene targeting can be initiated, the donor construct must be inserted into the target genome by *P*-element transformation. The pED7-*fru* construct was microinjected into white-eyed (*w*) fly embryos (Genetic Services Inc., Cambridge, MA). Mature adults were mated with flies of the white-eyed *w*¹¹⁸ line and transformants were isolated on the basis of red eye colour conferred by presence of the *mw* marker gene in the targeting construct. 45 independent transformant lines were selected and the chromosome of insertion for these lines was determined by a series of crosses to chromosome balancer lines.

When a gene on the third chromosome is to be targeted, *P*-element insertions on the second or X chromosomes are used. This is to enable distinction, in later steps, between targeted insertions at the desired locus and re-insertions of the donor DNA section at the point of the original insertion locus. Accordingly, a healthy transformant line possessing an insertion on the second chromosome was chosen as the starting point for the gene targeting process.

4.3.2 First Step Crosses: Integration at Target Locus

Once a suitable transformant line was established, the gene targeting process commenced using the genetic crosses outlined in Figure 4.4. The first step of gene targeting excises the donor construct from its original insertion site, enabling it to integrate at the target locus (Figure 4.4A).

For the first step, transformant virgin females were crossed to males of the M690 line. M690 carries the heat-shock *hid* (*hs-hid*) gene on the Y-chromosome, and heat-shock *FLP recombinase* (*hs-FLP*) and *Scel endonuclease* (*hs-I-Scel*) genes on the second chromosome. *hid* (head involution defective) is a cell death regulator, involved in the control of apoptosis during development (Kurada and White 1998). The heat-shock that induces expression of *hs-FLP* and *hs-I-Scel* also engenders *hs-hid* expression, killing all male progeny and ensuring that all female offspring are collected as virgins. 150 virgin females were grouped with 50 males in a bottle for two full days. On the morning of the third day, surviving adults were transferred to a fresh bottle. The initial bottle, containing young larvae, was immediately heat-shocked for one and a half hours at 38°C and then again for one hour, 24 hours after the initial heat-shock. In total 1100 virgin females were crossed and each group was transferred into a fresh bottle approximately ten times.

From this cross, 7500 virgin females were collected for the second cross of the gene targeting process (4.4B). Collected females usually had completely white eyes due to absolute loss of the targeting construct in somatic cells, but some had white and red mosaic eyes due to partial retention of the construct in the soma. Here, 200 females were grouped with 100 M699 males in bottles. Again, after three days, adults were transferred to fresh bottles. Although both parental lines in this cross have white eyes, a small number of maternal gametes possess a re-integration of the targeting construct, which leads to red-eyed

offspring. In total, approximately 110,000 flies were screened for red eye colour. All red-eyed progeny were selected and crossed to M700 and M701 lines to determine on which chromosome the re-integration events had occurred.

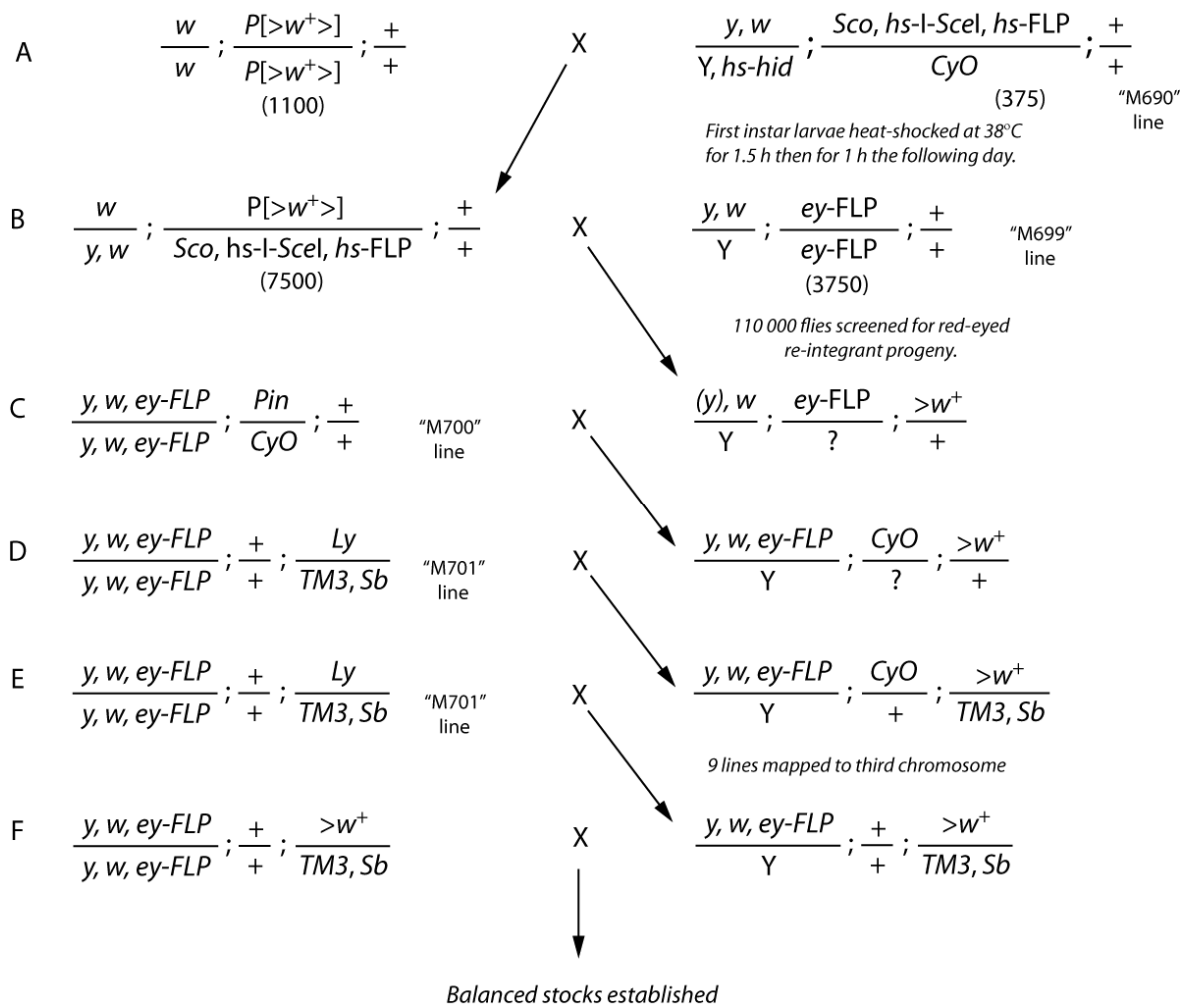


Figure 4.4 - Genetic Crossing Scheme to Achieve Targeted Integration of Donor Construct at *fru* Locus. (A) First instar larvae were heat-shocked to excise the randomly integrated donor construct and induce a DSB to facilitate re-integration at the target locus. The heat-shock is also lethal to all male progeny. Numbers of flies crossed in parentheses. (B) Progeny of the next cross to M699 males are screened for red eye colour conferred by the w^+ marker gene, indicating a putative re-integration event. (C-E) Crosses to second and third chromosome balancer lines (M700 and M701) to establish the chromosome of insertion for all re-integration lines. (F) All independent lines carrying re-integration events on the third chromosome were established as balanced stocks for molecular verification. Fly lines M690 and M699-M701 donated as kind gift by B. Dickson (IMBA, Austria).

The M699 line, and all subsequent lines used in the first step of the targeting scheme, carried the *ey-FLP*. This transgene places *FLP* recombinase under the control of an eye-specific enhancer element from the *eyeless* gene, and is

expressed in the eye disc from second instar stage onwards (Halder *et al.* 1995). Expression of *ey-FLP* in progeny of the remaining crosses ensured the excision of any copies of the gene targeting construct that may have evaded initial heat-shock mobilisation. This confirmed that all observed red-eyed progeny possessed this eye colour phenotype due to re-integration of the targeting construct. As *fru* is on the third chromosome, all lines with targeting construct re-integrations mapping to the third chromosome were selected to isolate targeted integration events. Seventeen recombinant lines in total were identified with successful re-integration events and of these lines, nine were found to map to the third chromosome (Figure 4.4F).

4.3.3 Analysis of Integration Events

4.3.3.1 Verification by PCR

4.3.3.1.1 Excision and Re-Integration

Primers were designed to confirm that the FRT sites of the targeting construct had come together, by the action of *FLP* recombinase, and that the excised donor construct had been re-integrated into the genome (Figure 4.5B-E). Genomic DNA (gDNA) was isolated from all nine of the re-integration events on the third chromosome and subjected to PCR analysis, as was gDNA from the original insertion line and *Canton-S* flies to act as negative controls (see Figure 4.5E). As expected, the original line carrying the *P*-element inserted construct on chromosome two did not generate a PCR product, as the FRT sites had not been brought together. Likewise a wild-type (*Canton-S*) negative control did not generate a PCR product as no FRT sites are present in the wild-type genome. The results for the re-integrants showed that, in all nine lines, the donor construct had been excised as an extrachromosomal circle and had re-integrated with the FRT sites adjacent to each other.

4.3.3.1.2 Targeted Insertion and Inclusion of Mutations

The first PCR amplification confirmed excision and re-integration of the donor construct but further analysis was required to determine whether these re-integrations on the third chromosome were targeted to the *fru* locus or non-targeted, random events. PCR primers specific to the *fru* locus were used to determine targeted integration. The primers were designed such that a product

would be generated from the endogenous *fru* locus and the introduced *fru* sequence of a successfully targeted donor re-integration event, but not a non-targeted event (see Figure 4.6A-D). The amplified region included exon A and, as the mutant version of this exon carried by the targeting construct also included a novel restriction enzyme site (*SalI*), this PCR product could then be used to determine whether the mutation was present in targeted events at the *fru* locus.

Genomic DNA, isolated from all nine transformant lines, was used for PCR analysis. Successfully amplified products were restriction digested with *SalI* and size fractionation revealed that five re-integrant lines, not only possessed targeted events at the *fru* locus, but also carried a copy of exon A with the engineered mutation (lines 1 and 3-6). As expected, the initial *P*-element construct line produced a PCR product which was cut with *SalI*, as it carried a copy of the targeting construct in its original conformation. The *Canton-S* control line produced a PCR product which was not cut by *SalI*, as the mutation was not present. Of the nine putative targeted lines, all successfully produced an amplification product of expected size, but only five lines (1 and 3-6) possessed the engineered novel *SalI* restriction site at the *fru* locus, which allowed their status as bona fide targeted re-integrations to be verified.

A similar pair of primers was designed to detect lines which possessing a targeted event that had also retained a mutant version of exon B. However, as with the amplification of fragment IV for assembly of the targeting construct, it was not possible to generate a large PCR product including the region immediately 3' of the mutation engineered into exon B. As it was not feasible to amplify this region in two sections and still perform the screen for targeted events, a new pair of PCR primers designed to screen solely for mutated versions of exon B. All nine re-integrant lines successfully produced an amplification product of expected size, but only eight lines (lines 1-2 and 4-9) were shown by restriction digest mapping to contain a novel mutant version of exon B.

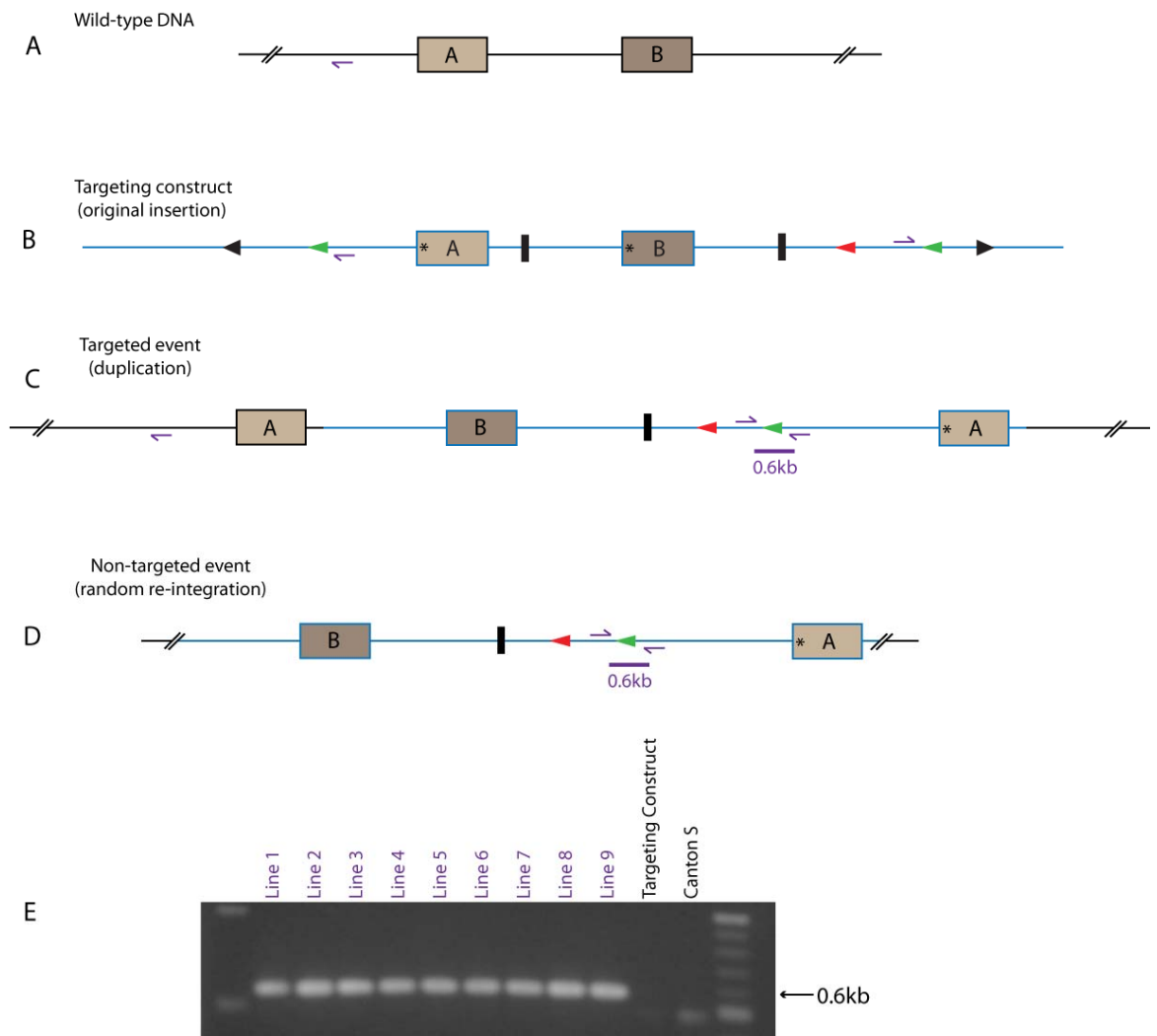


Figure 4.5 - Verification of Re-integration Events by PCR. (A-D) Predicted molecular organisation of region of interest within screened lines. Direction of PCR primers is indicated by half arrows (purple). One PCR primer binds at the beginning of *fru* region used as the donor DNA stretch in gene targeting. The other primer binds within the targeting vector DNA sequence. (A) In wild-type there is no targeting vector insert so no PCR product can be generated. (B) In the second chromosome initial insertion line the primers bind at opposite ends of the integrated construct in an orientation which prevents the generation of PCR products. (C and D) In targeted and non-targeted re-integration events the opposing ends of the donor construct are brought together by *FLP* recombinase. This enables a PCR product of approximately 600bp to be generated. (E) Amplification products from 9 re-integrant lines were electrophoresed on a 1% agarose gel. Genomic DNA from the original insertion line (Targeting Construct) and a wild-type control (*Canton-S*) were also screened as negative controls. All recombinant lines were in heterozygous combination with a wild-type third chromosome. Lines that generated the diagnostic 0.6kb are confirmed re-integration events and are shown in purple.

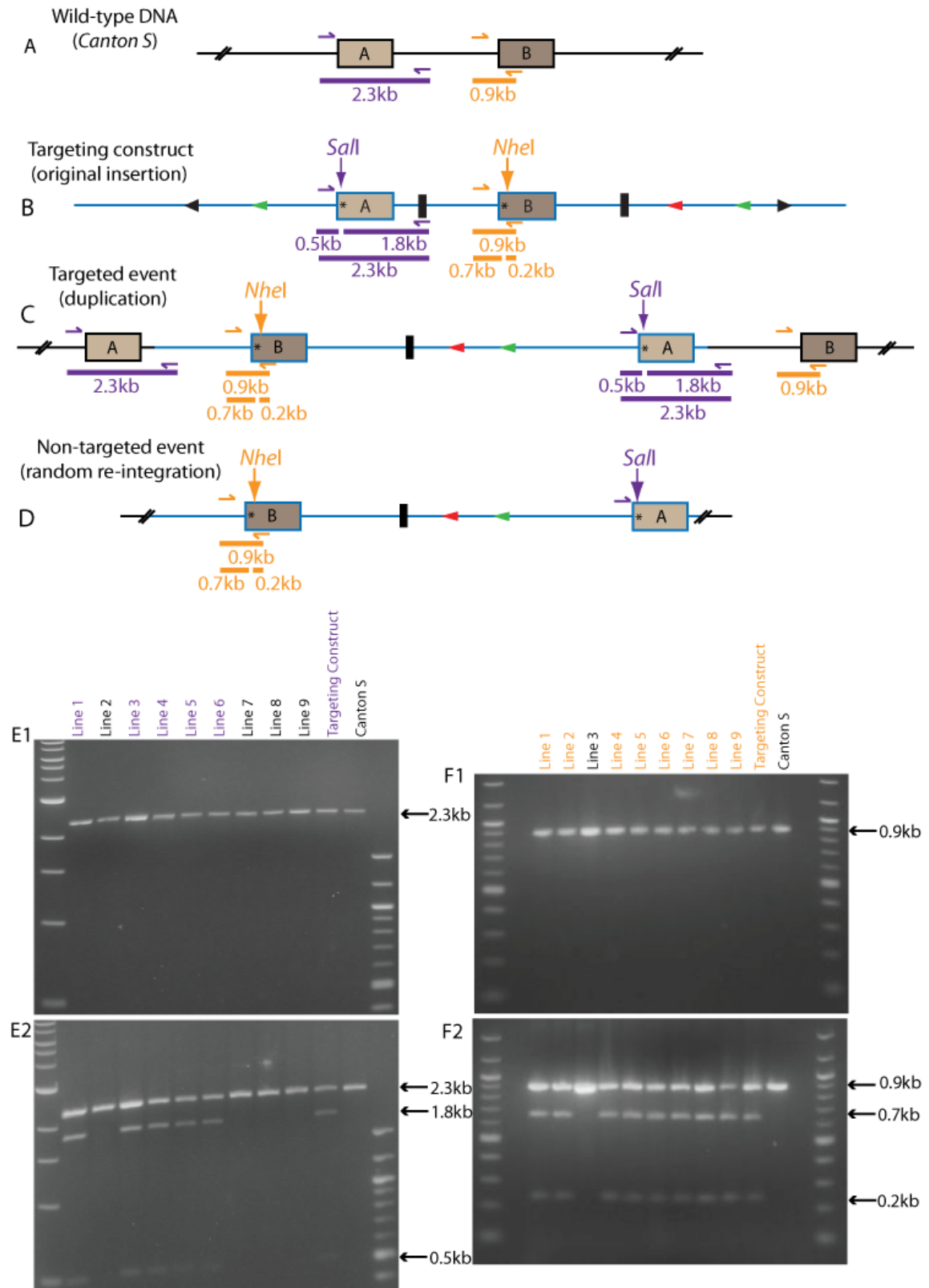


Figure 4.6 - Verification of Targeted Events and Mutation Screens by PCR and Restriction Digestion.

Figure 4.6 - Verification of Targeted Events and Mutation Screens by PCR and Restriction Digestion. (A-D) Predicted molecular organisation of region of interest within screened lines. Direction of PCR primers for exon A and exon B screens is indicated by half arrows (purple and orange respectively). (A) In the wild-type control only uncut DNA is produced as the wild-type line does not carry the engineered mutations. (B) The initial insertion line generated products that were cut with both diagnostic restriction enzymes. (C and D) Both targeted and non-targeted events were able to produce PCR products carrying the exon B mutation. Only targeted events were able to generate PCR products possessing the exon A mutation. (E1-2 and F1-2) Screen for mutation engineered into exon A. (E1 and F1) Amplification products from 9 re-integrant lines were electrophoresed on 1.5%(E) and 2%(F) agarose gels. Genomic DNA from the original insertion line (Targeting Construct) and a wild-type control (*Canton-S*) were also screened as positive and negative controls respectively. All lines generated the predicted PCR products. (E2 and F2) PCR products were cut with relevant restriction enzyme (*SalI* or *NheI*) to determine whether the novel restriction site, associated with each engineered mutation, was present within each line. Presence of mutation in exons A is indicated by cutting of the original 2.3kb PCR product into 1.8kb and 0.5kb bands. The B mutation is characterised by cutting of the 0.9kb PCR product into a 0.7kb and 0.2kb band. Lines carrying A or B mutations are shown in purple and orange respectively. Five re-integrant lines (1, 3-6) exhibited presence of the engineered mutation within exon A whilst eight lines (1-2, 4-9) were found to carry the mutation in exon B. Due to the design of the PCR primers, the detection of the exon A mutation in 5 re-integrant lines also confirms that these lines (1, 3-6) represent targeted events at the *fru* locus. As predicted, both mutations were detected within the original insertion line (Targeting Construct) and as expected no mutations were detected in the negative control line. All lanes show presence of uncut, wild-type-like, product as all recombinant lines were in heterozygous combination with a wild-type third chromosome.

4.3.3.2 Verification by Southern Blot

To further molecularly verify the re-integration events, Southern blot analysis was performed. Genomic DNA probes were designed to hybridise to exon A and exon B regions. The exon A region probe was able to produce a clear hybridisation banding pattern and was used to investigate each of the nine recombinant lines. Several probes were synthesised to hybridise to the exon B region but, for reasons unknown, none were able to produce clear membrane hybridisation. The region surrounding exon B also proved difficult to amplify, both in this study and in previous attempts to generate an Fru^B antibody (Troy Carlo, pers. Comm.).

To analyse the exon A region, gDNA was isolated from each of the nine recombinant lines and restriction digested with *Sa*I (the restriction site engineered into exon A mutation). Southern blotting was then used to hybridise with a 1.3kb gDNA probe designed to screen the exon A region (see Figure 4.7). Genomic DNA isolated from all eight lines used in the gene targeting procedure were included in the blot as controls, as was gDNA from the targeting construct initial insertion line. All control bands were 16.2 kb in size, representing a wild-type *fru* locus. The five recombinant lines identified by PCR as carrying a mutant copy of exon A as part of a targeted duplication of the *fru* locus (*lines 1, 3-6*) all exhibited two additional smaller bands as predicted, in addition to a larger band corresponding to the wild-type version of exon A, present within the duplication. Of the remaining four recombinant lines, two (*lines 2 and 7*) produced a single, large band as expected, representing a targeted duplication at the *fru* locus without carrying a mutated copy of exon A. The two other lines (*lines 8 and 9*) produced a large band corresponding to a wild-type copy of exon A, but also exhibited two smaller bands. One of these bands was smaller than that observed in the four targeted duplication lines possessing a mutant copy of exon A. No mutant version of exon A was detected in PCR screens with *lines 8* and *9*, but the exon A PCR screen was designed to detect only copies of exon A that were present at the *fru* locus. The PCR and Southern blot results suggest that these two lines represent non-targeted re-integrations on the third chromosome at a location other than the target locus. This will be investigated further in chapter 5.

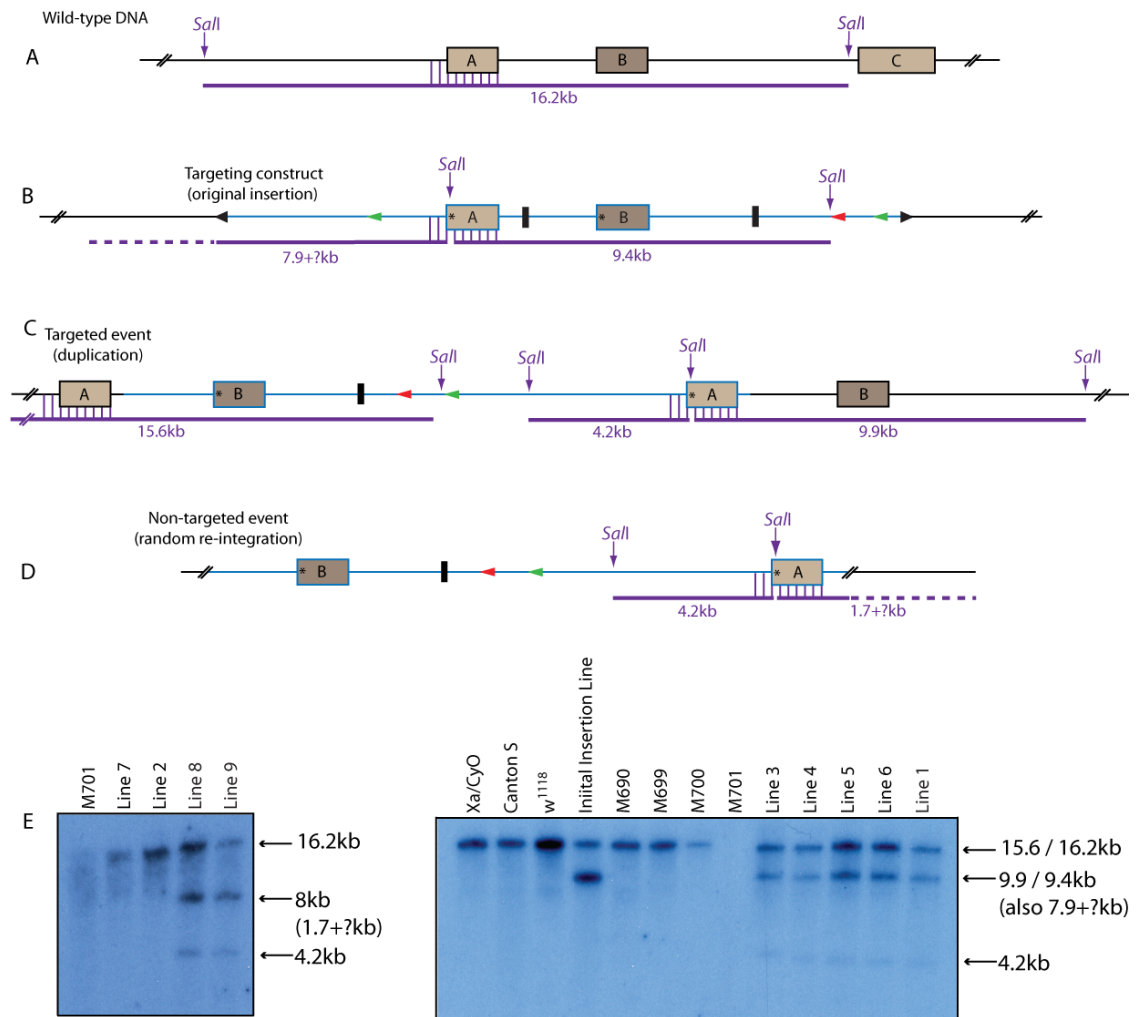


Figure 4.7 - Southern Blot Analysis of Targeting Events. (A-D) Schematic diagram showing the predicted molecular organisation within screened lines. *SalI* restriction sites are indicated by purple arrows and the region of DNA hybridised by the probe is shown by hatched purple lines. (A) The wild-type *fru* locus produces a single 16.2kb band. (B) The original construct insertion is expected to produce one 9.4kb band and a second band 7.9kb or larger, depending upon its insertion site. (C) A targeted duplication at the *fru* locus containing the expected single mutant version of exon A produces three bands of sizes 15.6kb, 9.9kb and 4.2kb. (D) A non-targeted re-integration event is expected to produce one band of 4.2kb and a second band of 1.7kb or larger, depending upon the site of insertion. As all novel recombinant lines were present in heterozygous combination with a wild-type third chromosome, a 16.2kb band was observed for all nine lines as expected. (E) Genomic DNA was restriction digested with *SalI* and the membrane was hybridised with a 1.3kb gDNA exon A probe.

4.3.4 Second Step Crosses: Resolution of Duplication

Nine recombinant lines had been isolated, though only a subset of these appeared to contain both mutant exons A and B. The second step in the gene targeting process is to resolve the resulting duplication by inducing a double stranded break between the two copies of the target locus. Resolution of the duplication will be accompanied by complete or partial loss of the *mw* marker gene, and reduction events will be characterised by either a white or mosaic eye colour.

To achieve resolution single virgin females carrying a heat-inducible *I-Crel* endonuclease transgene were paired with single males from one of the duplication lines (Figure 4.8A). Three days later, the mating pairs were transferred to a fresh vial and the initial vials were heat-shocked at 36°C for one hour. Thereafter the adults were transferred to fresh vials, every two days, for on average ten times. Males from six independent duplication lines (lines 1-6) were used, as use of multiple lines increases probability of obtaining resolution of the target locus duplication (E. Demir and B. Dickson, pers. comm.).

Males with the appropriate genetic markers were crossed to the females of the third chromosome balancer line M701. Progeny of both sexes with the correct genetic markers were screened for loss of the *mw* marker gene. Despite approximately 50,000 flies being screened none exhibited loss of the *mw* marker.

The possibility that no resolution events were isolated because such events are extremely rare is unlikely. Previous studies suggested that tandem duplications at the target locus are resolved, on average, in one third of flies of the appropriate genotype (Rong *et al.* 2002). This implied that cutting at the *I-Crel* site was not efficient. To assess the technique used to induce resolution of the *fru* locus duplication, a strain carrying a previously studied tandem duplication was obtained from Y. Rong. Resolution events are known to occur efficiently with this line (Y. Rong, pers. comm.). The resolution process was repeated using this control line and all flies carrying both the targeted locus and *I-Crel* endonuclease exhibited eye-colour mosaicism. This illustrated that the resolution step conditions are able to induce reduction of duplicated loci to a single copy and suggested that the *I-Crel* site within the targeting construct of

the targeted *fru* integrant lines may be defective. To investigate this further, the I-*Crel* site in the pED7 vector was sequenced. The sequence present was found to differ at two base pairs, within the region usually conserved in functional I-*Crel* sites (Jurica *et al.* 1998). In light of this discovery a novel I-*Scel* site was introduced into the pED7-*fru* vector, which was sent for microinjection.

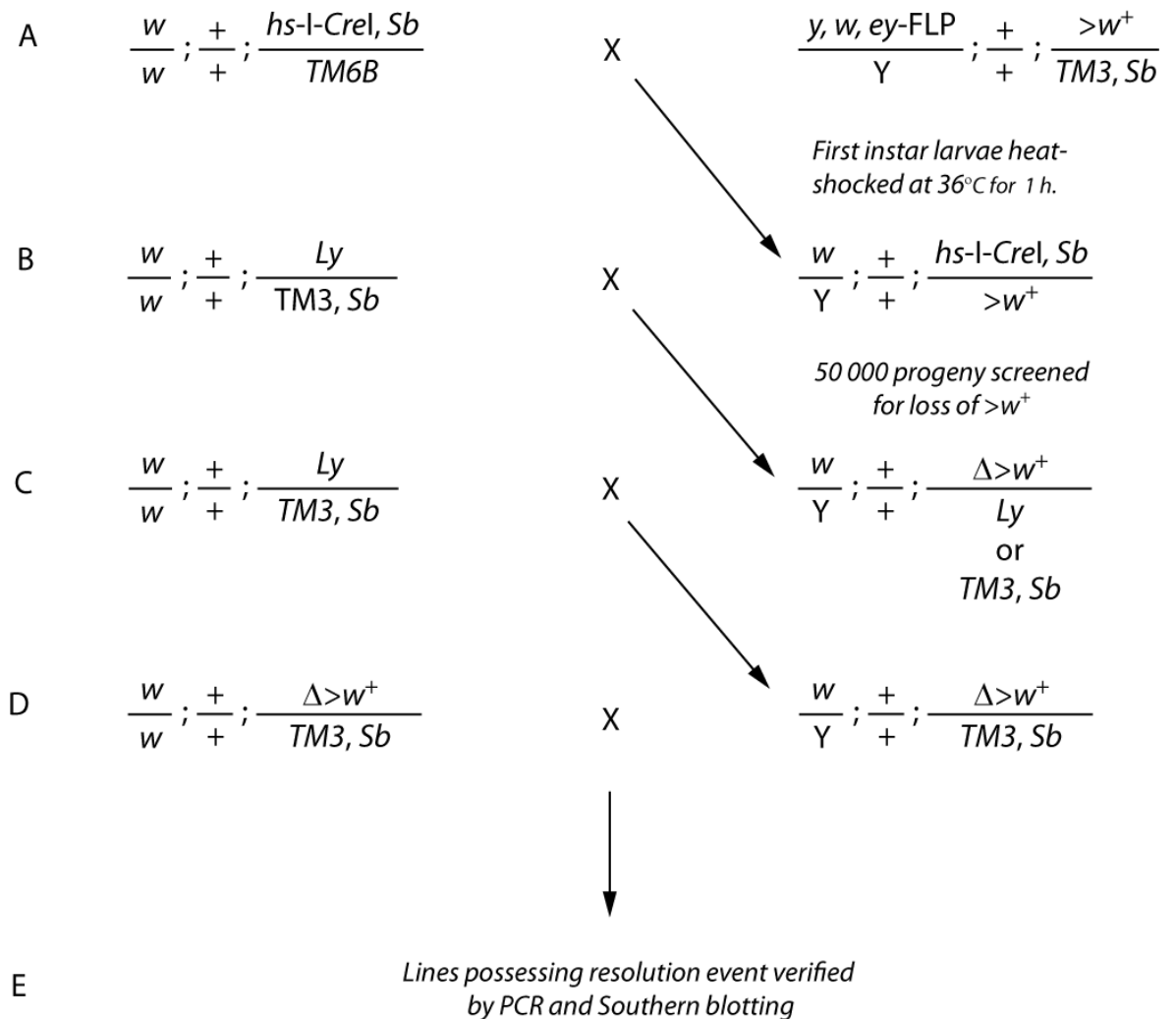


Figure 4.8 - Genetic Crossing Scheme to Resolve Targeted Duplication at *fru* Locus. (A) Six independent lines carrying a targeted duplication at the *fru* locus were crossed the *hs-I-Crel* line and heat-shocked to induce a DSB at the I-*Crel* cut site. (B) Male progeny carrying both a copy of *hs-I-Crel* and a targeted duplication were crossed to a third chromosome balancer and screened for loss of red eye colour. (C-E) Any progeny possessing resolution events should then be established as a balanced stock line for verification by PCR and Southern blotting.

4.4 Discussion

In this chapter, the design of a gene targeting construct was described and the two step process of ends-in gene targeting by homologous recombination was

outlined. Screening assays to detect targeted events at the *fru* locus were established, to isolate *fru* alleles in which specific isoform subsets were disrupted. The results and relative efficiency of each step in the targeting process is described in detail below.

4.4.1 Targeting Construct Design

The success of any gene targeting construct is dependent largely upon the design of both the targeting vector used to integrate the construct, and region of homology used to home in on the target locus.

4.4.1.1 Targeting Vector

The pTV2 vector was selected to integrate the entire targeting construct into the target genome as it has been used successfully to disrupt single gene loci (Rong *et al.* 2002) and multiple gene targets simultaneously (Dolezal *et al.* 2003) by ends-in targeting. Errors identified by this study in the sequence of the pTV2 vector supplied by the *Drosophila* stock centre (Bloomington, University of Indiana) required the withdrawal of this vector and dictated that an alternative targeting vector was required. Thus, the pED7 targeting vector was used to initiate ends-in gene targeting.

Following microinjection into *Drosophila* embryos, the *P*-element ends of the pED7 vector allowed the targeting construct to integrate successfully into the target genome, leading to the isolation of 45 transformant lines. That these transformants were successfully identified by the presence of red eye colour, also illustrated that the exogenous *mw* marker gene carried by the targeting vector was fully functional. Successful excision of the donor DNA section of the construct during the first step of the gene targeting process also provided evidence that the *FRT* sites of pED7 function fully *in vivo*. That no resolution events were observed in the second step of the gene targeting process appeared to be due the fault the I-*Crel* site, discovered by sequencing the site.

4.4.1.2 Target Homology

The gene targeting construct was designed to facilitate integration of exogenous DNA, carrying engineered mutations, into the *Drosophila* genome. In turn, the

gene targeting technique is reliant upon this stretch of DNA possessing sufficient homology to direct re-integration to the target locus.

As both exon A and exon B were targeted simultaneously using the same construct, and these exons are situated approximately 4kb apart in the *fru* locus, this dictated that at least 4kb of homology had to be included in the targeting construct. This is the recommended minimum size of homology to be used in gene targeting attempts in *Drosophila* (Rong and Golic 2000, Reviewed by Bi and Rong 2003). In this study it was decided to use 12kb of DNA as homology to the target locus. It has been found in *Drosophila* and other systems that the increasing the amount of donor:target homology can significantly raise the frequency of targeted events more than fivefold (Rong *et al.* 2002). However, the fact that multiple targeted events at the *fru* locus were achieved in this investigation suggests that 12kb of homology may be sufficient for similar studies on this scale. The engineered I-*Scel* site, situated within the region of homology, was successful in generating a DSB in the extrachromosomal DNA circle released by the action of *FLP* recombinase. Seventeen re-integration events were isolated, nine of which were on the third chromosome.

4.4.2 Efficiency of Gene Targeting at Fruitless Locus

4.4.2.1 The First Step: Targeting Fruitless Locus

The first stage of gene targeting was to excise the targeting construct from its integration site on chromosome two and promote its integration at the target locus by inducing a DSB at the I-*Scel* site within the construct.

Efficiency of gene targeting varies from locus to locus. The frequency of targeted events in *Drosophila* can vary from one targeted event in 1500 gametes (0.067%) to one event in 34000 gametes (0.003%, Rong *et al.* 2002). The frequency of targeted events observed in this study was one in 12200 events (0.008%), which is well within the range of frequencies previously recorded.

4.4.2.2 The Second Step: Resolution

The second stage of gene targeting was to induce a DSB between the tandem copies of the target locus using site-specific I-*Crel* endonuclease, causing the

duplication to be reduced to a single copy through the action of homologous recombination.

A previous study of six *Drosophila* loci suggested that resolution of a targeted duplication occurs, on average, 36 percent of the time (Rong *et al.* 2002). This figure was calculated from resolution events at three different loci and the numbers of flies screened for each locus varied from 125 to 1229. The absence of any detected resolution events in 50000 flies screened, suggests a fault with either the I-*Crel* site within the pED7 vector, the fly line carrying the heat-inducible I-*Crel* endonuclease, or some other aspect of the resolution step. However, observation that the duplication line received from Y. Rong exhibits eye colour mosaicism at levels approaching 100 percent, when the resolution step is performed as before, indicates that the fly line carrying I-*Crel* endonuclease and the heat-shock methodology are fine, and that the I-*Crel* site within the pED7 vector may be defective.

4.4.3 The I-*Crel* Endonuclease Recognition Site

The wild-type homing site recognised by I-*Crel* endonuclease is a degenerate palindrome 22 bps in length. Seven base pairs are conserved between each 11bp I-*Crel* half site and sequence variations at these positions is more likely to affect cleavage activity than at those not conserved between half sites (Jurica *et al.* 1998). The I-*Crel* site of the pED7 gene targeting vector varies, not only at all positions not conserved between I-*Crel* wild-type half sites, but also at the extreme ends (positions -11 and +11) which are conserved in the wild type recognition sequence. Although, genetic analysis indicates that any single nucleotide base pair may be altered while preserving cleavage activity (Argast 1998), and mutation at position +11 alone does not alter enzyme binding or activity (Jurica *et al.* 1998), the multiple sequence variations within the pED7 site may have caused reduced I-*Crel* endonuclease cleavage. The combined impact of sequence variation at positions -11 and +11, and perhaps more subtle effects of variation at the non-conserved half site positions, could have reduced the efficiency of the I-*Crel* mediated gene targeting step, leading to an absence of resolution events at the *fru* locus. Anecdotal evidence now suggests that other laboratories have had similar problems (Dr Paul Garrity; Brandeis University, USA).

In light of these problems, an additional I-*Crel* site, faithful to the wild-type sequence, has been subsequently introduced into the pED7-*fru* targeting construct. This modified construct will be used for future attempts at gene targeting at the *fru* locus, and should enable resolution to a single copy of the target region to be achieved. The bona fide pTV2 targeting vector, now available again, was also re-ordered to allow future gene targeting attempts to be performed with this well studied vector.

Another factor regarding the recognition site of I-*Crel* which may also have affected resolution of lines carrying a targeted duplication is that, unlike I-*Scel*, which has no recognition site in *Drosophila*, I-*Crel* is believed to have a cut site within the 28S ribosomal subunit gene. Here, a sequence identical to the wild-type I-*Crel* endonuclease recognition site at 17 of the 22bp is present and it has been shown that this sequence can be cut by I-*Crel* in vitro (Argast *et al.* 1998). Cutting at this site on the X chromosome may have caused high levels of lethality, particularly in males, reducing the potential of recovering males carrying resolution events at the first step of the resolution process (see Figure 4.8). Reduction of the length or the temperature of the heat-shock in the resolution step may be one way in which the risk of I-*Crel*-induced lethality could be reduced.

4.5 Conclusions

In this chapter a gene targeting construct was designed to generate mutants, defective in the production of specific zinc finger-containing *fru* isoforms, by homologous recombination. Analytical methods to confirm and characterise these targeted events were devised and the relative efficiencies of the mutagenesis steps were assessed.

Precise mutations, to introduce premature stop codons into targeted transcripts, and novel diagnostic restriction sites to track these mutations were successfully engineered into an amplified region of the *fru* locus. This donor stretch of DNA was incorporated into the *Drosophila* genome and mobilisation and re-integration at the target locus was achieved. Ideally, mutants carrying only a mutated version of each of the targeted exons were desired. However, the targeted duplication lines isolated did exhibit some instantly recognisable *fru*

phenotypes and these mutants will be investigated further in the following chapter to determine whether or not these phenotypic effects are the result of a reduction of *fru* function. The transgenic lines will also be assessed to ascertain whether these lines exhibit the loss of specific zinc finger-containing isoforms.

5 Genetic Dissection of Gene Targeting Mutants

5.1 Introduction

The previous chapter described the generation of several mutant lines by gene targeting. The aim of generating these mutants was to disrupt specific subsets of isoforms, and ultimately eliminate all Fru proteins containing A and/or B-type zinc finger 3' termini. These putative *fru* mutants were obtained by insertion of DNA homologous to the target region of the *fru* locus, but carrying mutant versions of exons A and B. When resolution of the targeted duplications was not achieved, the targeting vector, complete with newly engineered I-*Crel* site, was sent for re-injection. In spite of this, time constraints dictated that analysis would have to be performed on the existing targeted duplication lines, with the caveat that these lines may not actually represent *fru* alleles. However, preliminary observations suggested that some of these targeted duplication lines exhibited anatomical phenotypes previously associated with the *fru* syndrome (Anand *et al.* 2001, Billeter *et al.* 2006b).

In this chapter, these transgenic lines will be analysed at the neuronal level to determine whether the expression of *fru* transcripts is indeed affected in these mutants. Additionally, the mutants will be studied at morphological and reproductive levels to evaluate the phenotypic effects caused by any reduction in *fru* expression, and to attempt to quantify the contribution of individual *fru* isoforms to the gene's pleiotropic roles.

5.2 Dissecting the Functions of *fruitless* Isoforms

Much is known about the roles of *fru*'s sex-specific proteins (Fru^M) and sex non-specific proteins (Fru^{Com}) but little is known about the individual roles played by each of the different zinc finger domain isoforms. This is largely due to the classes of *fru* mutant generated thus far, and the transcripts that they disrupt. Almost all previously characterised *fru* mutants reduce or abolish the expression of all *fru* zinc finger isoforms, limiting functional assignment to the zinc finger triumvirate as a whole, and preventing genetic dissection of their individual roles.

The one exception to this trend was the isolation of the *fru*^{AC} allele during an EMS screen (Billeter *et al.* 2006b). This micro-deletion in exon C introduces a

premature stop codon upstream of the type-C zinc finger domain, and prevents production of both Fru^{ComC} and Fru^{MC} functional proteins. This was demonstrated by the absence of anti-Fru^C immunostaining in *fru^{AC}* homozygotes. However, in contrast to previous *fru* mutants, positive anti-Fru^A immunoreactivity showed that type-A isoforms are unaffected (the presence of Fru^B isoforms could not be assessed as a Fru^B antibody had not been generated at that time). Elimination of all Fru^C proteins leads to reduced courtship and diminished infertility, in addition to several anatomical abnormalities. The fertility of male *fru^{AC}* homozygotes is one third of levels recorded in wild-type males. A similar reduction in fertility is observed in males possessing *fru^{AC}* in heterozygous combination with *fru* deficiency lines *fru^{A-40}* or *fru³*, which abolish production of all Fru^M proteins but not Fru^{Com} proteins. This intragenic complementation demonstrates that the reduction in fertility observed in male *fru^{AC}* homozygotes is a consequence of the absence of Fru^{MC} proteins (Billeter *et al.* 2006b).

The diminished fertility observed in males heterozygous for *fru^{AC}* is accompanied by a decrease in viability, to a level of approximately half of that observed in wild-type controls (Billeter *et al.* 2006b). However, in contrast to the reduction in fertility, this decrease in viability is also observed in females, showing that *fru^{AC}* effects on viability are not sex-specific. Additionally, heterozygotes for *fru^{AC}* and either *fru^{A-40}* or *fru³*, are fully viable in either sex, demonstrating that complete viability is dependent upon Fru^{ComC} but not Fru^{MC} proteins. It was found that the reduction in viability was associated with a number of anatomical abnormalities in both sexes, but these defects were absent in *fru^{AC}* heterozygotes in combination with *fru^{A-40}* or *fru³*. Male fertility and viability of both sexes was also assessed with individuals heterozygous for *fru^{AC}* and *fru* variants that lack all *fru* transcripts (*fru^{w24}* and *fru^{sat15}*, Billeter *et al.* 2006b). The severity of fertility and viability defects in these heterozygotes was even greater than those observed in *fru^{AC}* homozygotes, which points to a functional role for Fru^A isoforms and/or Fru^B isoforms in viability and male fertility.

Accordingly, the potential *fru* mutants, isolated by gene targeting, will be assessed with antibodies to each of the zinc finger-containing 3' termini to determine whether *fru* expression is diminished in any of these lines. This information will then be used in combination with data from fertility, viability

and anatomical investigations with these mutants in an attempt to establish the roles played by type-A and -B *fru* isoforms, with the caveat that these isoforms may be unaffected.

5.3 Preparation of Gene Targeting Mutants for Phenotypic Analysis

Before investigating the genetic impact of the gene targeting events at the *fru* locus, all lines had to be outcrossed to a *Canton-S* wild-type strain. A recent study by O'Keefe *et al.* (2007) concluded that although gene targeting in *Drosophila* is an extremely powerful technique, generated lines accumulate a significant number of background mutations that can contribute to observed phenotypes or even induce novel phenotypes on their own. The source of these background mutations may lie in the use of ectopically expressed enzymes which could cleave at non-specific sites. Alternatively, these non-targeted may be derived directly from the various strains used in the targeting process (O'Keefe *et al.* 2007). As a consequence, the study recommended that all gene targeting mutants should be backcrossed at least four times to minimise the effects of background mutations. Accordingly, all nine lines were backcrossed to the *Canton-S* (*w^h*) strain six times, prior to detailed phenotypic analysis.

5.4 Expression of *fruitless* Isoforms in Generated Recombinant Lines

Expression of *fru* has been investigated, as seen in chapter 3, at various stages of development (Ito *et al.* 1996, Ryner *et al.* 1996, Lee *et al.* 2000, Song *et al.* 2002). However, these patterns of expression, including those of the individual isoform types, have been studied in most detail in mature adults (Goodwin *et al.* 2000, Lee *et al.* 2000, Anand *et al.* 2001, Billeter *et al.* 2006b). The greater part of that investigation has focussed upon the CNS. Almost all of the expression observed here is male-specific, and 20 distinct clusters of Fru^M expression have been well characterised in this region (Lee *et al.* 2000). For this reason it was decided to assess the expression of each *fru* zinc finger isoform in the male adult CNSs of mutant lines obtained by gene targeting. Additionally, by determining expression in adults it may be possible to investigate any direct

consequences of isoform disruption in a greater range of anatomical and behavioural phenotypes.

Three mutant lines were selected for immunocytochemical analysis based upon the mutations detected by PCR and restriction digestion (Table 5.1). One line possessing a mutated version of exon A (*line 3*), one line carrying a mutant copy of exon B (*line 8*) and one line carrying mutated copies of both exons (*line 1*) were chosen and assessed to investigate whether expression of each zinc finger *fru* isoform was affected in any way.

Name of Novel <i>fru</i> Mutant Line	Mutant Exon(s) Detected Molecularly	Organisation and Compliment of <i>fru</i> Zn-F Exons within each Duplication Mutant
<i>line 1</i>	A,B	AB*,A*BC
<i>line 4</i>	A,B	AB*,A*BC
<i>line 5</i>	A,B	AB*,A*BC
<i>line 6</i>	A,B	AB*,A*BC
<i>line 3</i>	A	AB,A*BC
<i>line 2</i>	B	AB*,ABC
<i>line 7</i>	B	AB*,ABC
<i>line 8</i>	B	ABC (A*B*)?
<i>line 9</i>	B	ABC (A*B*)?

Table 5.1 - Novel *fru* Mutant Lines and the Mutant Exons Incorporated During Gene Targeting. List of the nine *fru* mutant lines generated by gene targeting the mutant exon(s) detected molecularly in each line. Also listed is the molecular organisation and compliment of *fru* Zn-F exons (A-C) at the *fru* locus within each duplication mutant. “*” indicates a mutant version of the relevant Zn-F exon. Four lines possess mutant copies of both exon A and exon B within the duplication (*line 1,4,5* and *6*), whilst one line contains a mutant copy of exon A only (*line3*). In a further two lines, only a mutant copy of exon B is present within the duplication (*line 2* and *7*). In the final two lines (*line 8* and *9*), a mutant copy of exon B was also detected. However, molecular characterisation in Figure 4.7 suggested that these lines represented non-targeted events and the targeting construct had inserted into a third chromosome location other than the *fru* locus. Boxes shaded were chosen for further study.

Using CNSs taken from 5-day old adults, the expression of each *fru* isoform in male homozygotes of each mutant line was compared to the corresponding pattern of expression observed in wild-type males of the same age.

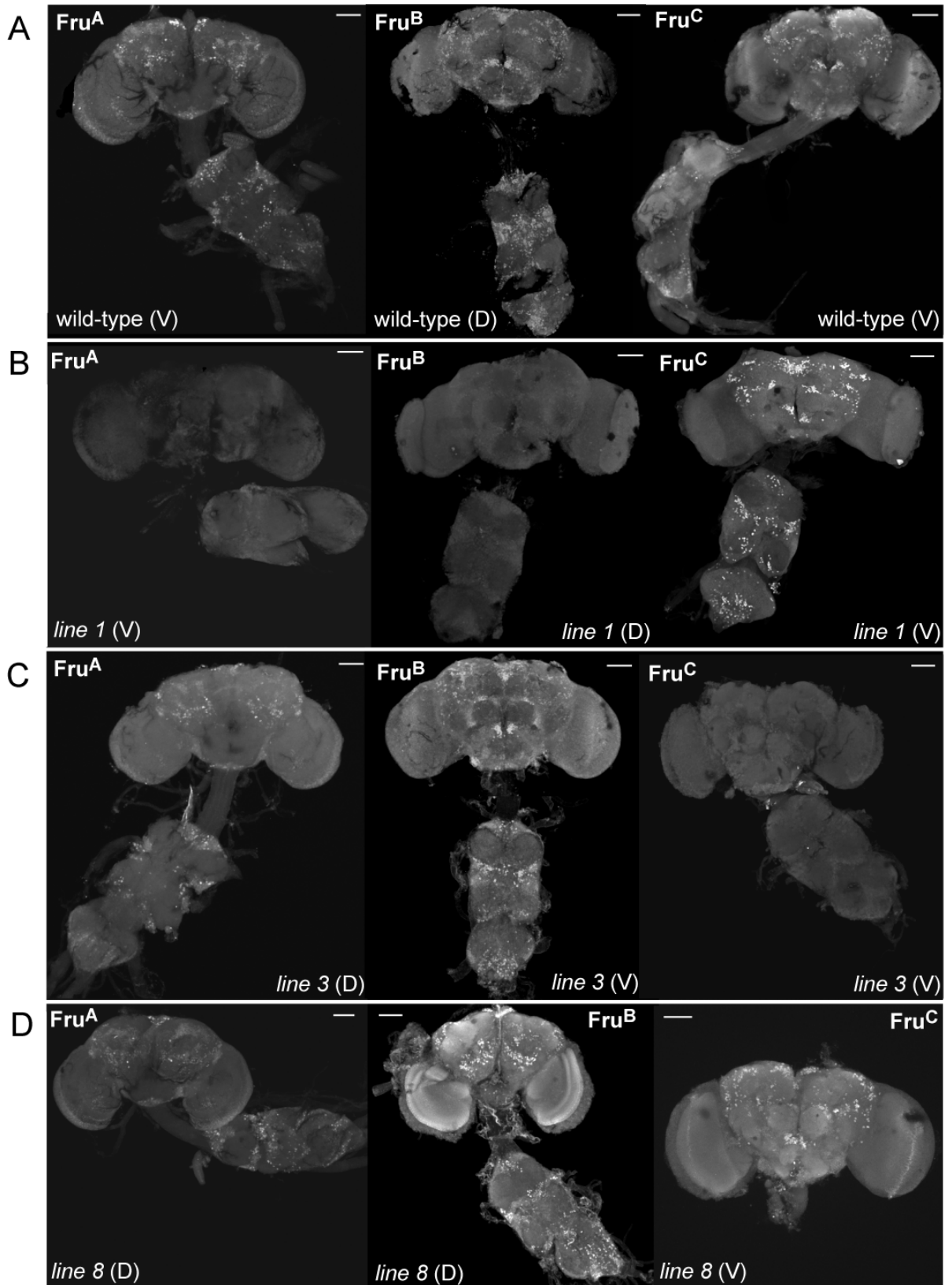


Figure 5.1 - Expression of *fru* Isoforms in Adult Male CNS of Novel *fru* Mutants. 5-day-old male adult CNSs stained with anti-Fru^A, anti-Fru^B or anti-Fru^C. Immunostaining for each Fru antibody in wild-type males (A), *line 1* males (B), *line 3* males (C) and *line 8* males (D). (A) All three isoforms are present in the wild-type CNS. (B) Fru^A and Fru^B proteins are absent in the CNS of *line 1* males. (C) Fru^A proteins are absent in CNS of *line 3* males. (D) All three isoforms were detected in the CNS of *line 8* males. View of brain is indicated as dorsal (D) or ventral (V). Scale bar = 50 μ m. n \geq 5.

Homozygous individuals carrying mutant versions of both exon A and exon B (*line 1*) are not able to eclose and die in their pupal cases. These pharate adults had to be dissected from their pupae cases before standard immunocytochemistry procedures could be performed. Homozygotes of both *line 3* and *line 8* eclosed successfully and were prepared as normal (See Materials and Methods section 2.1.4.1).

In *line 1* homozygotes, the expression of type-C isoforms did not differ from that observed in wild-type (see Figure 5.1A and B). All type-C proteins expressed in the male adult brain are male-specific, Fru^{MC}, proteins (Ryner *et al.* 1996, Goodwin *et al.* 2000, Billeter *et al.* 2006b) and *line 1* males exhibited strong anti-Fru^C immunostaining in all 20 previously characterised Fru^M expressing neuron clusters of the CNS (Lee *et al.* 2000). However, none of the anti-Fru^A or anti-Fru^B immunoreactivity observed in the wild-type CNS was apparent in the CNS of *line 1* mutants, suggesting that type-A and -B isoforms had been disrupted by the introduction of mutant versions of the corresponding A and B exons (see Figure 5.1B).

Isoform disruption was also observed in *line 3* mutants, however, this time the effect did not result directly from the introduction of a mutant copy of the corresponding exon. *line 3* individuals carry an additional mutant version of exon A, and also a second copy of exon B that has the wild-type sequence, but expression of both type-A and type-B proteins were detected in the CNS of 5-day old adult males. Conversely, no anti-Fru^C immunoreactivity was apparent in *line 3* individuals (see Figure 5.1C). Again it appeared that incorporation of an additional copy of exons A and B into the *fru* locus had eliminated expression of a specific set of *fru* proteins in the CNS. However, on this occasion, the isoforms affected did not correspond to the exons that were duplicated at the *fru* locus.

Analysis of the *fru* isoforms expressed in the adult CNS of *line 8* males produced a different result. Here, no disruption to expression was observed, and all three types of zinc finger containing isoform were detected at levels comparable to those in wild-type controls (see Figure 5.1D). This finding suggested that either, introduction of additional copies of exons A and B at the *fru* locus does not always disrupt the expression of specific *fru* isoforms, as implied by the results observed for the other two lines, or that the integration event in *line 8* was

somehow different to those in lines 1 and 3. The molecular screening assays in used in the previous chapter were not able to determine whether or not *line 8* does indeed possess a targeted event at the *fru* locus. It is tempting to speculate that this line may represent a non-targeted insertion elsewhere on the third chromosome and this will be possibility will investigated further.

In light of the observed specific effects on *fru* isoform expression, viability and fertility investigations were carried out, with interest, for each of the transgenic lines to determine if the detected isoform disruption correlated with any apparent mutant phenotypes.

5.5 Viability of Novel *fru* Mutants

In addition to its sex-specific roles, it is known that *fru* function is essential for the viability of both sexes (Ryner *et al.* 1996, Anand *et al.* 2001, Song *et al.* 2002). This function is provided by Fru^{Com} proteins, derived from P3 and P4 transcripts, and mutants that are unable to produce these proteins die during metamorphosis (Anand *et al.* 2001). It is not known whether type-A, -B and -C Fru^{Com} proteins are produced from both of these promoters (Goodwin *et al.* 2000) and, hence, it is not known which specific Fru^{Com} isoforms are necessary for survival to adulthood. As discussed previously, the new gene targeting mutant lines possess different combinations of additional mutant exons at the *fru* locus, leading to differing disruptive effects of the expression of particular isoforms. By considering the overall viability of each mutant line within the context of the isoforms that are absent, it may be possible to speculate which Fru^{Com} isoforms are essential for the viability of both sexes. To evaluate the function of these essential proteins in the novel *fru* mutants, a series of genetic crosses were performed to establish the viability of each line, both as a homozygote, and also in intragenic combination with the other recombinant lines, and extant *fru* mutants deficient in these vital functions.

5.5.1 Homozygote Viability

To investigate the homozygote viability of the new mutants, males heterozygous for one of the mutant lines, and a third chromosome balancer line (*TM3 Sb*), were mated with females of the same genotype. The observed ratio of homozygotes to heterozygotes was compared to that expected by normal

Mendelian segregation, if the line is fully viable as a homozygote (1:2). Once all of the offspring produced by a particular cross were counted, the number of progeny expected for the genotype of interest, if it were fully viable, was calculated. The viability of that genotype was then derived by calculating what percentage of the number of offspring expected was actually observed in the progeny of the cross. Heterozygotes of each novel mutant are expected to be fully viable, as individuals heterozygous for deficiencies that do not express any *fru* transcripts are fully viable (Anand *et al.* 2001).

Viability of mutant genotype (% of expected number of progeny observed)									
Genotype	<i>line 1</i>	<i>line 2</i>	<i>line 3</i>	<i>line 4</i>	<i>line 5</i>	<i>line 6</i>	<i>line 7</i>	<i>line 8</i>	<i>line 9</i>
<i>line 1</i>	0	9	100	0	0	0	97	103	105
<i>line 2</i>	9	0 ^a	98	7	0	12	98	96	107
<i>line 3</i>	100	98	95	103	93	95	96	97	99
<i>line 4</i>	0	7	103	0	0	0	94	99	100
<i>line 5</i>	0	0	93	0	0	0	99	101	104
<i>line 6</i>	0	12	95	0	0	0	106	93	110
<i>line 7</i>	97	98	96	94	99	106	0 ^a	105	103
<i>line 8</i>	103	96	97	99	101	93	105	102	110
<i>line 9</i>	105	107	99	100	104	110	103	110	108
<i>P14</i>	0	0	83	0	0	0	73	93	102
<i>fru</i> ^{sat15}	0	0	101	0	0	0	93	103	105
<i>fru</i> ^{w24}	0	0	90	0	0	0	81	99	106

Table 5.2 - Viability of Novel *fru* Mutants as Homozygotes and in Combination with Other *fru* Variants. Viability of each novel *fru* mutant line as a homozygote (purple boxes), in heterozygous combination with one of the other novel mutant lines (grey boxes), or in combination with extant *fru* variants which remove all *fru* transcripts (pink boxes). Viability shown as percentage of the number of offspring expected by for a particular genotype, actually observed in the progeny produced by the corresponding genetic cross (see text 5.5.1-3 for full definition). $n \geq 200$ for number of progeny screened from each cross. ^a A few escapers survived to adulthood for *line 2* and *line 7* homozygotes, but at frequencies were lower than 1%.

None of the homozygous mutants possessing mutant copies of both exons A and B (*lines 1, 4, 5* and *6*) were fully viable (Table 5.2). No homozygotes from these lines successfully eclosed and all individuals died as pharate adults in their pupal cases. In contrast, no decrease in the viability was apparent in homozygotes of *line 3*, which carry a mutant copy of exon A only. Homozygotes of *line 2* and *line 7*, possessing a mutant copy of exon B, displayed a severe reduction in overall viability. The overwhelming majority of homozygotes were unable to

eclose from their pupal cases and only a few homozygous escapers were detected (less than one percent of the numbers expected if homozygotes were fully viable). Finally, homozygotes of *line 8* and *line 9* did not exhibit any apparent reduction in viability, as the proportion of homozygotes was approximately one third of the total number of adults, as would be expected for normal Mendelian segregation. This is consistent with the Fru antibody immunoreactivity findings for *line 8* (Figure 5.1), which suggested that expression of all three *fru* isoforms was unaffected by the re-integration of the targeting construct on chromosome three.

5.5.2 Complementation of Novel *fru* Mutants

Once the viability of each individual line had been assessed, multiple crosses were performed to investigate the genetic fitness of various allelic *fru* combinations. Observation of the same phenotype in independently isolated alleles of the same gene provides strong evidence for loss of function in genes disrupted by gene targeting (Rong et al. 2002). More specifically, in the case these new *fru* mutants, creation of a *trans*-heterozygote from two independent lines, in which the same mutant exons have been detected, may make it possible to distinguish between phenotypes caused by the integration of these mutated exons and any others, caused by non-specific effects.

Accordingly, individuals heterozygous for one of the novel mutant lines, and a third chromosome balancer line (*TM3 Sb*), were mated separately to individuals heterozygous for each of the other novel mutant lines, and the same third chromosome balancer. Subsequently, the ratio of progeny not carrying the third chromosome balancer to balanced offspring, was compared to the ratio expected if non-balanced mutant combinations were fully viable, and a percentage figure was calculated. Reciprocal crosses were performed for each mutant combination to provide replicates, and to allow for any effects that may be dependent upon the sex of a given parent.

The viability results produced by *line 8* and *line 9* in combination with all other new *fru* mutant lines, including each other, were consistent with genotypes that were fully viable (Table 5.2). Conversely, the viability of all four 'double' mutants, carrying mutant copies of both exon A and exon B (*line 1*, *line 4*, *line 5* and *line 6*), when placed in heterozygous combination with each other was found

to be zero, as no individuals without the third chromosome balancer survived to adulthood. The viability of each of these lines was largely the same when they were combined with *line 2*, which carried a mutant copy of exon B. Almost all of the progeny produced from these crosses carried the third chromosome balancer, although a very small percentage of escapers were observed for three of the four mutants in combination with *line 2* (*line 1*, *line 4* and *line 6*).

Full viability for each of the 'double' mutant lines was restored when combined with the two remaining novel mutants (*line 3* and *line 7*). The finding that combinations with *line 7* were viable is interesting, given that each of the 'double' mutants and *line 7* were found to be non viable individually, as homozygotes. It is also important to note that although *line 2* and *line 7*, which both carry a mutant version of exon B, were molecularly indistinguishable by the screening methods used in chapter 4, and produced identical results for homozygote viability, only *line 7* is able to provide intragenic complementation of the 'double' mutant lines. All genetic crosses between *line 2*, *line 3* and *line 7* heterozygotes produced numbers of progeny, without third chromosome balancers, that were consistent with fully viable genotypes. This again demonstrated intragenic complementation between two lines, *line 2* and *line 7*, that were non-viable as homozygotes.

5.5.3 Novel Mutants in Combination with Extant *fru* Null Mutants

Lastly, each novel mutant was crossed to extant *fru* alleles (*fru^{w24}*, *fru^{sat15}* and *P14*) in which no functional Fru protein is produced (Gailey and Hall 1989, Ito et al. 1996). These intragenic combinations allowed the genetic fitness of lines, that were found to be homozygous viable, to be assessed in a genetic background that produced no additional Fru proteins. This was performed as it may allow determination of whether a single copy of a particular disrupted locus is sufficient to enable survival. Additionally, it allowed examination of those lines which do not survive as homozygotes, to investigate whether the loss of viability arose simply due to a loss of *fru* function or if the was the result of a more complex series of events. The viability each genotype combination was calculated in the same manner as those for the homozygous novel *fru* mutants and the complementation of the homozygous novel *fru* mutants.

Of the six novel *fru* mutant lines that are non-viable as homozygotes, five exhibited lethality when in heterozygous combination with the extant Fru-null mutants (*line 1*, *line 2*, *line 4*, *line 5* and *line 6*; Table 5.2). The exception was *line 7*, which was again able to provide intragenic complementation of homozygous lethal *fru* alleles. *line 3* was also found to be viable in heterozygous combination with all three Fru-null alleles. As with all of the previous combinations, *line 8* and *line 9* were fully viable with each of the *fru* variants.

The finding that *line 7* is viable in heterozygous combination with all of the extant *fru* alleles and new mutants, but not as a homozygote raises questions of validity of *line 7* as a *fru* allele. Approximately one third of all of the genes in the *Drosophila* genome are thought to be essential for viability (Miklos and Rubin 1996) and, although *line 7* was outcrossed to wild-type, it is possible that the lethality in *line 7* is the result of a mutation in close proximity to *fru* on the third chromosome. Additionally, the full viability observed for both *line 8* and *line 9*, coupled with the detection of all three *fru* isoforms in the CNS of *line 8* homozygotes suggests that *fru* expression in these lines may not be disrupted at all. One way to further investigate these issues further is to examine the morphology of these lines and screen for anatomical defects, previously identified as physical consequences of a loss in *fru* function.

5.6 Anatomical Defects in Novel *fru* Mutants

The loss of viability observed in several of the novel gene targeting mutants, in individuals of both sexes, was most likely due to a reduction in Fru^{Com} function. Previous investigations describing the phenotypic effects of a decrease in Fru^{Com} function, found reduction in viability to be associated with a number of anatomical defects (Anand et al. 2001, Billeter et al. 2006b). These studies showed that reduction of Fru^{Com} function can affect appendage, genitalia and bristle formation, in pharate and/or mature adults of both sexes.

To investigate if the re-insertion events at the *fru* locus, in the new *fru* mutants, had impacted upon the morphology of these individuals, homozygotes and heterozygotes, in combination with extant *fru* variants, were assessed for anatomical defects previously observed in extant *fru* mutants.

Genotype	Anatomical Defects Observed in Mature Adults (% of individuals of possessing specified mutant phenotype)					
	Humeral Setae Reduced / Absent		Genitalia Deformed / Absent		Leg Defects	
	M	F	M	F	M	F
<i>line 3 / line 3</i>	100	98	4	0	0	0
<i>line 7 / line 7</i>	100 ^a	100 ^a	0 ^a	0 ^a	0 ^a	0 ^a
<i>line 8 / line 8</i>	0	0	0	0	0	0
<i>line 9 / line 9</i>	0	0	0	0	0	0
<i>line 3 / P14</i>	100	100	23	0	0	0
<i>line 7 / P14</i>	94	100	33	0	0	0
<i>line 8 / P14</i>	0	0	0	0	0	0
<i>line 9 / P14</i>	0	0	0	0	0	0
<i>line 3 / Cha^{M5}</i>	0	0	0	0	0	0
<i>line 7 / Cha^{M5}</i>	0	0	0	0	0	0
<i>line 8 / Cha^{M5}</i>	0	0	0	0	0	0
<i>line 9 / Cha^{M5}</i>	0	0	0	0	0	0
<i>line 1 / Cha^{M5}</i>	0	0	0	0	0	0
<i>line 6 / Cha^{M5}</i>	0	0	0	0	0	0
<i>line 2 / Cha^{M5}</i>	0	0	0	0	0	0

Genotype	Anatomical Defects in Pharate Adults (% of individuals of possessing mutant phenotype when dissected from pupal case)					
	Humeral Setae Reduced / Absent		Genitalia Deformed / Absent		Leg Defects	
	M	F	M	F	M	F
<i>line 2 / line 2</i>	33	20	0	0	100	100
<i>line 1 / line 1</i>	30	32	0	0	100	100
<i>line 6 / line 6</i>	56	50	0	0	100	100
<i>line 2 / P14</i>	28	16	0	0	100	100
<i>line 1 / P14</i>	36	32	0	0	100	100
<i>line 6 / P14</i>	44	28	0	0	100	100

Table 5.3 - Frequency of Anatomical Abnormalities in Novel *fru* Mutants. Top half of table shows percentage of mature adults from novel *fru* mutant lines exhibiting morphological abnormalities (reduced/absent humeral setae, clubbed or deformed legs and deformed/absent genitalia). Bottom half of table shows results from homozygous lethal novel mutants, which do not survive to adulthood. For these lines, pharate adults were dissected from their pupal cases to allow examination of anatomical defects. Purple boxes show results observed in novel mutant homozygotes and pink boxes indicate findings from novel mutants in heterozygous combination with the *P14* deficiency line, which removes all *fru* transcripts. Orange boxes display results from novel *fru* mutants in heterozygous combination with the *Cha^{M5}* deficiency line, which removes *fru^M* transcripts only. ^a n≥25 for each sex of every genotype examined, except for *line 7*. Sufficient numbers of *line 7* homozygotes, as mature or pharate adults, could not be obtained as, apart from a few escapers, all individuals died prior to, or early into, the pupal stages of development. For this genotype, only five males and four females respectively, were examined.

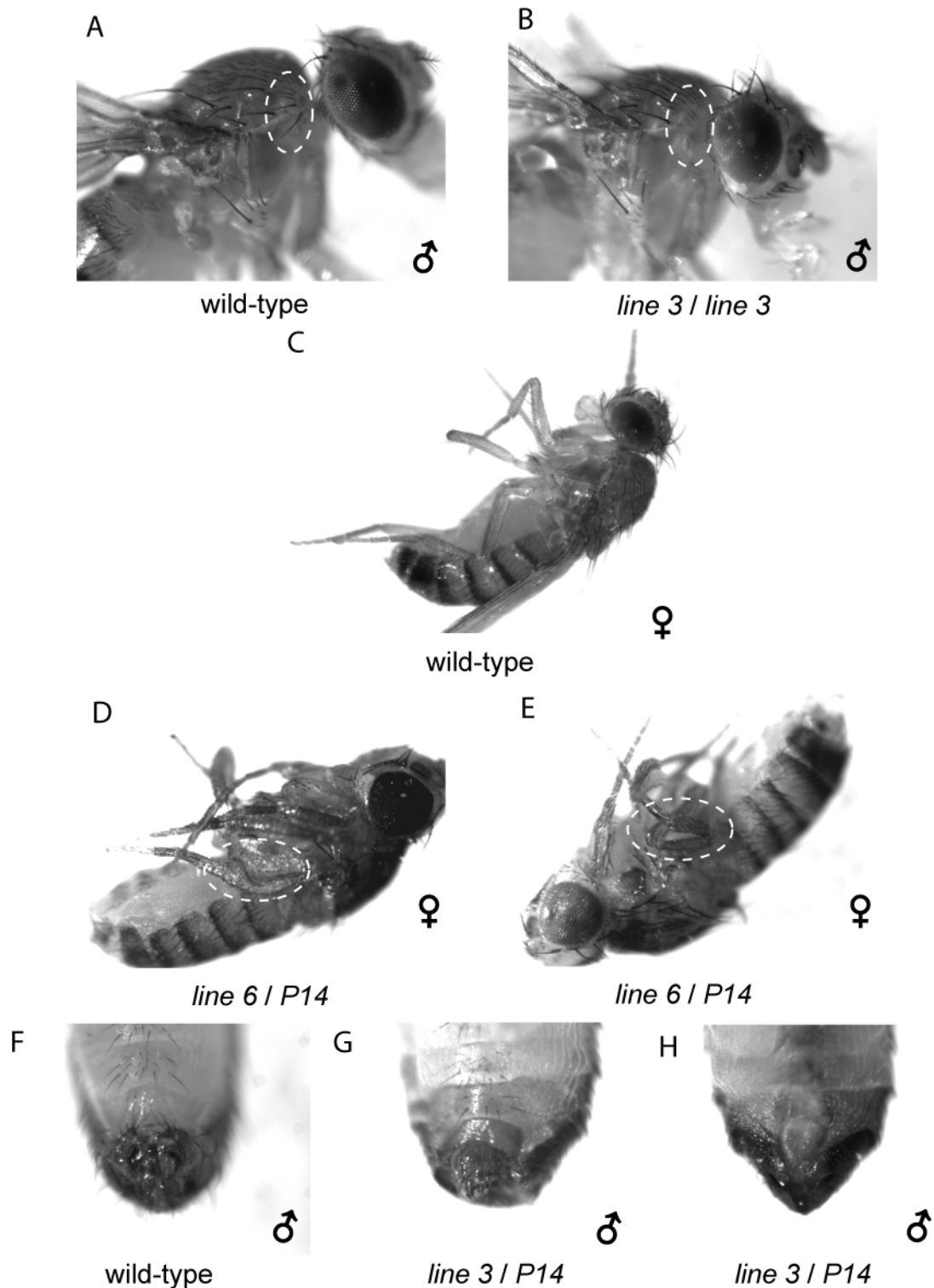


Figure 5.2 - Anatomical Defects Observed in Novel *fru* Mutants. (A) humeral setae in wild-type male. (B) Absence of humeral setae in *line 3* male homozygote. (C) Normal leg development in wild-type female. (D) Enlarged, defective leg joint in *line 6 / P14* heterozygote (female). (E) Abnormally bent leg joint in *line 6 / P14* heterozygote (female). Reduced (G) and absent (H) male genitalia in *line 3* heterozygotes in combination with *P14*.

Due to the observed variation in the viability of the new mutant lines carrying a mutant copy of *fru* exon B (*line 2*, *line 7*, *line 8* and *line 9*; Table 5.2), all four were subjected to anatomical analysis. As all four ‘double’ mutants, possessing mutant versions of exons A and B, produced broadly the same viability results, only two, *line 1* and *line 6*, were selected for inspection. *line 3* individuals, carrying a mutant copy of exon A but exhibiting absence of Fru^C, were also examined. Mature or pharate adults were examined depending upon the viability of each genotype, as stated in Table 5.3.

5.6.1 Disruption of Humeral Setae Formation

One of the more subtle effects on morphology, observed in certain *fru* animals, is the reduction or absence of humeral setae. Typically two macrochaetes are present on the humerus of wild-type individuals of both sexes (Figure 5.2A; Markow and O’Grady 2005). However, isolation of the *fru*^{AC} mutant led to the discovery that *fru* function is necessary for the formation of wild-type humeral setae (Billeter *et al.* 2006b, supplemental information). The study showed that all individuals homozygous for *fru*^{AC} displayed reduced or absent humeral setae in both sexes. All *fru*^{AC} heterozygotes in combination with the *fru*^{sat15} allele, which removes all *fru* transcripts, also exhibited disruption of humeral setae in both sexes, but no effect on humeral setae was apparent in *fru*^{AC} heterozygotes in combination with the *fru*³ allele, which removes *fru*^M transcripts only.

These findings demonstrated that the abnormality in humeral setae formation was the result of a loss of Fru^{ComC} function. The role of Fru^{ComC} in adult humeral bristle formation had not been identified before, as all previous mutants removing all *fru*^{ComC} transcripts also removed *fru*^{ComA} and *fru*^{ComB} transcripts, leading to lethality during metamorphosis (Gailey and Hall 1989, Ito *et al.* 1996, Ryner *et al.* 1996, Anand *et al.* 2001). The *fru*^{AC} mutant was the first *fru* allele to uncouple the functions of the different *fru* zinc finger isoforms, allowing the contribution of the *fru*^{ComC} isoform to overall morphology to be assessed.

Examination of the novel *fru* mutant genotypes that survive to adulthood revealed that homozygotes of *line 3* and *line 7* both display reduced or absent humeral setae in almost all individuals (Table 5.3 and Figure 5.2B). Humeral bristles were also disrupted in *line 3* and *line 7* heterozygotes in combination

with *P14*, which removes all *fru* transcripts. Humeral setae were unaffected in *line 3* and *line 7* heterozygotes in combination with *Cha^{M5}*, which removes only *fru^M* transcripts. No effect upon humeral setae was apparent in *line 8* or *line 9*, either as homozygotes, or in heterozygous combination with either *fru* variants.

Analysis of pharate adults in genotypes that were not able to eclose, revealed a reduction or absence of humeral setae in a proportion of individuals. Humeral bristles were affected in *line 2*, *line 1* and *line 6* homozygotes, and in heterozygotes in combination with *P14*, but not at the frequency observed in *line 3* and *line 7* mutants. Disruption of humeral setae was apparent at similar frequencies in both homozygotes, and heterozygotes in combination with *P14*. However, as with all other novel mutant lines investigated, no effect on humeral bristles was detected in heterozygotes in combination with *Cha^{M5}*.

5.6.2 Defects in Genitalia Development

Another phenotype uncovered by examination of *fru^{AC}* mutants was aberrant external genitalia in both males and females (Billeter *et al.* 2006b, supplemental information). The study found that this defect was apparent in 2% of homozygotes and 14% of heterozygotes in combination with *fru^{sat15}*, which removes all *fru* transcripts. Affected individuals displayed either reduced or absent external genitalia.

The novel *fru* mutants lines isolated in this study were also inspected for defects in external genitalia. Two of seven the lines examined, *line 3* and *line 7*, produced male progeny with aberrant genitalia (Figure 5.2G and H). Four percent of *line 3* homozygotes displayed reduced or absent male genitalia, and that figure increased to 23% in *line 3* males in heterozygous combination with *P14*. The low viability of *line 7* homozygotes prevented extensive investigation of genitalia in this genotype, and no genitalia defects were observed in the five escapers examined. However, *line 7* was viable in heterozygous combination with *P14*, and one third of males inspected exhibited reduced or absent genitalia. No effect was apparent in females of either mutant line.

The finding that both humeral setae and male external genitalia development are disrupted in individuals of *line 3* is consistent with the finding that *Fru^C* isoforms are not detected in *line 3* homozygotes (Figure 5.1C), given that both

phenotypes are associated with *fru^{AC}* animals (Billeter *et al.* 2006b). Identification of both phenotypes in *line 7* individuals also strongly suggests that *line 7* is indeed a *fru* allele.

5.6.3 Abnormal Leg Development

Perhaps the most striking anatomical phenotype observed in mutants with vastly reduced Fru^{Com} function is defective leg development (Anand *et al.* 2001). The study by Anand *et al.* found that pharate adults of different genotypes, lacking *fru^{Com}* transcripts from most, or all, *fru* promoters exhibited leg joint defects. This effect was observed in at least one leg, in a high percentage of males and females (frequencies of up to 100%). A less severe effect on leg development is also observed in a proportion of *fru^{AC}* homozygotes. This effect manifests itself in abnormally bent distal leg(s) in 9% of *fru^{AC}* homozygotes (Billeter *et al.* 2006b, supplemental information).

Examination of all novel *fru* mutant lines that were viable as both homozygotes, and in heterozygous combination with *P14*, revealed no apparent effect on leg development (*line 3*, *line 7*, *line 8* and *line 9*). Conversely, all individuals of mutant lines that were unable to eclose (*line 2*, *line 1* and *line 6*), either as homozygotes, or as heterozygotes in combination with *P14*, were found to have at least one visibly-defective leg joint (Figure 5.2D and E). None of the novel mutant lines, in heterozygous combination with *Cha^{M5}*, showed any apparent leg defects.

These findings not only demonstrate that the abnormalities in leg development observed in this study are caused by an absence of specific subsets of Fru^{Com} proteins, but also that failure of pharate adults to eclose from their pupal cases in these mutant lines is strongly linked to defective leg development. Indeed, it is a distinct possibility that one of the main reasons that these mutants are unable to eclose successfully is due to their abnormal leg structure. This assertion was backed up by the observation that, when these pharate adult mutants were dissected from their pupal cases, they did not appear to have full control of many, or indeed any, of their limbs when placed in an upright position.

5.7 Fertility of Novel *fru* Mutants

While it has been shown that the expression of Fru^{Com} is essential for the viability of both sexes (Ryner *et al.* 1996, Anand *et al.* 2001), expression of Fru^M throughout the male CNS is also known to be required for several morphological, neuronal and behavioural outcomes, observed exclusively in males (Usui-Aoki *et al.* 2000, Billeter and Goodwin 2004, Stockinger *et al.* 2005, Lee and Hall 2001, Kimura *et al.* 2005). However, the most characterised of the phenotypes, observed in *fru* alleles, in which Fru^M expression is reduced, are the effects upon male-specific courtship. Such deficiencies can induce courtship song defects, behavioural sterility and increased intermale courtship (Villella *et al.* 1997, Goodwin *et al.* 2000).

Individual defects, or combinations of these abnormalities, impact upon the reproductive ability of each mutant, causing reduced male fertility (Villella *et al.* 1997, Anand *et al.* 2001, Billeter *et al.* 2006b). Males lacking all Fru^M function are known to be infertile (Villella *et al.* 1997, Anand *et al.* 2001), whereas the *fru^{AC}* allele, which lacks a subset of Fru^M proteins, is known to induce incompletely penetrant sterility in males (Billeter *et al.* 2006b).

To investigate the effect of each novel *fru* mutant on fertility, caused by reduction in Fru^M function, the ability each new mutant line to produce progeny was assessed in homozygotes, and heterozygotes in combination with extant *fru* variants (*P14* and *Cha^{M5}*). In mutant lines lacking expression of a particular zinc finger isoform(s), combinations with *Cha^{M5}* will assess the effect on fertility of lacking only the male-specific version of this isoform(s). Combinations with *P14* will assess the effect of losing both the sex-specific and sex-non-specific versions of this isoform(s). Males and virgin females were placed separately with wild-type animals of the opposite sex, and evidence of progeny was assessed after a period of one week.

The fertility results observed for the novel *fru* mutants are shown in Table 5.4, divided into three sections according to the mutant exons that were previously detected in each line (Table 5.1). The produced results for male fertility correlated strongly within each mutant group, suggesting that Fru^M function might be similarly affected in each member of a particular group. No effect

upon female fertility was apparent in any of the genotypes tested. Similarly, all heterozygous *fru* allele combinations with wild-type were found to be fully fertile in both sexes. This demonstrates that none of the alleles represent dominant negative mutations.

Fertility (% of individuals of each genotype able to produce offspring)								
Genotype	<i>P14</i>		<i>Cha^{M5}</i>		wild-type (+)		homozygote	
	M	F	M	F	M	F	M	F
<i>line 1</i>	lethal	lethal	10	100	100	100	lethal	lethal
<i>line 4</i>	lethal	lethal	9	97	100	100	lethal	lethal
<i>line 5</i>	lethal	lethal	6	97	100	100	lethal	lethal
<i>line 6</i>	lethal	lethal	9	100	100	100	lethal	lethal
<i>line 3</i>	3	97	45	100	97	100	70	100
<i>line 2</i>	lethal	lethal	100	100	97	100	lethal	lethal
<i>line 7</i>	9	100	100	100	100	97	lethal	lethal
<i>line 8</i>	100	97	100	100	100	100	100	100
<i>line 9</i>	100	100	100	100	100	100	100	100
Wild-type	100	100	100	100	100	100		

Table 5.4 - Fertility of Novel *fru* Mutants in Combination with other *fru* Variants. Novel gene targeting mutants *line 1*, *line 4*, *line 5* and *line 6* possess mutant versions of exons A and B. *line 3* carries a only mutant copy of exon A, and a mutant version of exon B is present in *line 2*, *line 7*, *line 8* and *line 9*. Pink indicates novel gene targeting mutants in combination with *fru* variants removing all *fru* transcripts. Orange depicts combinations removing all sex-specific *fru* transcripts. Green represents combinations with wild-type, and purple indicates gene targeting mutant homozygotes. Fertility of males (M) and females (F) is shown in separate columns. Each genotype was crossed to wild-type individual(s) of the opposite sex. For each fertility cross, two males were placed with one virgin female, and vials were observed after a period of one week for presence of progeny. $n \geq 30$ for each cross.

The new mutant lines containing mutant versions of both exons A and B (*line 1*, *line 4*, *line 5* and *line 6*) were not viable either as homozygotes, or in heterozygous combination with extant Fru-null mutants. Accordingly, the fertility of these lines was assessed in heterozygous combination with *Cha^{M5}*, which removes only *fru^M* transcripts. In all four lines, male fertility in combination with *Cha^{M5}* was greatly reduced. Progeny were produced by only 10%, or less, of the males tested for each line (Table 5.4). This indicates that Fru^{MA} and/or Fru^{MB} are important for male fertility. As *line 1* homozygotes lack expression of both Fru^{MA} and Fru^{MB} in the male CNS (Figure 5.1B), and the other

'double' mutants, carrying mutant copies of both exon A and exon B, exhibit fertility results indistinguishable from *line 1* it is likely that these lines also lack Fru^{MA} and Fru^{MB} function.

Mutant *line 3* was viable, both as a homozygote, and in heterozygous combination with all *fru* variants used. However, male fertility was reduced in each case. Only two thirds of *line 3* homozygotes tested were fertile, and in *line 3* heterozygotes in combination with *Cha*^{M5}, fertility was only apparent in around half of the males tested (Table 5.4). The reduction in fertility was even more severe in males heterozygous for *line 3* and *P14*, where only 3% of males tested were able to produce progeny. All three *line 3* genetic combinations lack Fru^{MC} isoforms, but each combination displays a different level of fertility. The difference between *line 3* homozygotes and individuals in combination with *Cha*^{M5}, is that the heterozygotes produce, potentially, less Fru^{MA} and Fru^{MB} isoforms (since *Cha*^{M5} is a Fru^M-null). This suggests that a reduction in Fru^{MA} and Fru^{MB}, and not only a complete absence of Fru^{MA} and Fru^{MB} (as observed in *line 1* individuals), has an adverse effect on male fertility. The greater decrease in fertility observed between *line 3* homozygotes and *line 3* heterozygotes in combination with *P14*, is presumably due to a reduction in Fru^{ComA} and Fru^{ComB}, in addition that of Fru^{MA} and Fru^{MB}. This suggests that a reduction in Fru^{ComA} and Fru^{ComB} isoforms also has a direct or indirect effect on male fertility.

In terms of fertility results, the mutants possessing a mutant copy of exon B (*line 2*, *line 3*, *line 8* and *line 9*,) can be spilt into two pairs, with both members of each pair showing highly concordant results. As with all previous phenotypic assessments, no effect on *fru* function was observed in *line 8* or *line 9*, and all genetic combinations resulted in fully fertile male and female animals (Table 5.4). Conversely, *line 7* males did exhibit a marked decrease in fertility when in heterozygous combination with *P14* (Table 5.4). The lethality of *line 2* individuals, in combination with *P14*, prevented the analogous assessed to be made for *line 2*, but both *line 7* and *line 2* did produce identical fertility results, for individuals in combination with *Cha*^{M5}. Unlike the findings in the other novel *fru* mutants with reduced fertility, all *line 2* and *line 7* animals in heterozygous combination with *Cha*^{M5} appear to be completely fertile.

These results suggest that if a particular Fru^M isoform is indeed absent from *line 2* and *line 7* individuals, then that Fru^M isoform is not strictly necessary for male fertility. By considering the possible absence of Fru^M isoforms in these lines, in context of the results for *line 1* and *line 8*, it is probable that any Fru^M disruption is likely to affect Fru^{MA} or Fru^{MB} isoforms. This is because the fertility findings for *line 2* and *line 7* differ from those obtained for lines lacking Fru^{MC} (*line 3*), or Fru^{MA} and Fru^{MB} (*line 1*). By assessing the Fru^M expression in *line 2* and *line 7* it may be possible to determine if both Fru^{MA} and Fru^{MB} are responsible for the reduction in fertility in *line 1*, or if only one is important.

5.8 Discussion

Analysis of the novel *fru* transgenic lines revealed that expression of specific *fru* isoforms was disrupted in a number of these mutants. However, the isoform disruption observed in a particular line, did not always correlate directly with the mutant exon introduced by gene targeting. For instance, *line 3*, carrying a mutant version of exon A, and an additional wild-type copy of exon B, was found to express Fru^{MA} and Fru^{MB} isoforms, but not Fru^{MC} isoforms (Figure 5.1C). The additional phenotypes observed in *line 3* individuals (Table 5.2, 5.3, 5.4 and Figure 5.2) closely match those observed in *fru^{ΔC}* mutants (Billeter *et al.* 2006b). As such, it is highly likely that Fru^{ComC} isoforms are also disrupted in *line 3* animals.

However, the reason for the disruption of Fru^C expression is unclear. One possibility is that *fru* transcripts, which usually splice into exon C, are directed down alternative processing pathways by splice acceptor sites, introduced in the duplicated region of the *fru* locus present in the novel mutant lines. These acceptor sites may exist in the additional exon copies themselves, or the *mw* marker gene, introduced as part of the gene targeting construct. Such aberrant splicing has been observed before in *fru* (Goodwin *et al.* 2000). Here, a series of hypomorphic *fru* alleles (*fru²*, *fru³*, *fru⁴* and *fru^{sat}*), resulting from *P*-element insertions, were shown to produce aberrant transcripts by splicing into acceptor sites, provided by marker genes carried by the inserted transposons. However, as the *mw* marker gene of the targeting construct used in this study was designed to be positioned in the opposite orientation to the introduced *fru* exons, it is more likely that any aberrantly spliced transcripts result in the novel

fru mutants are spliced into the modified *fru* exons rather than *mw*. Another important point to consider is that *P*-element insertions in the hypomorphic *fru* alleles only affected transcripts from promoters located 5' to the insertion sites (Goodwin *et al.* 2000). Due to the positioning of the *fru* locus duplication in the novel *fru* mutants, 3' to all four *fru* promoters, it is possible that transcripts from all of the *fru* promoters could be affected. Such aberrant splice events could be identified using RT-PCR or northern blot analysis.

The immunocytochemistry analysis of the male adult CNS in pharate adults of *line 1* showed that Fru^{MA} and Fru^{MB} isoforms were absent, but Fru^{MC} isoforms were still present. In contrast to *line 3*, the isoforms disrupted in *line 1* match the mutant exon versions present in the duplication present at the *fru* locus. In spite of this difference, the mechanism of isoform disruption is probably similar to that proposed for *line 3*. The observation that the three other novel mutant lines carrying mutant copies of exons A and B (*line 4*, *line 5* and *line 6*) exhibit identical phenotypes to those observed in *line 1* suggests that Fru^{MA} and Fru^{MB} isoforms are also disrupted in these mutants.

The severe reduction in male fertility observed in these mutants, when in heterozygous combination with *Cha*^{M5}, demonstrated the importance of Fru^{MA} and/or Fru^{MB} isoforms in establishing male fertility. The difference in viability and morphology results observed between the 'double' mutants and *line 3*, suggests that Fru^{Com} isoforms other than Fru^{ComC} are disrupted in these lines. This assertion hints at a crucial role for Fru^{ComA} and/or Fru^{ComB} in adult viability and certain morphological outcomes, since no homozygotes from *line 1*, *line 4*, *line 5* or *line 6* survive to become mature adults (Table 5.2), or develop fully functional leg structures (Table 5.3). To assess the proposed absence of these Fru^{Com} isoforms, immunocytochemistry could be performed at a stage of development, prior to the production of *fru*^M transcripts, where Fru^{Com} expression is more abundant. One such stage is L3 larvae, where expression is found in the CNS, imaginal discs and support cells ensheathing neurite bundles (Lee *et al.* 2000, Dornan *et al.* 2005).

The isoform disruption in *line 2* and *line 7* is less clear. Both lines possess a mutant copy of exon B and produce similar findings when tested for male fertility. However, morphological analysis of these mutants reveals a disparity

between the two lines. *line 7* individuals exhibit severe reduction in humeral setae and abnormal genitalia in a proportion of males, much like individuals from the *line 3* (Table 5.3). In contrast, *line 2* homozygotes display leg development abnormalities such as those found in homozygotes of *line 1* and *line 6*, and a reduced level of humeral setae disruption. In the case of viability results, the two lines differ again. Neither line is viable as a homozygote, but *line 7* is able to complement all four novel 'double' mutant lines fully. In contrast, when *line 2* is crossed to each of the four 'double' mutant lines, only a small number of progeny, heterozygous for each mutant line, are observed. The explanation for the variation in the effects observed between these two mutants is unclear, but is presumably due to differences in Fru^{Com} expression. One possibility is that, in these mutant lines, different aberrant splice events occur in transcripts from certain promoters, leading to a variation in the isoforms produced by individual promoters. To resolve this uncertainty, immunocytochemistry could be performed to assess Fru^{Com} and Fru^M expression in these mutant lines. Given that both lines display full male fertility in heterozygous combination with *Cha*^{M5}, discovery of disruption in either Fru^{MA} or Fru^{MB} expression in either line may point to a functional redundancy in terms of male fertility one of these isoforms.

Southern blot analysis in chapter 4 suggested that *line 8* and *line 9* may possess an insertion of the targeting construct at a location on chromosome three other than the *fru* locus. The expression, viability, morphology and fertility analysis performed in this chapter is consistent with that assertion and it is likely that these lines represent non-targeted insertion events. To further verify this conclusion a pair of PCR primers, analogous to those used to identify lines containing a mutant copy of exon B, has been designed to amplify the region including exon A. This primer pair differs from that used to identify mutant versions of exon A in chapter 4, in that it should amplify *all* copies of exon A, irrespective of their position in the genome, and not only those included in a targeted insertion at the *fru* locus. Generation of a PCR product with these novel primers using DNA from these lines would suggest that the re-integration events here were non-targeted. Subsequent cutting by restriction digestion at the novel restriction enzyme site engineered in the mutant version of exon A would confirm that the targeting construct insertion in these lines is non-targeted.

5.9 Conclusions

In this chapter it has been demonstrated that a proportion of the novel *fru* mutants generated in chapter 4 do indeed disrupt the expression specific *fru* isoforms. This disruption impacts upon a number of developmental outcomes, inducing a wide range of phenotypes, which vary greatly between individual mutant lines. The subset of mutants in which Fru^A and Fru^B isoforms are disrupted have provided a valuable insight into the functional roles of these two isoforms, suggesting one or both of them are crucial in both male fertility and the viability and development of both sexes. Further characterisation of these mutant lines should enable the understanding of the individual functions of each isoform to be developed further.

6 Final Discussion

The main objective of this work was to investigate the extent to which different *fru* isoforms are utilised to accomplish a diverse range of developmental and behavioural outcomes. Much of the understanding of how *fru* performs these functions has come from mutations isolated within the *fru* locus, which affect all transcripts produced from one or more of the four promoters (Gailey and Hall 1989, Ito *et al.* 1996, Ryner *et al.* 1996). This has revealed the promoters from which transcripts, necessary for adult viability, are produced, and also the roles of sex-specific transcripts produced only from the distal *fru* promoter (Anand *et al.* 2001). Such findings, however, do not investigate the individual contribution of each of the *fru* Zn-F isoforms (A, B and C) and functional assignment is limited to that Zn-F triumvirate as a whole. The recent isolation of a coding mutation, which results in the complete loss of all type-C Zn-F isoforms, has enabled the individual roles of both sex-specific and sex-non-specific type-C isoforms to be established (Billeter *et al.* 2006b). Accordingly, of primary importance in this work, was the generation of null mutants for each of the remaining Zn-F isoforms (A and B), to dissect the contributions of each isoform to overall *fru* function throughout development.

The work within this thesis extends what is known of the functional roles of *fru* Zn-F isoforms A and B by demonstrating that mutants lacking expression of the male-specific versions of both *fru* Zn-F isoforms exhibit vastly reduced male fertility. Additionally, generation of a polyclonal antibody specific to Fru^B isoforms enabled the individual expression pattern of Fru^B to be studied for the first time, and revealed that Fru^{MB} is expressed in all of the serotonergic neurons of the adult male abdominal ganglion. Interestingly, these serotonergic neurons have projections that innervate the internal male reproductive organs and are known to be involved in controlling the synchronised emission of sperm and seminal fluid (Lee and Hall 2001, Lee *et al.* 2001). This is consistent with the finding that the generated mutant lines lacking expression of Fru^{MA} and Fru^{MB} exhibit an extreme reduction in male fertility.

In addition to enhancing the understanding of the function of the male-specific *fru* isoforms, the findings in this work also expanded what is known of the roles of sex-non-specific *fru* isoforms. Expression of these Fru^{Com} proteins begins early in embryogenesis (Song *et al.* 2002) and Fru^C immunocytochemistry revealed a novel pattern of Fru^{ComC} expression in a group of coalescing cells in stage 13

embryos. It is known that Fru^{Com} expression is necessary to regulate appropriate axon pathfinding in the embryonic CNS, but this expression appears to be in haemocytes (see section 6.2), which are involved in phagocytosis and organ remodelling (Song *et al.* 2002, Abrams *et al.* 1993, Holz *et al.* 2003). Examination of the generated novel *fru* mutants also revealed severe effects upon viability and morphology, indicating that expression of sex-non-specific transcripts had also been disrupted in a number of these lines.

In light of these results, a succession of experiments, using the reagents generated in this study, should be performed to extend the findings of this work and, in turn, reveal more about the functional role played by *fru*. By developing this research in such a manner, it should be possible to further extrapolate the understanding of what developmental processes *fru* participates in and how, as a transcription factor, it able to achieve this.

6.1 Further Characterisation of Novel *fru* Mutants

Following preliminary phenotypic characterisation of the novel *fru* mutants, a number of questions still remain regarding the *fru* isoforms that are absent in these mutants and the functional role that they play in wild-type individuals.

6.1.1 Do Both Fru^{MA} and Fru^{MB} Play a Significant Role in Establishing Male Fertility?

Of the nine isolated lines possessing a re-integration event on the third chromosome, seven were shown to represent a duplication event at the *fru* locus. Four of these lines (*line 1*, 4, 5 and 6) carried mutant versions of both exon A and exon B at the *fru* locus, and *line 1* male homozygotes exhibited absence of Fru^{MA} and Fru^{MB} expression in the pharate adult CNS. Adult heterozygotes in combination with *Cha*^{M5}, which removes all Fru^M isoforms, display a severe reduction in male fertility. As these four mutant lines were molecularly indistinguishable, and displayed identical results for each phenotype investigated (including a reduction in male fertility), it is highly likely that all four lines lack both Fru^{MA} and Fru^{MB} expression.

Verification by immunostaining, with the isoform-specific Fru antibodies (A, B and C) in the remaining three lines, would confirm that Fru^{MA} and/or Fru^{MB} have

important roles in establishing male fertility. Fru^{MB} in particular would be expected to have a significant part to play in male fertility, given that it is expressed in the serotonergic neurons in the abdominal ganglion, whose projections innervate the male internal reproductive organs (Lee *et al.* 2001). Similarly, Fru^{MC} is also expressed in all of the serotonergic neurons of the abdominal ganglion and it has previously been demonstrated that this isoform plays an important role in male fertility (Billeter *et al.* 2006). As Fru^{MA} is not expressed in either of the male serotonergic neuron clusters in the abdominal ganglion, it is tempting to speculate that it may be the absence of Fru^{MB} alone that is reducing male fertility in these mutants. One way to address this possibility would be to attempt rescue of male fertility in *fru* duplication-*Cha*^{M5} heterozygotes using the *fru(16)-gal4* driver and GAL4-responsive Fru^{MA} or Fru^{MB} isoforms.

An alternative way to investigate the contribution of individual *fru* isoforms to male fertility would be to perform immunostaining with the isoform-specific Fru antibodies in the two novel *fru* mutants that have no effect upon male fertility (*line 2* and *7*). If either Fru^{MA} or Fru^{MB} isoforms are absent in the male CNS of pharate adults, it would indicate that the absent isoform is not necessary for full male fertility to be established.

6.1.2 Are all three Fru^{Com} Zn-F Isoforms Required to Confer Full Viability and Appropriate Morphology?

In addition to displaying concordant male fertility results, *line 1*, *4*, *5* and *6* also have identical effects upon the viability and morphology of both sexes. These severe mutant phenotypes are caused by a reduction in sex-non-specific Fru^{Com} proteins, derived from transcripts of promoters P2-P4 (Anand *et al.* 2001). Presumably, as predicted with the male-specific isoforms, the same sex-non-specific isoforms are absent in each of these four mutant lines. However, to confirm which particular Zn-F isoforms are absent, immunostaining with the isoform-specific Fru antibodies should be performed at a developmental stage where all Fru^{Com} proteins are normally present but Fru^M expression is absent, such as in 3rd-instar larvae (Lee *et al.* 2000). By performing similar analysis in the remaining three novel mutants (*line 2*, *3* and *7*) and comparing the expression of Fru^{Com} in each mutant line to the corresponding effects upon

viability and morphology it may be possible to determine which Zn-F Fru^{Com} isoform(s) is involved in each developmental outcome.

6.1.3 Are Fru^{MA} or Fru^{MB} Involved in Male Serotonergic Neuron Differentiation or MOL Development?

In wild-type adult males, Fru^{MC} is expressed in all of the serotonergic neurons in the abdominal ganglion (Billeter *et al.* 2006b). However, in Fru^{MC}-null males, the number of neurons in each cluster of serotonergic neurons is severely reduced, with one cluster often entirely absent. In Fru^M-null males, both clusters of serotonergic neurons are absent, but expression of a Gal4-responsive Fru^{MC} isoform, using the *fru(16)-gal4* driver line, is sufficient to rescue both the dorsal and ventral cluster. Fru^{MC} isoform expression is also able to rescue development of the dorsal cluster in Fru^{MC}-null males and, to a lesser extent, the ventral cluster. This demonstrates the importance of the role played by Fru^{MC} in the development of serotonergic neurons in the adult male abdominal ganglion (Billeter *et al.* 2006b).

As illustrated by this study, Fru^{MB} is expressed in all of the serotonergic neurons of the male abdominal ganglion. In contrast, Fru^{MA} expression is absent from both clusters of serotonergic neurons (Billeter *et al.* 2006b). This is consistent with the finding Fru^{MB} isoform expression, but not that of Fru^{MA}, is able to rescue development of one of the clusters of serotonergic neurons in the abdominal ganglion of Fru^M-null males (Billeter *et al.* 2006b), and suggests that Fru^{MB} but not Fru^{MA} is involved in the differentiation of these neurons. To further investigate this possibility, pharate adult males of the novel mutant lines deficient for the production of both Fru^{MB} and Fru^{MA} should be analysed to determine whether there has been a reduction in the number of male serotonergic neurons in the abdominal ganglion. This could be achieved by immunostaining the mutant male abdominal ganglion with both anti-Fru^M and anti-5HT, and counting the number of serotonergic neurons present in each cluster. If any reduction in the number of neurons within either cluster is observed, rescue could be attempted using *fru(16)-gal4* and Gal4-responsive Fru^{MA} and Fru^{MB} isoforms.

However, to obtain a definitive answer regarding the potential contribution of Fru^{MA} and Fru^{MB} isoforms to differentiation of serotonergic neurons in the

abdominal ganglion, mutants lacking only one of these isoforms must be studied. With this in mind, anti-Fru^A and anti-Fru^B immunostaining of the pharate adult CNS of novel mutants *line 2* and *line 7* should be undertaken to investigate whether either line lacks Fru^{MA} or Fru^{MB} expression. However, as male fertility in these two lines is not diminished, one may expect the serotonergic neurons of the male abdominal ganglion to be similarly unaffected.

In addition to an important role in serotonergic neuron differentiation in the male abdominal ganglion, Fru^{MC} expression is also necessary and sufficient for development of the male-specific MOL (Billeter *et al.* 2006b). The overwhelming majority of Fru^{MC}-null and Fru^M-null mutants lack any discernable MOL, and those that do possess only a vestigial MOL. As is the case with the male serotonergic neurons, expression of Fru^{MC} under the control of *fru(16)-gal4* rescues formation of the MOL in both mutant backgrounds. Expression of Fru^{MA} or Fru^{MB} does not rescue development of the MOL (Billeter *et al.* 2006b). The inability of Fru^{MA} and Fru^{MB} to rescue MOL development, suggests that neither isoform is involved in its formation. To test this theory, pharate adult males from the novel mutant lines lacking Fru^{MA} and Fru^{MB} expression should be analysed for any disruption in MOL formation. As Fru^{MC} is present in these individuals, one would still expect wild-type MOLs to be observed.

6.1.4 To What Extent is Male Courtship Affected in the Novel fru Mutants?

fru mutant males which lack expression of any Fru^M isoforms are behaviourally sterile as they do not copulate (Lee *et al.* 2000, Goodwin *et al.* 2000). In addition to exhibiting reduced levels of courtship towards females, these mutant males also display increased levels of courtship towards other males, including formation of intermale courtship chains (Gailey and Hall 1989, Villella *et al.* 1997). Similarly, males lacking only Fru^{MC} isoforms (*fru^{AC}* mutants) also exhibit a reduction in courtship behaviour towards females, and an increase in intermale courtship. Both courtship and wing extension indices (CI and WEI) performed by *fru^{AC}* males towards females are significantly lower compared to those of wild-type males. Additionally, CI and WEI levels performed by *fru^{AC}* males towards other males are dramatically increased compared to wild-type levels, as is the formation of intermale courtship chains (ChI) (Billeter *et al.* 2006b). This

demonstrates the importance of Fru^{MC} in establishing wild-type male courtship behaviour. To investigate the potential roles of Fru^{MA} and Fru^{MB} isoforms in establishing male courtship behaviour, males from the novel mutant lines lacking Fru^{MA} and Fru^{MB} (*line 1, 4, 5 and 6*) expression should be subjected to courtship analysis.

Preliminary courtship analysis of *line 1* and *line 6* males in heterozygous combination with the *Cha*^{M5} deficiency, which produces no Fru^M proteins, was performed (data not shown). Initial results suggested that courtship behaviour (CI) towards females in these mutant males was almost completely abolished. This is consistent with the severely reduced male fertility recorded for these genotypes. Reduced courtship was also accompanied by a slight increase in courtship towards other males compared to that of wild-type. A significant increase in intermale chaining behaviour (ChI) was also observed in *line 1* and *line 6* heterozygotes. Intermale chaining was also observed in *line 3* male homozygotes, which lack Fru^{MC} expression. This is consistent with the increased chaining behaviour observed between *fru*^{AC} mutant males.

To adequately assess whether male courtship behaviour is affected in each of the novel *fru* alleles, mutant males should be analysed for levels of courtship performed towards wild-type males and females. Heterozygotes in combination with a deficiency removing all Fru^M proteins (*Cha*^{M5}, *fru*⁴⁻⁴⁰ or *fru*³) should be analysed for all seven mutant lines, in addition to homozygous males in the case of *line 3*. CI and WEI should be recorded for male-female and male-male single courtship pairings, as should ChI recordings from ten mutant males of the same genotype grouped together. Care should also be taken to investigate whether or not certain steps of the male courtship routine are completely absent in these mutants, or whether loss of particular Fru^M isoforms simply leads to a global reduction of all courtship steps.

6.1.5 What Aberrant Splicing Events Occur at the *fru* Locus within the Novel Mutant Lines?

All of the seven lines possessing a duplication of exons A and B at the *fru* locus displayed mutant phenotypes known to be associated with the *fru* syndrome. Since the original, wild-type copies of these exons are still present at the *fru* locus, it suggested that aberrantly spliced transcripts were being produced from

one or more of the *fru* promoters, as a result of the duplication and insertion of a portion of the pED7 gene targeting vector. In at least one of the mutant lines (*line 3*), Zn-F isoform disruption (type-C isoforms) did not correspond to the mutant Zn-F isoform-encoding exon that had been introduced at the locus (exon A). This demonstrated that loss of a particular Zn-F isoform in each of these mutants was not due to transcripts preferentially splicing into the corresponding mutant version of a particular Zn-F isoform-encoding exon.

Immunocytochemistry can determine which Fru proteins are produced in each of these mutants, but to understand the splicing mechanisms involved, one must investigate expression at an RNA level. To investigate the molecular mechanisms that produce the expression patterns of male-specific Fru^M isoforms in novel *fru* mutant males, northern blotting should be performed with mRNA isolated from sexed heads of each of the mutant lines. By hybridising with a probe common to *fru* P1 transcripts from both sexes (but not present in *fru* transcripts from other promoters), and comparing the sizes of the transcripts produced in each of the mutant lines to those produced in wild-type, it should be possible to screen for aberrant splicing events. Identification of novel transcripts of different size in any of the mutants would suggest that aberrant splicing events are occurring in P1 transcripts. Lack of variation in transcript size may suggest that preferential splicing of certain P1 transcripts into mutant versions of exons A and/or B are the reason for the absence of a particular Fru^M isoform.

To determine the molecular identity of any detected aberrant splicing events, RT-PCR should be performed with the isolated mRNA. A forward primer within the sequence specific to P1 transcripts of both sexes, in addition to reverse primers within each of the Zn-F-encoding exons (A, B and C) should be designed. Also included, should be reverse primers within regions suspected to be involved in aberrant P1 transcript splicing events at the 3' end. These would include the section of the pED7 targeting vector that was integrated at the *fru* locus during gene targeting. Another candidate region would be the final common exon (see figure 1.2) that is found in all *fru* transcripts. This exon is present in the 4kb of *fru* sequence preceding exon A that was also incorporated into the gene targeting vector and, hence, a second copy of this exon is also present in the *fru* duplication mutants. The second copy of this common exon could also act as a

splice acceptor site for P1 transcripts. All RT-PCR products should then be sequenced to confirm predicted splice patterns.

Similar RT-PCR analysis should also be performed for transcripts produced from promoters P2-P4. This could be achieved by substituting the P1 transcript-specific primer for a forward primer unique to sequences found only in transcripts derived from one of the more proximal promoters. However, in the case of P3 transcripts, RNA should be collected at the pupal stage as P3 expression is weak in the heads of adults (Dornan *et al.* 2005).

Northern blot and RT-PCR analysis should help to explain the aberrant splicing mechanisms present in the *fru* duplication mutants. However, despite the absence of immunostaining for particular Fru^M isoforms in each of the mutants, it is possible that the corresponding *fru*^M transcripts and indeed the Fru^M proteins themselves are still expressed in these mutants, only at a much reduced level. Such expression may affect subsequent phenotypic analysis of the novel *fru* mutants. Accordingly, the modified *fru* genomic sequence containing the engineered exon A and B mutations has been cloned into the pED7 vector, enhanced with an additional I-Cre1 site, faithful to the wild-type sequence. Gene targeting of the *fru* locus using this targeting vector has begun and inclusion of the novel I-Cre1 site should enable resolution of future duplication events. Further options for future *fru* mutagenesis would be to perform gene targeting with pED7-*fru* in a *fru*^{A^C} mutant background. This would theoretically allow any combination of *fru*^A, *fru*^B and *fru*^C mutants to be obtained. Additionally, gene targeting of *fru* exon D could be performed to investigate whether *fru*^D transcripts have a functional role in *Drosophila*.

6.2 Novel Pattern of Fru^C Embryonic Expression

Detection of Fru^C expression in a group of cells which coalesce towards the anterior end of stage 13 embryos represented a novel Fru expression pattern. Initially, these cells appeared to be precursors of Garland cells. However, closer inspection showed that these cells lacked the characteristic crescent-shaped clustering of Garland cells and the cells are more likely to be a subset of haemocytes (B. Denholm, pers. comm.).

During embryonic development in *Drosophila*, haemocytes are responsible for phagocytosis of apoptotic cells, making them important for tissue formation. In metamorphosis haemocytes are also required for organ remodelling (Abrams *et al.* 1993, Holz *et al.* 2003). To investigate whether Fru^C is indeed expressed in a subset of haemocytes, a haemocyte GAL4 driver such as *srp-gal4* (*serpent-gal4*; Milchanowski *et al.* 2004) could be used to drive expression of a GAL4 responsive reporter gene such as *UAS-GFP* in embryonic haemocytes. Detection of Fru^C and GFP expression in the same cells would suggest that the novel pattern of embryonic Fru^C expression is indeed within haemocytes.

6.3 Searching for Targets of Fru

fru encodes a vast array of transcription factors and each one is potentially able to bind to the promoters of a different set of genes. Many of the important developmental processes that these different *fru* Zn-F isoforms regulate have been uncovered, but little is known of their actual binding sites and the partners that Fru presumably co-operates with to activate transcription.

In an attempt to identify proteins which interact with Fru, a yeast two-hybrid screen was performed using a library generated from *Drosophila* head cDNAs fused to the activation domain of the yeast transcription factor Gal4 (M. Neville, pers. comm.). The library plasmids were each co-transformed with a plasmid expressing the Gal4 DNA binding domain attached to Fru, into a modified yeast strain containing the UAS recognised by Gal4 upstream of reporter genes. If a protein from the library interacts with Fru, the attached Gal4 activation domain is brought into contact with the Gal4 DNA binding domain, which fused to Fru, and activates the reporter genes integrated into the host genome (Giot *et al.* 2003).

Six proteins were identified as potential Fru interactors. One of these was Fru itself, suggesting that the protein can dimerise through its BTB domain (Ito *et al.* 1996, Ryner *et al.* 1996). One of the other potential interactors is Kismet, which is believed to act as a universal activator of RNA Polymerase II in *Drosophila*. The longer of the two isoforms encoded by *kismet* (KIS-L) is related to members of the SWI2/SNF2 and CHD families of chromatin-remodelling factors, which can dissociate nucleosomes from the chromosome to activate transcription. KIS-L is

also found to be associated with nearly all sites of transcriptionally active chromatin, in a pattern that overlaps with RNA Polymerase II (Srinivasan *et al.* 2005). It is possible that Fru may recruit Kismet to promoters of target genes to initiate transcription. To investigate this possibility further, a binding target gene of Fru in the must be uncovered to prove interaction between these proteins in *Drosophila*.

One way to identify targets of Fru is by chromatin immunoprecipitation (ChIP). ChIP enables protein-DNA interactions to be revealed by immunoprecipitating protein-DNA complexes out of cellular lysates. By using an antibody specific to the protein of interest, selective enrichment of the relevant chromatin fractions can be performed to isolate DNA binding sites in the genome for that particular protein. The isolated DNA binding sites can then be identified by PCR. Use of micro-array technology allows *in vivo* protein-DNA interactions to be on a genome-wide scale (ChIP-on-chip), and the novel ChIP-seq technique combines ChIP technology in parallel with high-throughput sequencing, to precisely map the global binding sites for a protein of interest.

To perform such techniques, a ChIP-grade antibody to the protein of interest is required. A good indication of whether an antibody will be suitable for ChIP analysis is to subject it to western blot analysis. If the isoform-specific Fru antibodies are able to detect the correct protein products on a western blot, they may be applicable to ChIP techniques, to search for binding sites of the targets of each isoform. If a suitable antibody is not available for the protein of interest, an alternative solution is to engineer the protein of interest to carry a tag such as FLAG-tag. The presence of such tags enables isolation the protein-DNA complexes of interest.

Two genes have previously been proposed as potential targets of Fru. The first is the cuticle pigmentation gene *yellow* (Radovic *et al.* 2002). In late L3 larvae Fru and Yellow immunostaining colocalise, while mutations in both *yellow* and *fru* have been shown to cause defects in wing extension, prior to courtship song production (Drapeau 2003). The second potential target is *takeout*. Identified in a screen for genes under the control of the sex-determination gene *tra-2*, *takeout* is expressed in the fat bodies surrounding the male adult brain and in the third antennal segment. Selective feminisation of the male brain with *UAS-*

tra^F, under the control of a *takeout-gal4* driver, produces males whose ability to court beyond the stage of initial orientation is significantly reduced (Dauwalder 2002). The effects upon male courtship behaviour in *yellow* and *takeout* mutants are consistent with the possibility that these genes are targets of the male-specific products of *fru* P1 transcripts.

Male courtship behaviour in *Drosophila* is a complex and dynamic process, involving recognition of multiple environmental sensory inputs, which must be correctly processed in order to execute the appropriate motor response. The groups of sensory, motor and interneurons in which Fru^M is expressed represent the neural circuits by which male courtship behaviour is controlled, and the importance of Fru^M in linking each of these circuits has been demonstrated by disrupting Fru^M expression in different regions of the brain to induce termination of male behaviour at disparate courtship stages. The existence of multiple interlinked neuronal circuits controlling male sexual behaviour, as opposed to one predominant linear pathway, is supported by the rescue of male fertility but not overall courtship behaviour in *fru^{ΔC}* males, when Fru^{MC} is restored in only a subset of its normal expression pattern (Billeter *et al.* 2006b). Future identification of target binding sites of Fru, and proteins it interacts with at these genomic locations, should illuminate how *fru* operates within these neural networks to regulate such a wide range of developmental outcomes.

References

- Abrams, J. M., White, K., Fessler, L. I. and Steller, H. (1993). Programmed cell death during *Drosophila* embryogenesis. *Development* 117, 29-43.
- Acebes, A., Grosjean, Y., Everaerts, C., and Ferveur, J.F. (2004) Cholinergic control of synchronized seminal emissions in *Drosophila*. *Curr. Biol.* 14, 704-710.
- Adams, M.D., Celniker, S.E., Holt, R.A., Evans, C.A. Gocayne, J.D., Amanatides, P.G., Scherer, S.E., Li, P.W., Hoskins, R.A. *et al.* (2000). The genome sequence of *Drosophila melanogaster*. *Science.* 287, 2185-2195.
- Albagli, O., Dhordain, P., Deweindt, C., Lecocq, G., Leprince, D. (1995). The BTB/POZ domain: a new protein-protein interaction motif common to DNA- and actin-binding proteins. *Cell Growth Differ.* 6, 1193-1198.
- Anand, A., Villella, A., Ryner, L. C., Carlo, T., Goodwin, S. F., Song, H-J., Gailey, D. A., Morales, A., Hall, J. C., Baker, B. S., and Taylor, B. J. (2001). Molecular genetic dissection of the sex-specific and vital functions of the *Drosophila melanogaster* sex determination gene *fruitless*. *Genetics.* 158, 1569-1595.
- Amrani N., Sachs M.S. and Jacobsen A. (2006) Early nonsense: mRNA decay solves a translational problem. *Nature Reviews Molecular Cell Biology* 7(6):415-25.
- Argast, G.M., Stephens, K.M., Emond, M.J., Monnat, R.J. (1998). I-*PpoI* and I-*Crel* homing site sequence degeneracy determined by random mutagenesis and sequential *in vitro* enrichment. *J. Mol. Biol.* 280, 345-353.
- Arthur, B.I. Jr, Jallon, J.M., Caflisch, B., Choffat, Y., and Nothiger, R. (1998). Sexual behaviour in *Drosophila* is irreversibly programmed during a critical period. *Curr. Biol.* 8, 1187-1190.
- Ashburner, M. (1989). *Drosophila*, a laboratory handbook. New York: Cold Spring Harbor Laboratory Press.
- Bainbridge, P.S., and Bownes, M. (1982). Staging the metamorphosis of *Drosophila melanogaster*. *J. Embryol. Exp. Morph.* 66, 57-80.
- Bellaïche, Y., Mogila, N., Perrimon., N. (1999) I-*Scel* endonuclease, a new tool for studying DNA double-stranded break repair mechanisms in *Drosophila*. *Genetics.* 152, 1037-1044.
- Bertossa, R.C., van de Zande, L., Beukeboom, L.W., (2009) The Fruitless gene in *Nasonia* displays complex sex-specific splicing and contains new zinc finger domains. *Mol Biol Evol.* 26,1557-69.
- Dauwalder, B., Tsujimoto, S., Moss, J., Mattox, W. (2002) The *Drosophila* takeout gene is regulated by the somatic sex-determination pathway and affects male courtship behavior. *Genes Dev.* 16, 2879-92.
- Bi, X. and Rong, Y.S. (2003). Genome manipulation by homologous recombination in *Drosophila*. *Brief Funct. Genomic Proteomic.* 2, 142-146.

- Billeter, J.C. (2003). Targeting *fruitless* Neurons: Neurogenetic Dissection of Male Sexual Behaviour in *Drosophila melanogaster*. PhD Thesis, University of Glasgow.
- Billeter, J.C. and Goodwin, S.F. (2004). Characterization of *Drosophila fruitless*-Gal4 transgenes reveals expression in male-specific *fruitless* neurons and innervation of male reproductive structures. *J. Comp. Neurol.* *475*, 270-287.
- Billeter, J.C., Rideout, E.J., Dornan, A.J., Goodwin, S.F. (2006a). Control of male sexual behavior in *Drosophila* by the sex determination pathway. *Curr. Biol.* *16*, R766-776.
- Billeter, J.C., Vilella, A., Allendorfer, J.B., Dornan, A.J., Richardson, M., Gailey, D.A., Goodwin, S.F. (2006b) Isoform-specific control of male neuronal differentiation and behavior in *Drosophila* by the *fruitless* gene. *Curr. Biol.* *16*, 1063-1076.
- Brand, A.H. and Perrimon, N. (1993). Targeted gene expression as a means of altering cell fates and generating dominant phenotypes. *Development* *118*, 401-415.
- Castrillon, D.H., Gonczy, P., Alexander, S., Rawson, R., Eberhart, C.G., Viswanathan, S., DiNaro, S., and Wasserman, S.A. (1993). Toward a molecular genetic analysis of spermatogenesis in *Drosophila melanogaster*: Characterization of male-sterile mutants generated by single *P*-element mutagenesis. *Genetics.* *153*, 489-505.
- Christiansen, A.E., Keisman, E.L., Ahmad, S.M., Baker, B.S. (2002). Sex comes in from the cold: the integration of sex and pattern. *Trends Genet.* *18*, 510-516.
- Cline, T.W. and Meyer, B.J. (1996). Vive la difference: males vs females in flies vs worms. *Annu. Rev. Genet.* *30*, 637-702.
- Consoulas, C., Duch, C., Bayline, R.J., and Levine, R.B. (2000) Behavioural transformations during metamorphosis: re-modelling of neural and motor systems. *Brain Res. Bull.* *53*, 571-583.
- Currie, D.A., and Bate, M. (1995). Innervation is essential for the development and differentiation of a sex-specific adult muscle in *Drosophila melanogaster*. *Development* *121*, 2549-2557.
- Demir, E. and Dickson, B.J. (2005). *fruitless* splicing specifies male courtship behaviour in *Drosophila*. *Cell.* *121*, 785-794.
- Deng, C. and Capecchi, M.R. (1992). Reexamination of gene targeting frequency as a function of the extent of homology between the targeting vector and the target locus. *Mol. Cell. Biol.* *12*, 3365-3371.
- Dolezal, T., Gazi, M., Zurovec, M., Bryant, P.J. (2003) Genetic analysis of the *ADGF* multigene family by homologous recombination and gene conversion in *Drosophila*. *Genetics.* *165*, 653-666.

- Dornan, A.J., Gailey, D.A., and Goodwin S.F. (2005). GAL4 enhancer trap targeting of the *Drosophila* sex determination gene *fruitless*. *Genesis* 42, 155-64.
- Drapeau, M.D. (2003) A novel hypothesis on the biochemical role of the *Drosophila* Yellow protein. *Biochem Biophys Res Commun.* 311, 1-3.
- Evans, M.J., and Kaufman, M.H. (1981). Establishment in culture of pluripotent cells from mouse embryos. *Nature.* 292, 154-156.
- Ewing, A.W. (1979). The neuromuscular basis of courtship song in *Drosophila*: the role of the direct and axillary wing muscles. *J. Comp. Physiol. A.* 130, 87-93.
- Ferveur, J.F., Stortkuhl, K.F., Stocker, R.F., Greenspan, R.J. (1995). Genetic feminization of brain structures and changed sexual orientation in male *Drosophila*. *Science.* 267, 902-905.
- Ferveur, J.F. and Greenspan, R.J. (1998). Courtship behaviour of brain mosaics in *Drosophila*. *J. Neurogenet.* 12, 205-226.
- Gailey, D.A. and Hall, J.C. (1989). Behavior and cytogenetics of *fruitless* in *Drosophila melanogaster*: different courtship defects caused by separate, closely linked lesion. *Genetics.* 121, 773-785.
- Gailey, D.A., Billeter, J.C., Liu, J.H., Bauzon, F., Allendorfer, J.B., Goodwin, S.F. (2006) Functional conservation of the *fruitless* male sex-determination gene across 250 Myr of insect evolution. *Mol. Biol. Evol.* 23, 633-43.
- Gill, K.S. (1963). A mutation causing abnormal courtship and mating behavior in males of *Drosophila melanogaster*. *Am. Zool.* 3, 507.
- Giot, L., Bader, J.S., Brouwer, C., Chaudhuri, A., Kuang, B., Li, Y., Hao, Y.L., Ooi, C.E., Godwin, B., Vitols, E., Vijayadamodar, G., Pochart, P., Machineni, H., *et al.* (2003). A protein interaction map of *Drosophila melanogaster*. *Science.* 302, 1727-1736.
- Gloor, G.B., Nassif, D.M., Johnsonschlitz, D.M., Preston, C.R., and Engels, W.R. (1991). Targeted gene replacement in *Drosophila* via *P*-element-induced gap repair. *Science.* 253, 1110-1117.
- Golic K.G., and Lindquist, S. (1989). The FLP recombinase of yeast catalyzes site-specific recombination in the *Drosophila* genome. *Cell.* 59, 499-509.
- Gong, W.J., and Golic K.G. (2003). Ends-out, or replacement, gene targeting in *Drosophila*. *Proc. Natl. Acad. Sci.* 100, 2556-2561.
- Gong, M., and Rong, Y.S. (2003) Targeting multi-cellular organisms. *Curr Opin Gen Dev.* 13, 215-220.
- Goodwin, S.F., Taylor, B.J., Vilella, A., Foss, M., Ryner, L.C., Baker, B.S., Hall, J.C. (2000). Aberrant splicing and altered spatial expression patterns in *fruitless* mutants of *Drosophila melanogaster*. *Genetics.* 154, 725-745.

- Greenspan, R.J. (1995). Understanding the genetic construction of behavior. *Sci. Am.* 272, 74-79.
- Greenspan, R.J. and Ferveur, J.F. (2000). Courtship in *Drosophila*. *Annu. Rev. Genet.* 34, 205-232.
- Guan, C., Li, P., Riggs, P.D., and Inouye, H. (1987) Vectors that facilitate the expression and purification of foreign peptides in *Escherichia coli* by fusion to maltose-binding protein. *Gene.* 67,21-30.
- Halder, G., Callaerts, P., Gehring, W.J. (1995). Induction of ectopic eyes by targeted expression of the eyeless gene in *Drosophila*. *Science.* 267, 1788-1792.
- Hall, J.C. (1977). Portions of the central nervous system controlling reproductive behavior in *Drosophila melanogaster*. *Behav. Genet.* 4, 291-312.
- Hall, J.C. (1978a). Courtship among males due to a male-sterile mutation in *Drosophila melanogaster*. *Behav. Genet.* 8, 125-141.
- Hall, J.C. (1978b). Behavioral analysis in *Drosophila* mosaics. In "Genetic mosaics and cell differentiation" (Ed. W.J. Gehring). Springer-Verlag, Berlin. Pp 259-305.
- Hall, J.C. (1979). Control of male reproductive behavior by the central nervous system of *Drosophila*: Dissection of a courtship pathway by genetic mosaics. *Genetics.* 92, 437-457.
- Hall, J.C. (1994). The mating of a fly. *Science* 264, 1702-1714.
- Hamilton, B.A. and Zinn, K. (1994). From clone to mutant Gene. In "*Drosophila melanogaster*: Practical uses in cell and molecular biology" (Eds. L.S.B. Goldstein and E.A. Fyrberg). Academic Press, New York. Pp. 81-97.
- Hanahan, D. (1983). Studies on transformation of *Escherichia coli* with plasmids. *J. Mol. Biol.* 166, 557-580.
- Hanahan, D., Jessee, J., and Bloom, F.R. (1995). Techniques for transformation of *E. coli*. In "DNA cloning 1: core techniques" (Eds. D.M. Glover and B.D. Hames). IRL Press: Oxford-Washington DC. Pp. 1-36.
- Hastings, P.J., McGill, C., Shafer, B., Strathern, J.N. (1993). Ends-In vs. Ends-Out Recombination in Yeast. *Genetics.* 135, 973-980.
- Hasty, P., Rivera-Perez, J., Chang, C., Bradley, A. (1993). Target frequency and integration pattern for insertion and replacement vectors in embryonic stem cells. *Mol. Cell. Biol.* 11, 4509-4517.
- Heinrichs, V., Ryner, L.C., Baker, B.S. (1998). Regulation of sex-specific selection of *fruitless* 5' splice sites by *transformer* and *transformer-2*. *Mol. Cell. Biol.* 18, 450-458.
- Hinnen, A., Hicks, J.B., Fink, G.R. (1978) Transformation of yeast. *Proc. Natl. Acad. Sci. USA.* 75, 1929-1933.

- Holz, A., Bossinger, B., Strasser, T., Janning, J., Klapper, R. (2003) Two origins of hemocytes in *Drosophila*. *Development* 130, 4955-4962.
- Ito, H., Fujitani, K., Usui, K., Shimizu-Nishikawa, K., Tanaka, S., Yamamoto, D. (1996). Sexual orientation in *Drosophila* is altered by the *satori* mutation in the sex-determination gene *fruitless* that encodes a zinc finger protein with a BTB domain. *Proc. Natl. Acad. Sci. USA.* 93, 9687-9692.
- Joiner, M.I.A. and Griffith, L.C. (1997). CaM kinase II and visual input modulate memory formation in the neuronal circuit controlling courtship conditioning. *J. Neurosci.* 17, 9384-9391.
- Jurica, M.S., Monnat, R.J.Jnr., Stoddard, B.L. (1998) DNA recognition and cleavage by the LAGLIDADG homing endonuclease I-*Crel*. *Molecular Cell* 2, 469-476.
- Kapust, R.B., and Waugh, D.S. (1999). *Escherichia coli* maltose-binding protein is uncommonly effective at promoting the solubility of polypeptides to which it is fused. *Protein Sci.* 8, 1668-1674.
- Kimura, K., Ote, M., Tazawa, T., Yamamoto, D. (2005). *fruitless* specifies sexually dimorphic neural circuitry in the *Drosophila* brain. *Nature.* 438, 229-233.
- Kitamoto, T. (2002). Conditional disruption of synaptic transmission induces male-male courtship behavior in *Drosophila*. *Proc. Natl. Acad. USA.* 99, 13232-13237.
- Kosaka, T. and Ikeda, K. (1983) Reversible blockage of membrane retrieval and endocytosis in the garland cell of the temperature-sensitive mutant of *Drosophila melanogaster*, *shibire^{ts1}*. *J Cell Biol.* 97, 499-507.
- Kubli, E. (2003). Sex-peptides: seminal peptides of the *Drosophila* male. *Cell. Mol. Life. Sci.* 60, 1689-1704.
- Kurada, P., and White, K. (1998) Ras promotes cell survival in *Drosophila* by downregulating *hid* expression. *Cell* 95, 319-29.
- Laski, F.A., Rio, D.C., and Rubin, G.M. (1986). Tissue specificity of *Drosophila P*-element transformation is regulated at the level of mRNA splicing. *Cell.* 44, 7-19.
- Lawrence, P.A., and Johnston, P. (1986). The muscle pattern of a segment of *Drosophila* may be determined by neurons and not by contributing myoblasts. *Cell* 45, 505-513.
- Lee, G., Foss, M., Goodwin, S.F., Carlo, T., Taylor, B.J., Hall, J.C. (2000). Spatial, temporal and sexually dimorphic expression patterns of the *fruitless* gene in the *Drosophila* central nervous system. *J. Neurobiol.* 43, 404-426.

- Lee, G., and Hall, J. (2001). Abnormalities of male-specific FRU protein and serotonin expression in the CNS of *fruitless* mutants in *Drosophila*. *J. Neurosci.* 21, 513-526.
- Lee, G., Vilella, A., Taylor, B.J., Hall, J.C. (2001). New reproductive anomalies in *fruitless*-mutant *Drosophila* males: extreme lengthening of mating durations and infertility correlated with defective serotonergic innervation of reproductive organs. *J. Neurobiol.* 47, 121-149.
- Lee, G., Hall, J.C., Park, J.H. (2002). *doublesex* gene expression in the central nervous system of *Drosophila melanogaster*. *J. Neurogenet.* 16, 229-248.
- Liu, H. and Kubli E. (2003) Sex-peptide is the molecular basis of the sperm effect in *Drosophila melanogaster*. *Proc. Natl. Acad. Sci. USA.* 100, 9929-9933.
- Lloyd, T.E., Atkinson, R.A., Wu, M.N., Zhou, Y., Pennetta, G., Bellen, H.J. (2002) Hrs regulates endosome membrane invagination and tyrosine kinase receptor signaling in *Drosophila*. *Gene* 246, 103-109.
- Manoli, D.S. and Baker, B.S. (2004). Median bundle neurons coordinate behaviours during *Drosophila* male courtship. *Nature.* 430, 564-569.
- Manoli, D.S., Foss, M., Vilella, A., Taylor, B.J., Hall, J.C., Baker, B.S. (2005). Male-specific *fruitless* specifies the neural substrates of *Drosophila* courtship behaviour. *Nature.* 436, 395-400.
- Mansour, S.L., Thomas, K.R., Capecchi, M.R. (1988). Disruption of the proto-oncogene int-2 in mouse embryo-derived stem cells: a general strategy for targeting mutations to non-selectable genes. *Nature.* 336, 348-352.
- Markow, T.A., and O'Grady, P.M. (2005) *Drosophila: a guide to species identification and use.* Academic Press. p80.
- Martin, G.R. (1981) Isolation of a pluripotent cell line from early mouse embryos cultured in medium conditioned by teratocarcinoma stem cells. *Proc. Natl. Acad. Sci. USA.* 78, 7634.
- McBride, S.M.J., Giuliani, G., Choi, C., Krause, P., Correale, D., Watson, K., Baker G., Siwicki, K.K. (1999). Mushroom body ablation impairs short-term memory and long-term memory of courtship conditioning in *Drosophila melanogaster*. *Neuron* 24, 967-977.
- Miklos, G.L., and Rubin, G.M. (1996). The role of the genome project in determining gene function: insights from model organisms. *Cell* 86, 521-529.
- Milchanowski, A.B., Henkenius, A.L., Narayanan, M., Hartenstein, V., Banerjee, U. (2004) Identification and characterization of genes involved in embryonic crystal cell formation during *Drosophila* hematopoiesis. *Genetics.* 168, 325-39.
- Moses, K., Ellis, M.C., and Rubin, G.M. (1989) The glass gene encodes a zinc finger protein required by *Drosophila* photoreceptor cells. *Nature* 340, 531-536.

- O'Dell, K.M., Armstrong, J.D., Yang, M.Y., and Kaiser, K. (1995). Functional dissection of the *Drosophila* mushroom bodies by selective feminization of genetically defined subcompartments. *Neuron* 15, 55-61.
- O'Keefe, L.V., Smibert, P., Colella, A., Chataway, T.K., Saint, R., Richards, R.I. (2007). Know thy fly. *Trends in Genetics* 23, 238-242.
- Papadopoulou, B. and Dumas, C. (1997). Parameters controlling the rate of gene targeting frequency in the protozoan parasite *Leishmania*. *Nucleic Acids Res.* 25, 4278-4286.
- Radovic, A., Wittkopp, P.J., Long, A.D., Drapeau, M.D. (2002). Immunohistochemical colocalization of Yellow and male-specific Fruitless in *Drosophila melanogaster* neuroblasts. *Biochem Biophys Res Commun.* 293,1262-4.
- Robertson, H. M. (1983). Chemical Stimuli eliciting courtship by males in *Drosophila melanogaster*. *Experientia* 39, 333-335.
- Rideout, E.J., Billeter J.C. and Goodwin S.F. (2007). The sex determination genes *fruitless* and *doublesex* specify a neural substrate required for courtship song. *Curr. Biol.* 17, 1473-1478.
- Riziki, T.M. (1978) The circulatory system and associated cells and tissues. The genetics and biology of *Drosophila*. Academic Press, London. 397-452.
- Rong, Y.S. and Golic, K.G. (2000). Gene targeting by homologous recombination in *Drosophila*. *Science.* 288, 2013-2018.
- Rong, Y.S. and Golic, K.G. (2001). A targeted gene knockout in *Drosophila*. *Genetics.* 157, 1307-1312.
- Rong, Y.S., Titen, S.W., Xie, H.B., Golic, M.M., Bastiani, M., Bandyopadhyay, P., Olivera, B.M., Brodsky, M., Rubin, G.M., Golic, K.G. (2002). Targeted mutagenesis by homologous recombination in *D. melanogaster*. *Genes Dev.* 16, 1568-1581.
- Rubin, G.M. and Spradling, A.C. (1983). Vectors for *P* element-mediated gene transfer in *Drosophila*. *Nucleic Acid Res.* 11, 6341-6351.
- Ryner, L.C., Goodwin, S.F., Castrillon, D.H., Anand, A., Villella, A., Baker, B.S., Hall, J.C., Taylor, B.J., Wasserman, S.A. (1996). Control of male sexual behaviour and sexual orientation in *Drosophila* by the *fruitless* gene. *Cell.* 87, 1079-1089.
- Sambrook, J., and Russell, D.W. (2001). In "Molecular Cloning: A Laboratory Manual", Third Edition. Cold Spring Harbor Laboratory Press, Cold Spring Harbor, New York. Pp. 8.81-8.85
- Seum, C., Pauli, D., Delattre, M., Jacquet, Y., Spierer, A., and Spierer, Pierre. (2002). Isolation of *Su(var)3-7* mutations by homologous recombination in *Drosophila melanogaster*. *Gen. Soc. Amer.* 161, 1125-1136.

- Song, H.J., Billeter, J.C., Reynaud, E., Carlo, T., Spana, E.P., Perimon, N., Goodwin, S.F., Baker B.S. and Taylor B.J. (2002) The *fruitless* gene is required for proper formation of axonal tracts in the embryonic central nervous system of *Drosophila*. *Genetics* 162, 1703-1724.
- Srinivasan, S., Armstrong, J.A., Deuring, R., Dahlsveen, I.K., McNeill, H., and Tamkun, J.W. (2005). The *Drosophila* trithorax group protein Kismet facilitates an early step in transcriptional elongation by RNA Polymerase II. *Development* 132, 1623-1635.
- Stocker, R.F. and Gendre, N. (1989). Courtship behavior of *Drosophila* genetically or surgically deprived of basiconic sensilla. *Behav. Genet.* 19, 371-385.
- Stocker, R.F. (1994). The organization of the chemosensory system in *Drosophila melanogaster*: a review. *Cell Tissue Res.* 275, 3-26
- Stockinger, P., Kvitsiani, D., Rotkopf, S., Tirian, L., Dickson, B.J. (2005). Neural circuitry that governs *Drosophila* male courtship behavior. *Cell.* 121, 795-807.
- Taylor, B.J., and Knittel, L.M. (1995). Sex-specific differentiation of a male-specific abdominal muscle, the Muscle of Lawrence, is abnormal in hydroxyurea-treated and in *fruitless* male flies. *Development* 121, 3079-3088.
- Tepass, U., Fessler, L.I., Aziz, A., and Hartenstein, V. (1994). Embryonic origin of hemocytes and their relationship to cell death in *Drosophila*. *Development* 120, 1829-1837.
- Thompson, A.J., Yuan, X., Kudlicki, W., and Herrin, D.L. (1992). Cleavage and recognition pattern of double-strand-specific endonuclease (*I-Crel*) encoded by the chloroplast 23S rRNA intron of *Chlamydomonas reinhardtii*. *Gene.* 119, 247-251.
- Tissot, M., and Stocker, R.F. (2000) Metamorphosis in *Drosophila* and other insects: the fate of neurons throughout the stages. *Prog. Neurobiol.* 62, 89-111.
- Trimarchi, J.R. and Schneiderman, A.M. (1994). The motor neurons innervating the direct flight muscles of *Drosophila melanogaster* are morphologically specialized. *J. Comp. Neurol.* 340, 427-443.
- Usui-Aoki, K., Ito, H., Ui-Tei, K., Takahashi, K., Lukacsovich, T., Awano, W., Nakata, H., Piao, Z.F., Nilsson, E.E., Tomida, J., Yamamoto, D. (2000). Formation of the male-specific muscle in female *Drosophila* by ectopic *fruitless* expression. *Nat. Cell Biol.* 2, 500-506.
- Villella, A., Gailey, D.A., Berwald, B., Ohshima, S., Barnes, P.T., Hall, J.C. (1997). Extended reproductive roles of the *fruitless* gene in *Drosophila melanogaster* revealed by behavioural analysis of new *fru* mutants. *Genetics.* 147, 1107-1130.
- Villella, A., Ferri, S.L., Krystal, J.D., Hall, J.C. (2005). Functional analysis of *fruitless* gene expression by transgenic manipulations of *Drosophila* courtship. *Proc. Natl. Acad. Sci. USA.* 102, 16550-16557.

- Villella A., Peyre J.B., Aigaki T. and Hall J.C. (2006) Defective transfer of seminal-fluid materials during matings of semi-fertile *fruitless* mutants in *Drosophila*. *J. Comp. Phys. A* 192(12):1253-69.
- von Schilcher, F. and Hall, J.C. (1979). Neural topography of courtship song in sex mosaics of *Drosophila melanogaster*. *J. Comp. Physiol. A.* 129, 85-95.
- Williams, J.A., and Seghal, A. (2001). Molecular components of the circadian system in *Drosophila*. *Annu. Rev. Physiol.* 63, 729-755.
- Wolfner, M.F. (1997). Tokens of love: functions and regulation of *Drosophila* male accessory gland products. *Insect Biochem. Mol. Biol.* 27, 179-192.
- Yamamoto, D., Jallon J.-M., Komatsu, A. (1997). Genetic dissection of sexual behavior in *Drosophila melanogaster*. *Ann. Rev. Entomol.* 42: 551-585.
- Yao, K. M., Samson, M.L., Reeves, R., White, K. (1993). Gene *elav* of *Drosophila melanogaster*: a prototype for neuronal-specific binding protein gene family that is conserved in flies and humans. *J. Neurobiol.* 24, 723-739.
- Zaffran, S. (2000) Molecular cloning and embryonic expression of *dFKBP59*, a novel *Drosophila* FK506-binding protein. *Gene* 246, 103-109.
- Zhang, S.D. and Odenwald, W.F. (1995). Misexpression of the *white (w)* gene triggers male-male courtship in *Drosophila*. *Proc. Natl. Acad. Sci. USA.* 92, 5525-5529.